ICES COOPERATIVE RESEARCH REPORT
RAPPORT DES RECHERCHES COLLECTIVES

NO. 312

APRIL 2012

Fishery applications of optical technologies

Editors

James Churnside • Michael Jech • Eirik Tenningen

Authors

Pierre M. Clement • Arne Fjälling • Jules S. Jaffe
Emma G. Jones • Bo Lundgren • Gavin J. Macaulay
Howard McElderry • Richard O'Driscoll • Tim E. Ryan
Mark R. Shortis • Stephen J. Smith • W. Waldo Wakefield

International Council for the Exploration of the Sea
Conseil International pour l'Exploration de la Mer

H. C. Andersens Boulevard 44–46
DK-1553 Copenhagen V
Denmark
Telephone (+45) 33 38 67 00
Telefax (+45) 33 93 42 15
www.ices.dk
info@ices.dk

Recommended format for purposes of citation:

Churnside, J., Jech, M., and Tenningen, E. (Eds). 2012. Fishery applications of optical technologies. ICES Cooperative Research Report No. 312. 91 pp.

Series Editor: Emory D. Anderson

ISBN 978-87-7482-102-1

ISSN 1017-6195

Contents

1 Introduction

The optics of the ocean are very different from those of the atmosphere. Light is much more strongly absorbed and scattered. Despite the difficulties, optical systems have been widely applied in fishery research and management. These applications include, but are not limited to: abundance surveys using video and still cameras, airborne lidar (light detection and ranging), supporting data for acoustic measurements, behavioural studies, observations of fishery operations, and habitat classification. New applications are continually being developed and made possible by the array of optical technologies available. Many use simple digital still or video cameras. For operation at depths greater than a few tens of metres, where there is little ambient light, low-light-level cameras and artificial lighting are often used. Lasers have found application in a number of configurations, including airborne lidars that operate like vertical echosounders, holographic cameras, and laser-imaging systems designed to increase image contrast in the presence of scattering in the water. There are a number of practical factors that affect the performance of optical systems. These include the capability of the platform, geolocation, data processing, metadata, calibration, and of course estimate of measurement uncertainties.

1.1 Overview of this report

This report begins with a brief review of the optical properties of the ocean, which determine what is possible with optical systems. These properties can vary considerably from familiar acoustical properties. For example, in the clearest waters, 66% of the light is scattered and absorbed over distances of tens of metres, whereas sound can travel much farther, depending on wavelength. However, the transmission of optical energy through the air–sea interface is ca. 98% at near-normal incidence, whereas the corresponding transmission for acoustic energy is ca. 0.1%, and all acoustic systems in use are operated in contact with the ocean. This review is followed by a description of available optical technologies, some of the issues that must be considered in their use, and practical applications.

Several commonly used optical techniques have not been included in order to concentrate on more recent technology. Visual observations, often aided by binoculars, from aircraft and surface vessels have long been used, especially for counts of seabirds and marine mammals. Similarly, visual observations by divers have been important in, for example, coral reef monitoring (Samoilys and Carlos, 2000). The use of microscopes in plankton studies is considered to be a well-developed technology and beyond the scope of this report. Underwater cameras and video have been used extensively by divers, and by manned and unmanned submersibles, to collect images without quantitative analysis. We will only discuss applications where images have been used for quantitative analyses.

2 Ocean optics

James Churnside

This section presents a brief overview of the optical properties of the ocean that are relevant to the techniques described in this report. More details can be found in several good books on the topic (Jerlov, 1976; Shifrin, 1988; Mobley, 1994). There are three physical optical effects to be considered: refraction, absorption, and scattering. These produce the inherent optical properties, which depend only on the characteristics of the medium, and the apparent optical properties, which also depend on the characteristics of illumination. There are also two bio-optical processes of importance: fluorescence and bioluminescence. Standard notations for commonly used parameters are presented in Table 2.1.

Table 2.1. Common ocean-optics parameters and units.

Symbol	Definition	Unit
n	Refractive index	unitless
λ	Wavelength	nanometre (nm)
a	Absorption coefficient	m^{-1}
P	Power	watts
b	Scattering coefficient	m^{-1}
Ψ	Scattering angle	sr or degree
β	Volume scattering function	$m^{-1}\,sr^{-1}$
$\tilde{\beta}$	Phase function (β/b)	sr^{-1}
b_b	Backscattering	m^{-1}
c	Total attenuation	m^{-1}
ω_0	Single-scattering albedo (b/c)	unitless
Z_s	Secchi depth	m
K_D	Diffuse-attenuation coefficient	m^{-1}
R_{RS}	Remote-sensing reflectance (ratio of the water-leaving radiance in the zenith direction to the irradiance incident on the surface)	sr^{-1}

Light is a transverse electromagnetic wave that propagates at $3.00 \times 10^8\,m\,s^{-1}$ in a vacuum, but slightly slower through a material medium such as seawater. Because it is a transverse wave, the medium can also affect the azimuthal angle of the electric field with respect to some reference plane. This azimuth angle defines polarization, which can be linear if the angle does not change, or circular if the angle rotates around the direction of propagation. In unpolarized light, the azimuthal angle is completely randomized. As an example of the principles, sunlight is unpolarized, but light scattered from the sky is partially linearly polarized by the scattering process.

2.1 Inherent optical properties

The refractive index is, in general, a complex number. The real part n is the ratio of the speed of light in a vacuum to that in the medium. For seawater, n is ca. 1.33, with a weak dependence on wavelength, temperature, and salinity. For visible light, the correction is less than 1% for the range of temperatures and salinities encountered in nature. This produces a surface reflection of ca. 2% for near-normal incidence. It is this low surface reflection that allows optical systems to operate across the air–water interface. The in-water propagation angle is ca. 75% of the in-air angle for small (near-normal incidence) angles. The imaginary part is the absorption of the material, but the absorption coefficient is more commonly used.

The absorption coefficient a includes contributions from water, dissolved substances, and particles. It is defined as the fractional decrease in power through absorption as a function of range, and has units of m^{-1}. This implies that

$$P(s_1) = P(s_0)\exp\left[-a(s_1 - s_0)\right]$$

describes the power P in a beam that has propagated along the line from s_0 to s_1 in a uniformly absorbing medium. The absorption of pure seawater is strongly wavelength-dependent, with a minimum in the blue region of the visible spectrum (Figure 2.1). Dissolved organic substances absorb more strongly at shorter wavelengths, and chlorophyll has an absorption minimum at ca. 600 nm. The combined effect is to shift the absorption minimum towards green in coastal waters.

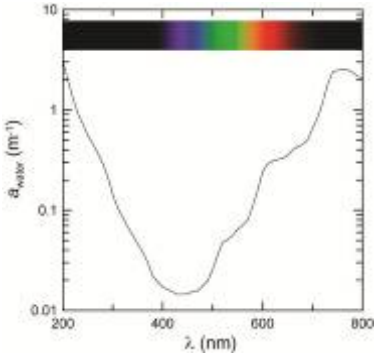

Figure 2.1. Absorption coefficient of pure seawater a_{water} (no dissolved organic material) vs. wavelength λ, with the visible spectrum at the top for reference. (Source: Mobley, 1994.)

The scattering coefficient b includes contributions from molecules as well as larger particles. It is defined in the same way as the absorption coefficient. Molecular scattering is isotropic, because molecules are much smaller than optical wavelengths. Most optical scattering, on the other hand, is by particles that are much larger than optical wavelengths, and most of the scattering is in the forward direction. The scattering in any particular direction Ψ is described by the volume scattering function β (Figure 2.2), which has units of m^{-1} sr^{-1}. The integral of β over all solid angles is b. The ratio β/b is the phase function $\tilde{\beta}$. The integral of β over all solid angles with scattering angle $> \pi/2$ is the backscatter coefficient b_b. The total attenuation of a narrow optical beam is given by $c = a + b$. The ratio b/c is the single-scattering albedo ω_0. Table 2.2 presents typical values of absorption and scattering parameters for the same typical water types considered in Figure 2.2.

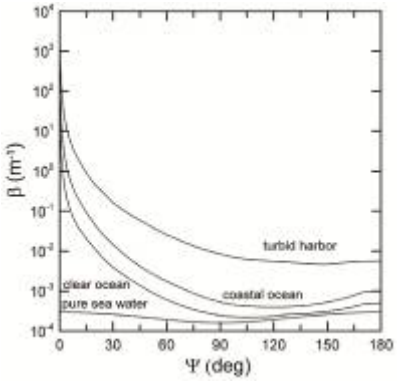

Figure 2.2. Measured values of the volume scattering function β vs. scattering angle Ψ for several water types at λ = 514 nm. (Source: Mobley, 1994.)

Table 2.2. Typical absorption coefficient *a*, scattering coefficient *b*, beam-attenuation coefficient *c*, single-scattering albedo ω_0, backscattering ratio b_b/b, and median value of the scattering angle Ψ (in degrees) for pure water and several natural water types. All values are for green ($\lambda = 514$ nm or 530 nm) light.

Water type	a(m^{-1})	b(m^{-1})	c(m^{-1})	ω_0	b_b/b	Median Ψ
Pure seawater	0.0405	0.0025	0.043	0.058	0.500	90.00
Clear ocean	0.114	0.037	0.151	0.247	0.044	6.25
Coastal ocean	0.179	0.219	0.398	0.551	0.013	2.53
Turbid harbour	0.366	1.824	2.190	0.833	0.020	4.68

Scattering also affects the polarization properties of light. Polarized light is generally described by the four-element Stokes vector, where the four elements describe optical intensity, the degree of linear polarization in a reference plane defined by an arbitrary azimuth angle, the degree of linear polarization in a plane with azimuth angle 45° from the reference plane, and the degree of circular polarization. In the most general case, the scattering coefficient is replaced by the 4×4 Mueller matrix, which relates the scattered Stokes vector to the incident Stokes vector.

A full polarimetric description of light in the ocean is beyond the scope of this report, but a couple of general features are worth noting: (i) laser light is generally polarized, but scattering in the ocean tends to decrease the degree of polarization; and (ii) natural light is unpolarized, but scattering in the ocean tends to increase the degree of polarization.

2.2 Apparent optical properties

One of the easiest of the optical properties to measure is Secchi depth Z_S, which is the depth at which a white disk with a diameter of 30 cm is no longer visible. Typically, the disk is slowly lowered and the depth at which it disappears from sight is noted. The disk is then lowered slightly farther and slowly raised until it reappears. The average of the two depths is taken to be the Secchi depth. If done in calm seas with the sun nearly overhead, this provides a measure of water clarity.

Another useful optical property is the diffuse-attenuation coefficient K_D, which describes the attenuation of natural light with depth. This quantity also depends on wavelength, and is typically measured by lowering a number of radiometers sensitive to different wavelengths into the water. As with Secchi depth, the diffuse-attenuation coefficient provides a good indication of water clarity for measurements made in calm seas with the sun high in the sky. Under these conditions, the diffuse-attenuation coefficient is approximated by $K_D = a + b_b$. We can also obtain a rough estimate of Secchi depth from (Hou *et al*., 2007)

$$Z_S = \frac{4.8}{K_D + c}$$

with K_D and c measured at a wavelength near the peak of the human visual response at 530 nm.

The characteristics of the diffuse-attenuation coefficient have been used to characterize different water types (Jerlov, 1976; Austin and Petzold, 1986). Figure 2.3 presents the spectral dependence of the diffuse-attenuation coefficient for the open ocean (I, IA, IB, II, and III) and coastal (1, 3, 5, 7, and 9) types. Waters are also characterized as Case 1, in which the optical properties are dominated by the effects of phytoplankton, or Case 2, in which the effects of suspended sediments, dissolved

organic matter, and terrigenous particles are evident. These cases generally correspond to the Jerlov open-ocean Types I–III and coastal Types 1–9, respectively.

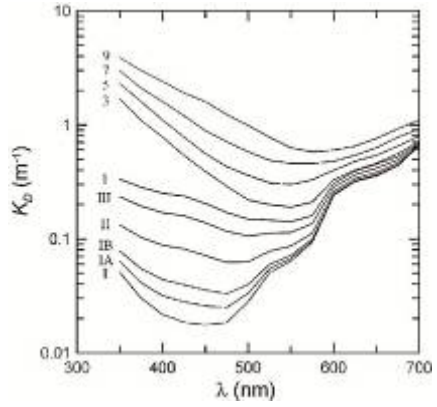

Figure 2.3. The diffuse-attenuation coefficient K_D vs. wavelength λ for open ocean (I, IA, IB, II, and III) and coastal (1, 3, 5, 7, and 9) water types. (Source: Mobley, 1994.)

For more than ten years, measurements of ocean colour have been available from satellite instruments. These instruments measure the incident radiance at the top of the atmosphere at several wavelengths. These measurements are converted into an apparent optical property of the ocean, referred to as the remote-sensing reflectance R_{RS}, which is defined as the ratio of the water-leaving radiance in the zenith direction to the irradiance incident on the surface. From the wavelength dependence of this quantity, estimates can be made for chlorophyll concentration, level of suspended sediments, and the diffuse-attenuation coefficient. Much more information is available on the National Aeronautics and Space Administration (NASA) ocean colour website (http://oceancolor.gsfc.nasa.gov/).

2.3 Bio-optical properties

In addition to the physical properties described above, there are two ocean properties of interest here that are biological in origin. The first is fluorescence, which is the process by which a complex molecule absorbs a photon of light at one energy level and emits a photon at a lower energy level. Of particular importance in the ocean is the fluorescence of the pigment chlorophyll *a*, which absorbs in the blue–green region of the visible spectrum and fluoresces in the red.

The other biological property of interest is bioluminescence, in which light is produced through a chemical reaction. It is exhibited by a wide variety of organisms in the ocean. Certain bacteria will luminesce for long periods of time once a critical cell density is reached. Dinoflagellates will emit light when they are physically stimulated. Certain deep-water fish use bioluminescence to attract prey. Cephalopods use bioluminescence in mating rituals.

3 Optical technologies

James Churnside, Arne Fjälling, Jules S. Jaffe, Michael Jech, Bo Lundgren, Tim E. Ryan, and W. Waldo Wakefield

This chapter provides a brief description of the technologies available at the time this report was written. There continues to be rapid advances in optical technologies in terms of price and performance that create new opportunities. Examples include the number of pixels available from charge-coupled device (CCD; visible) and microbolometer (infrared) arrays.

3.1 Cameras

In essence, a camera is a device that uses an optical lens to project an image onto a sensor that allows permanent storage of that image. Recent advances in electronic sensors and digital storage media have made the silver halide-based photographic emulsion that has been the basis of photography for more than a hundred years, almost obsolete. There are a number of different electronic-sensor technologies that have different performance characteristics and, therefore, different applications. This section categorizes and discusses cameras according to their sensor technologies.

The basic principles of photography are well documented, and the reader is referred to the many texts and resources on this subject. In any application, several factors need to be considered. A lens of longer focal length will provide greater magnification and hence a finer spatial resolution, but a smaller field of view. In a "zoom" lens, the effective focal length can be adjusted to provide the best combination of field of view and spatial resolution for the conditions. A smaller aperture (larger f-stop) will generally produce a greater depth of focus, but less sensitivity at low light levels. This parameter is also variable on many photographic lenses. A slower shutter speed will generally produce greater sensitivity at low light levels, but more motion blur if the camera or subject is moving.

Camera sensitivity is often specified in lux (lx), where 1 lx = 1 lumen m^{-2} = 1 candela sr m^{-2}. The candela (cd) is a fundamental SI unit, defined as:

> the luminous intensity, in a given direction, of a source that emits monochromatic radiation of frequency 540×10^{12} Hz (a wavelength of ca. 555 nm) and that has a radiant intensity in that direction of 1/683 watt per steradian (Thompson and Taylor, 2008).

The illuminance at the surface on a clear day with the sun directly overhead is ca. 10^5 lx. On a cloudy day, it will be around 10^3 lx. These values decrease rapidly with depth at a rate determined by the diffuse-attenuation coefficient. For example, consider the "coastal ocean" case in Table 2.2. On a cloudy day, the illuminance will be ca. 10 lx at a depth of 25 m.

Cameras are somewhat arbitrarily separated into "video" or "still" cameras, depending on whether images are taken at video-frame rates (for example 25 or 30 Hz). This distinction is breaking down to some extent because a convergence between the two modes is occurring; many still cameras now have the capability to record in a video mode and/or take still images at increasingly fast frame rates. Similarly, video cameras offer still-capture capability, and/or the resolution of "captured" video frames can be of sufficient quality to use as still images. When choosing between systems, it is perhaps helpful to consider the primary objective of

the camera. Is it to capture moving images or to "freeze" them at a moment in time? At the time of writing, we see still- and video-camera systems continue their rapid advances. Therefore, it seems that dedicated still or video systems, in keeping with their respective primary purposes, will continue to provide the highest possible performance for some time to come.

3.1.1. Charge-coupled devices, complementary metal oxide semiconductors

The most common camera type is a silicon CCD, which provides a digital image. These types of sensors are used for consumer digital still and video cameras as well as a variety of specialized industrial applications. Consumer still and video cameras are advancing so rapidly that whatever we might say about their specifications will be obsolete before publication. The most up-to-date information can be found from the manufacturers.

A CCD has an array of capacitors, which are photoactive, and a transmission area. As the light from an image is focused on the capacitor array via the lens, the capacitors accumulate an electric charge that is proportional to the amount of light received. A circuit then controls the transfer of each capacitor's contents to each of its neighbours, which, in turn, pass the contents to their neighbours and ultimately to a charge amplifier and digitizer. This digital information is then stored for later processing or visualization. The sensitivity of the photoactive region is the limiting factor for acquiring an image in low-light conditions. The most common material for the photoactive region is silicon with mixes of other elements.

Some cameras also use complementary metal oxide semiconductor (CMOS) imaging chips, which can be lighter and use less power, but are generally less sensitive. For example, almost all cameras in mobile phones use CMOS technology. Recent advances in CMOS technology, such as the scientific CMOS (sCMOS, www.scmos.com) have improved image quality to the point where multimegapixel images can be obtained with high dynamic range and quantum efficiency.

Digital still cameras can be broadly grouped into three categories.

1) compact "point-and-shoot" style cameras, which are small and light, with most having only automatic exposure and focus controls;

2) "bridge" cameras, which are physically similar to single-lens reflex (SLR) cameras and generally have more functionality and user control than compact cameras;

3) digital single-lens reflex (DSLR) cameras. These cameras offer through-the-lens framing, various degrees of manual and automatic control, the ability to interchange lenses, and the ability to interface with external strobes. They are generally more expensive, heavier, and larger than the first two categories.

A key consideration when building a system will be whether the camera can be controlled externally and what additional information (e.g. camera settings, GPS (global positioning system) time and position) can be stored with the images.

Recording video cameras (camcorders) integrate a video camera, recording media, and battery power supply into a portable hand-held unit. For some applications, they offer a very convenient and cost-effective solution. As is the case for digital still cameras, external control can be an important consideration. The ability to overlay text, such as time or position data, on the video image may also be desirable. There is a choice between cameras with one or three CCDs, with the former being cheaper,

but the latter generally having better low-light capability and colour definition. Common video standards include phase alternating line (PAL) outside North America, National Television System Committee (NTSC) within North America, and, more recently, high definition (HD). The HD cameras operate with either a full scan of the array at 50 or 60 Hz (progressive high definition, or HDp) or with alternate scans of even and odd numbered rows to produce images at 25 or 30 Hz (interlaced high definition, or HDi). The recording media are moving from tape and optical disk towards direct-to-disk internal hard drive (i.e. solid state) or flash memory (a.k.a. flash RAM). An alternative to using recording video cameras is to feed a video output from a stand-alone video camera to a video-capture device. The output of the video-capture device can then be recorded directly to a computer hard drive. Machine-vision cameras are now becoming available for underwater uses. Machine-vision cameras are digitally controlled and tend to be more complex to operate, but they provide greater control over image quality and acquisition.

Commercially produced underwater camera systems have the advantage of being available "off the shelf" and designed as a "turn-key" solution to a range of common situations. They are already proven in the field and well supported by the suppliers. An exhaustive list of CCD manufacturers is not possible because the market is changing rapidly. We provide a few examples of cameras that have been used in fishery applications and provide examples of image quality that is currently available. Deep Sea Power and Light Micro-SeaCam 1050 and Deep Sea Power and Light SSC-5000 low-light cameras are two robust cameras that have been used to image Atlantic herring (*Clupea harengus*) in the Northwest Atlantic (e.g. Figure 3.1). The Micro-SeaCam 1050 is a small (10 cm length by 5 cm diameter) camera with a ⅓ in CCD sensor that can acquire images down to 0.05 lx (at f/1.2) or 0.27 lx at f/2.8. The SSC-5000 is a "low-light" camera that is larger (25 cm length by 9.5 cm diameter), but has a ½ in CCD sensor that can acquire images to 10^{-3} lx at f/0.8.

Figure 3.1. Digital image of spawning Atlantic herring (*Clupea harengus*) during October 2001 on Georges Bank. The image was acquired with a Micro-SeaCam 1050 CCD black-and-white camera. External lighting was used for illumination. (Image courtesy of W. Michaels, NOAA Fisheries.)

The newest generation CCD cameras can obtain high-resolution (e.g. 2048 × 2048 pixels) images with high dynamic range (e.g. 16 bit) and at high frame rates (e.g. 10–30 frames per second (fps), depending on resolution). For example, PCO's

(www.pco.de) Pixelfly 1024 × 1280 pixel resolution CCD camera, with 12 bits of dynamic range, has been used to image the seabed in order to survey the geological and biological habitat (Figure 3.2; Armstrong *et al*., 2006).

Figure 3.2. A 1024 × 1280 pixel image of fish and invertebrates on the seabed. Compare with Figure 3.1, which was taken nearly a decade earlier. (Photo courtesy of H. Singh, Woods Hole Oceanographic Institution.)

Provided that there is the capability to design and build, customized systems offer many advantages.

1) They give access to a diverse range of products that can be selected according to the application. Depending on the application, the designer has a choice ranging from very low-cost products from the mass consumer market to professional-grade, high-end products.

2) It is possible to adopt new models, usually with a better specification, lower cost, or both, as they come onto the market.

3) They can allow a high degree of control on how the camera operates and, importantly, integrates and synchronizes with (or to) other instruments.

The disadvantages are that customized systems require in-house expertise and cannot be simply purchased off the shelf. The development and build lead-times can be lengthy, and a newly built system requires testing and carries the risk of failure.

One potential application, of course, is airborne video for documenting surface schools. Figure 3.3 is an example of a school of Atlantic menhaden (*Brevoortia tyrannus*) taken with an HD video from an altitude of 300 m. This school is at a colour front on the shallow shelf in the western Atlantic and extends from the surface to the bottom.

Figure 3.3. Video image of a fish school (dark region just above the time stamp). (Photo courtesy of J. Churnside.)

3.1.2. Low light level

The silicon intensifier-target (SIT) and intensified silicon intensifier-target (ISIT) camera technologies, which have been the mainstay of low-light cameras for the past few decades, are becoming obsolete technologies. For example, Kongsberg produced its final SIT camera in 2006. The sensor was based on glass vacuum-tube technology, which is the main reason for its recent demise. Although the SIT technology was originally developed for night-vision applications on land, the SIT sensor sensitivity peaked in the blue–green region of the visible spectrum, which was advantageous for working underwater. ISIT cameras still have some of the best sensitivities of 10^{-5} to 10^{-6} lx (e.g. Wardle and Hall, 1993) and are still utilized for applications where a power supply is not an issue (e.g. Heger *et al*., 2008).

The intensified charge-coupled device (ICCD), as its name suggests, intensifies light and can be used in lower light environments than standard CCD cameras. It is important to note that both ultimately use a CCD detector. These cameras have extensive use in night-vision applications. In addition to intensifying the incident light, intensifiers can be designed to accentuate different wavelengths (or part of the electromagnetic spectrum) and because of the intensified light, gate speeds (i.e. shutter speed) can be faster than with CCD cameras. For example, ICCD cameras can utilize intensifiers that accentuate the UV–blue range, visible, or near-infrared regions and have gate speeds on a picosecond time-scale. The high gate speeds makes these devices useful for range-gated laser imaging (see Section 3.6). Fourth generation (Gen IV) intensifiers were introduced recently, although earlier technology (Gen II and Gen III) are still available. The performance of intensifiers is often stated in terms of quantum efficiency (QE), which is the fraction of incident photons that are detected. Gen II intensifiers have QEs of ca. 25%, whereas the later-generation intensifiers have QEs of 40–50%. For comparison with CCD cameras, a Remote Ocean Systems (ROS), Inc. low-light-level ICCD television camera has a sensitivity of 10^{-4} lx (full video) to 10^{-5} lx (at the faceplate) with a Gen III Ultra Blue intensifier.

The low-light capability makes ICCDs useful for several applications, including operations near the bottom of the photic zone and in the air. Below the photic zone, faint, red illumination can be used (Widder *et al*., 2005) to collect images without affecting animal behaviour. The Eye-in-the-Sea (http://www.teamorca.org/cfiles/eyeinthesea.cfm) is an example of an underwater application of an ICCD using faint red illumination. Figure 3.4 shows the image of a squid taken with this instrument. An ICCD is capable of detecting fish schools at night from aircraft through bioluminescence, if sufficient concentrations of bioluminescing organisms are present (Roithmayr, 1970; Squire and Krumboltz, 1981). Because of the low-light capability, an image intensifier has also been used in a hyperspectral camera (Bowles *et al*., 1998). The amount of light within a narrow spectral band may be low, even if the total light level is not.

Figure 3.4. ICCD image of a squid taken with the Eye-in-the-Sea. (Photo courtesy of E. Widder.)

A recent technology for low-light levels is the electron multiplying charge-coupled device (EMCCD). Although the ICCD has an amplification stage on the front of the CCD, the EMCCD adds an electron-multiplication register after the CCD readout register (Coates *et al*., 2004; Weber *et al*., 2010). The sensitivity can be similar to an ICCD. This technology is likely to overtake ICCD technology low-light-level underwater cameras in future. It should be noted that images from both ICCD and EMCCD under low-light levels tend to be noisy. This is a fundamental limitation caused by quantum fluctuations in photon number when the number of detected photons per pixel is low.

3.1.3. Infrared

Infrared (IR), or thermal, cameras are for capturing images of heat radiated in either the 3–5 or 7–14 μm wavelength bands where the atmosphere is relatively transparent. The ocean is not transparent at these wavelengths, with a penetration depth of only ca. 10 μm. Thus, they are only useful for above-surface operation and only for warm-blooded animals, such as birds or marine mammals.

The National Oceanic and Atmospheric Administration (NOAA) and Airborne Technologies, Inc. have used a commercial thermal-IR camera for aerial surveys. The

camera is a Raytheon Control IR 2000 B, designed for industrial and surveillance applications. It uses an uncooled ferroelectric (barium strontium titanate) detector array with a spectral response of 7–14 μm. The array is 320 × 240 pixels, which is converted to NTSC format, and then digitized at 720 × 480 pixels. Camera sensitivity was measured to be ca. 0.1 Kelvin.

The primary application was the detection of sea lions at night. This was based on earlier work (Thomas and Thorne, 2001), in which a thermal IR camera on a surface ship was used to document Steller sea lions (*Eumetopias jubatus*) feeding on herring (*Clupea pallasii*) at night. The camera was flown at an altitude of ca. 300 m, producing a pixel size at the surface of 34 cm. Sea lions and birds were clearly visible (Figure 3.5), although better image resolution would provide better identification. The wakes behind whales near the surface were also detected (Churnside *et al*., 2009b), although the whales themselves were not.

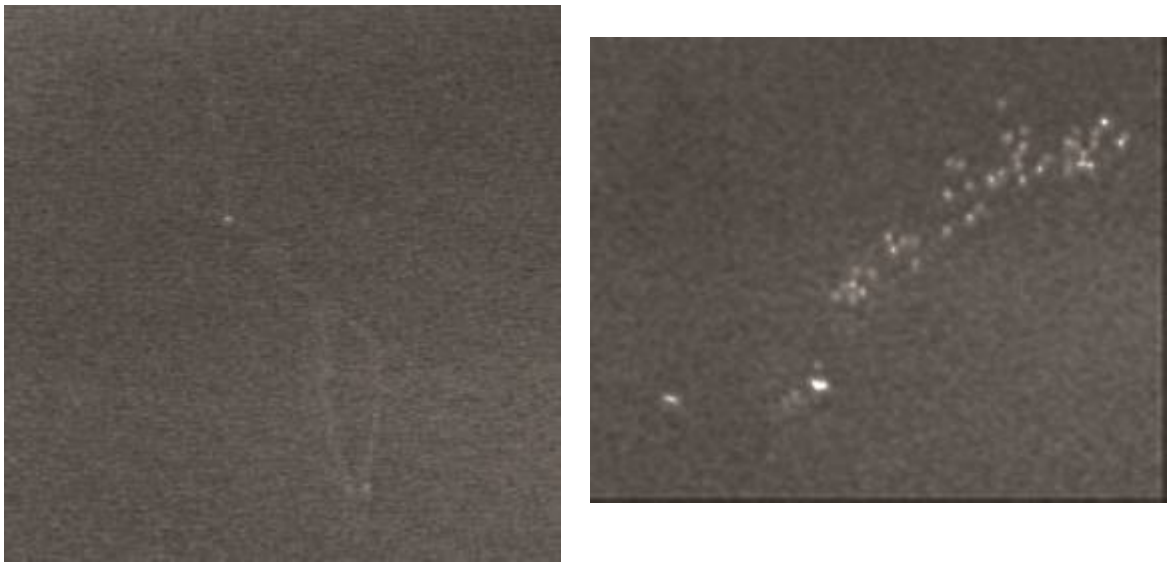

Figure 3.5. Thermal-IR images. (Left) Three sea lions. Each head is a bright (warm) spot in the image. The animals are moving toward the bottom of the image, leaving a warm wake. This wake is caused by the disruption of the cool skin layer at the surface. (Right) Seabirds on the surface. Each bird is an unresolved bright (warm) spot. Species identification is not possible with this resolution.

The camera used is typical of those on the market, with a spectral response of 7–14 μm, detector array of 320 × 240 pixels, and sensitivity of ca. 0.1 Kelvin. There are cameras available that operate in the 3–5 μm band. These use cooled detectors, which have been largely superseded by uncooled detectors working at the longer wavelengths. They can be more sensitive, however, because of the cooled detector. Higher resolution cameras (640 × 480 pixels) are also available and are likely to become more common. The cost of these cameras starts at ca. US$7000–8000, but is expected to continue to drop, as more commercial applications lead to larger production volumes. One other difference between these cameras is whether they are calibrated to provide an absolute temperature scale. For those that do, the accuracy is typically 2–3 Kelvin. Commercially available cameras range from the IR camera ICI7320, which weighs 0.15 kg and requires only a universal serial bus (USB) connection, to more advanced infrared (FLIR) systems that come in pods mounted externally on aircraft, with complete motion stabilization and control and feature tracking.

3.2 Lidar

Shortly after airborne lidar was tested for defence applications, it was recognized that fish schools could be detected by the same technique (Squire and Krumboltz, 1981). The appeal for fishery applications is the same as that for military applications: large areas of the ocean can be covered much more quickly by an aircraft than by a ship, but neither sound nor most forms of electromagnetic energy can penetrate into the ocean from above the surface. Light in the blue–green region of the spectrum is the notable exception, and backscatter lidars have been used for the detection of fish schools, individual fish, and plankton layers, validating theoretical predictions (Krekova *et al.*, 1994; Mitra and Churnside, 1999). Fluorescence lidar can provide airborne estimates of concentrations of chlorophyll *a* and other pigments (Gauldie *et al.*, 1996), but will not be discussed here.

The operation of a backscatter lidar is very similar in concept to a vertical echosounder. A short pulse of laser light is directed down into the ocean. As it travels down, it is scattered from fish and smaller particles in the ocean; the strength of the return provides information about the density of scatterers, whereas the time taken for the return provides depth information. Repeated pulses as the aircraft moves along build up an image of the depth profiles of scatterers along the flight track. Figure 3.6 is an example of raw data from the NOAA airborne fish lidar, FLOE (Fish Lidar, Oceanic, Experimental).

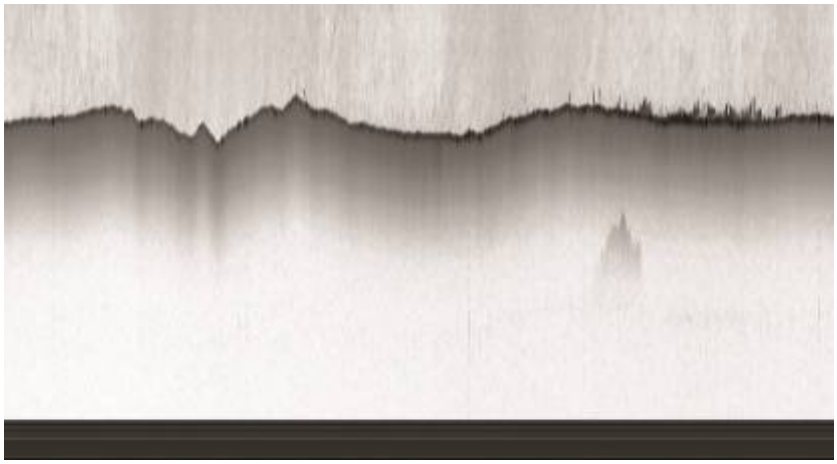

Figure 3.6. Sample of raw data file from the Bering Sea. The dark band near the top of the image is the water surface. Birds are seen just above the surface, and a school of fish is at the right. (Source: Churnside *et al.*, 2011b.)

FLOE provides a good example of the capabilities. The laser produces 10 nsec, 100 mJ pulses of linearly polarized green (532 nm) light at a rate of 30 pulses s^{-1}. The cross-polarized, reflected light is collected by a telescope onto a photomultiplier tube, and the return is digitized at a rate of 1 giga-sample s^{-1}, providing a sample at depth intervals of 11 cm. The use of the cross-polarized return provides a lower signal level than a copolarized return, but the contrast between fish and the background water scattering is greater (Churnside *et al.*, 1997). The specific wavelength is selected because of the availability of a very robust laser source. It is very close to the optimum wavelength for productive water, and not too far from the optimum for clear blue water.

Processing of the lidar returns involves several steps, depending on the final product desired (Churnside and Hunter, 1996; Churnside *et al.*, 2001a).

1) The surface return is identified for each pulse, and depths are measured from this point. This is necessary to account for variations in aircraft altitude.

2) The contribution to the signal from background light is measured for each pulse after the laser light has decayed to nothing. This level is subtracted from the rest of the profile.

3) The features of interest are separated from background scattering levels in the ocean. This can be done in one of several ways:

- manually select regions of interest in the data;
- automatically identify regions where the return is above the exponentially decaying return that would be expected for a vertically uniform collection of scatterers;
- automatically identify regions where the return is above the median return over some horizontal scale size. This last technique is useful where it is desirable to separate localized fish schools from larger plankton layers.

In the automated processing techniques, it is generally necessary to apply a threshold to the data to remove the effects of noise. In all three techniques, the background scattering level is estimated using the lidar return from outside the regions of interest. This level is subtracted from the total return, and the attenuation of the background scattering level is used to correct for the effects of attenuation on the signals of interest.

4) Finally, a calibration factor is applied to obtain a quantitative result. Figure 3.7 is an example of a processed lidar return, showing the same school of fish as in Figure 3.6.

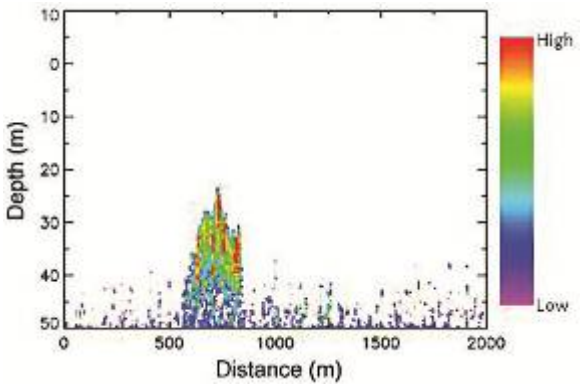

Figure 3.7. Processed data from the right side of Figure 3.6, showing the fish school between 25 and 40 m depth. Relative backscatter strength is shown by the colour bar at the right.

Several comparisons between lidar and ship-based echosounders have demonstrated good agreement in the relative backscatter levels from fish. Churnside *et al*. (2003) made direct comparisons of the same fish schools off the west coast of Florida and observed a correlation of 0.99. A study in the Gulf of Alaska compared acoustic and lidar transects with a difference of up to four days between them, and found correlations ranging from 0.55 to 0.59 with the four acoustic frequencies (Brown *et al*., 2002). A similar study in the Atlantic around the Iberian Peninsula produced a similar overall correlation of 0.55. That study found that the correlation depended on

the type of fish aggregation: from 0.50 for scattered fish to 0.93 for pelagic layers (Carrera *et al*., 2006). A zooplankton comparison in Prince William Sound, Alaska, produced a correlation of 0.78, and demonstrated the importance of selecting the threshold level correctly in order to separate zooplankton from phytoplankton (Churnside and Thorne, 2005).

Two of the most challenging problems in acoustics, namely target identification and target strength (TS), also apply to lidar. When fish schools are visible from aircraft, they can generally be identified (e.g. Figure 3.5). The depolarization of the return signal can also provide information, in a similar fashion to multifrequency information in acoustics. More commonly, some directed sampling will be required, as is done in acoustic surveys. TS measurements on live fish have only been attempted for sardine (*Sardinops sagax*; Churnside *et al*., 1997), mackerel (*Scomber scombrus*; Tenningen *et al*., 2006), and menhaden, although several other species have been measured using thawed fish (Churnside and McGillivary, 1991). One encouraging feature of lidar TS is that it is much less sensitive to fish orientation than acoustic TS (Churnside *et al*., 2001b), at least for typical echosounder frequencies above 38 kHz.

Three problems in lidar surveys not shared by acoustics are: depth coverage, scanning, and eye safety. Unlike a typical echosounder, lidar can detect fish right up to the surface in calm seas. In strong winds, breaking waves produce a bubble layer in the top few metres of the ocean that cannot be separated from fish signals. However, it is unlikely that fish will be right at the surface under these conditions, because of the strong turbulence they would experience. The more serious problem is that lidar is restricted to the top few tens of metres, depending on water clarity. In open-ocean waters, penetration to below 50 m is possible. In coastal waters, 20–30 m is more common. In very turbid waters, penetration may be limited to ≤10 m. In recent surveys in Chesapeake Bay, the depth penetration varied from 7 to 15 m (Churnside *et al*., 2011a). Scanning adds complexity and expense, but can increase the effective swathe width to approximately twice the aircraft altitude. However, for fish that form large schools or school groups, scanning does not increase the detection probability (Lo *et al*., 2000). A lidar system can easily be made eye-safe for humans at the ocean surface by diverging the laser beam. A 5 m spot on the surface suffices for a 10 ns 100 mJ pulse. This same level is also safe for marine mammals (Zorn *et al*., 2000).

Airborne lidar is ideal for epipelagic species such as sardine, mackerel, and menhaden that occupy large areas. This technique can capture synoptic views that are impossible from a ship. At the same time, aerial surveys are most effective when combined with acoustics and sampling from a ship that is directed to the areas of greatest interest using the lidar data. Airborne lidar is also well suited to measurements of the distribution of zooplankton (Churnside and Donaghay, 2009), although ground-truth for species composition is particularly important in this application.

3.3 External lighting

Light, whether natural or artificial, is a requirement for all optical technologies. The distance at which targets can be seen in water depends on the absorption and scattering properties of the water and the quantity of suspended particles in the water (Gilbert and Pernicka, 1967). Absorption is the irreversible loss of luminous energy as light propagates through the water. Although irreversible, methods are being developed for correcting an image in post-processing based on *in situ*

absorption (e.g. Figure 3.8). Two common ways to alleviate or minimize the effects of absorption are: to increase the amount of light, or to increase the sensitivity of the camera (receiver). Scattering of light by suspended particles is the other factor affecting the amount of light that can be used for acquiring a clear image. Suspended particles (e.g. turbidity) will scatter light, or redirect it in three dimensions, and essentially diffuse it so that the contrast between the target and background decreases and the target becomes imperceptible.

The location of light relative to the camera and the type of light (e.g. monochromatic, full spectrum, strobe) will dictate how far clear images can be acquired (Jaffe *et al*., 2001; Kocak *et al*., 2008). Short ranges can be imaged with the light source next to the camera, whereas longer ranges require the separation of the light source or the use of more complicated configurations and light sources, such as lasers and range-gated or synchronous-scanning technology.

Artificial light can be generated directly for the measurements, as in lidar, laser-line scanners, optical counters, or other laser-based technologies (see elsewhere in this chapter). For still-camera and video technologies, the camera requires a minimum level of illumination in order to generate a useful image. Light levels at or below the minimum produce suboptimal or useless images (see Section 3.1). Light levels can also be too high and may cause "washing", or "whitening", of the image, in which objects within the image become all-white. Using natural light has the advantage of requiring no additional power and no mechanical structures for mounting lamps. The additional power-draw and structures may not be an issue for a towed vehicle that can be connected to the ship's power, but it can be a problem for autonomous vehicles that need to have low drag and have a limited power supply. Unfortunately, natural light levels sufficient for electronic imaging are not present at depths much greater than 50–100 m in the ocean, and they are not available at night.

Power and spectral requirements are the two main considerations when selecting a light source. All light sources require power, but some, such as light-emitting diode (LED) technology, require considerably less energy than others. The spectral bandwidth is also a major consideration. To obtain true-colour images, full-spectrum light is required so that the image is as close to a true-colour representation of the objects as possible. This is often required for object identification (Bazeille *et al*., 2007). A drawback of full-spectrum light, or "white light", is that the colours (wavelengths) are differentially absorbed in the water. If the images are acquired close to the camera, the absorption is small and may be ignored. However, if the images are acquired farther from the camera, some wavelengths are absorbed, and the object colour will be represented incorrectly. This is especially true of the shorter wavelengths. One option is to correct the colours in the image by measuring or estimating the absorption *in situ* and then correcting the colours in the image (e.g. Gallager *et al*., 2005).

Initially, light sources were based on gas-filled elements/bulbs or conventional filament lamps. Halogen lamps have been popular during the past decade. Halogen produces a wide-spectrum light, which is advantageous for colour imaging. The disadvantages of halogen lamps are their high power requirements and the high temperatures that they generate, which require them to be operated only underwater. Although these lamps have been the mainstay of underwater light sources, within the past few years, LEDs are becoming the preferred light source. The advantages of LED lamps are: longevity, rapid on–off switching (i.e. strobe), dimming without changing the emitted colour, electrical efficiency, and monochromatic or wideband colour

selection (Olsson *et al*., 2007). For monochromatic emission, specific wavelengths can be chosen and LEDs made to emit at those wavelengths, as opposed to coloured LED lamps, and their cost is currently higher than conventional filament or gas-discharge lamps. Continued development of LED lamps should reduce the cost over time.

High-intensity-discharge (HID) technology is also being used for underwater lighting. These lamps can produce intense light with relatively low power requirements, although they can be expensive.

Artificial light works well in clear water, or when there are few suspended particles. Suspended particles will scatter the light, and an increased amount of light can make it difficult to acquire a clear image (think of using a motor vehicle's "high-beams" on a foggy night). Polarizing the transmitted and/or received light is an alternative means of improving image quality. Polarizing light reduces glare in an image and can improve the contrast between target and background significantly. Circular polarization (Gilbert and Pernicka, 1967), or other active methods of illumination using polarized light (e.g. Tyo *et al*., 1996; Walker *et al*., 2000), as well as passive methods (e.g. Chang *et al*., 2003) of polarizing ambient light, significantly increase image contrast in turbid water. Methods are even being developed for very thin (i.e. nanoscale) layers for CCD and CMOS sensors to polarize the incident light (Gruev *et al*., 2007). Polarizing techniques have also been used for stereoscopy (e.g. Osborn, 1997) applications, but these are used after images have been acquired.

Even with artificial light, colours in an image can be attenuated by the environment. Colour is becoming recognized as the key component in identifying objects in images (Ahlen and Bengtsson, 2005; Gallager *et al*., 2005; Armstrong *et al*., 2006). Underwater imagery is affected by non-linear attenuation of the visible spectrum (i.e. Beer's Law); thus most underwater images tend to be saturated in the blue–green region (Figure 3.8). Typically, image colour correction is done by either predicting or measuring attenuation across the colour spectrum and then modifying the image based on the range to the target and the attenuation coefficient. Attenuation can be measured *in situ* using spectrometers or estimated if the optical properties of the water (e.g. turbidity) are known. When done properly, image quality is improved significantly, and accurate identification of objects is possible (Figure 3.8).

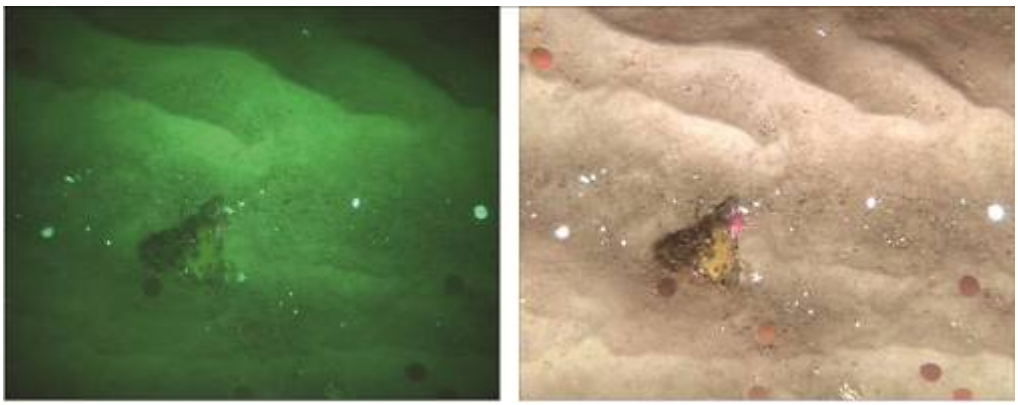

Figure 3.8. (Left) An image of a rock and scallops on sand prior to colour correction; (right) the same image after colour correction. (Image courtesy of H. Singh, Woods Hole Oceanographic Institution.)

3.4 Optical counters

When collecting and processing acoustic data from surveys for biomass estimates of plankton or fish populations, one of the most important tasks is the proper

identification of species and size distributions. It is, therefore, necessary to conduct frequent biological sampling of the populations, which is often time consuming and expensive. Acoustical identification methods are being increasingly used to reduce sampling requirements, but acoustical methods alone have only been partly successful. This section describes some optical methods, developed for automatic or semi-automatic species identification of small plankton species, that could be scaled up for use as supplements for acoustical identification methods.

3.4.1 Fish counters

An early electronic device using a photocell to count small marine organisms was developed in the 1960s (Mitson, 1963). Since about the same time, photocells have been used to count migrating fish in fish ladders. Counters were usually custom built, and no commercial supplier of complete systems of the early designs has been located. Generally for these early systems, a step counter was activated when a light beam was interrupted. Several problems were known to occur with systems using a single photocell; among other things, they were very sensitive to debris. Later systems using two or more photocells, arranged so that only objects passing upstream would trigger the counter, were less sensitive. Some of these systems are still in use. A significant basic weakness in these photocell systems is that the data output only encompasses the number of registrations, and possibly the direction of the (presumed) fish. Quality controls of derived data must be done in parallel by manual observation, unless the system is supplied with an external camera triggered by the photocell counter.

During recent decades, a more sophisticated photocell-based type of fish-counter system was developed in Norway (Larsen *et al*., 1995) and in Iceland (Shardlow and Hyatt 2004; Porcella and Nishijima, 2006). In this system, several photocells are installed in one of the vertical inner sides of a rectangular frame. The photocells are recessed in order not to be activated by stray light. On the other (facing) inner side of the frame, corresponding to the photocells, IR lamps (LEDs) are arranged. Each LED and its corresponding photocell is repeatedly, and in strict sequence, activated during a split second. In this way, a simple profile of a passing object that, by and by, masks some of the photocells, can be calculated. Taken together, it is possible to estimate individual body length and weight, and even to determine the species from this profile. Also, direction and velocity of the passing object can be calculated. This fish counter was first developed for fish-farming purposes, but has since been adapted for use in fishery management and research. Currently, it is often used for counting migrating salmonids. The main supplier is Vaki Aquaculture Systems Ltd, Iceland. Other suppliers include Storvik A/S, Norway, and Aqua Pro Counter AB, Sweden, as well as smaller suppliers. The inner diameter of the frame of the optic counter is limited by the range of the IR light, ca. 0.5 m. The performance of the optic counter depends on prudent installation. Water whirls and bubbles may disturb function. Ideally, the water flow that passes the counter frame is laminar, fairly deep, and free from debris. It is also important that only a smaller part of the total water flow passes through the frame. Several frames can be mounted next to each other to handle larger water flows. This type of fish counter is most common in Iceland, Sweden, Ireland, UK, USA, and Denmark.

There are several other techniques for fish counting using visual information. One is a manual system where monitoring takes place by direct observation through a window, sometimes assisted by video techniques (Trefethen and Collins, 1975; Wagner, 2007). These systems are usually custom-built for each site. They are used in

some large water bodies in the USA, Canada, and France. One semi-automatic type of system for fish counting involves closed-circuit television and a simple image-processing system that saves potentially valid sequences for later manual analysis (Lauver, 2006). Another type of system uses mechanical triggers to save video sequences (Lamberg *et al*., 2001). This type is, at present, the most common one in Norway. Fully automatic computerized image-processing systems are few; one is marketed by Poro AB, Sweden. Generally, technology for image processing is advancing rapidly and may offer new approaches (e.g. Morais *et al*., 2005).

A different technology, based on electric conductivity and first described by Lethlean (1953), was developed in the UK and Ireland for counting upstream-migrating Atlantic salmon (*Salmo salar*). The principle for all resistivity (or rather conductivity) counters is that a fish has a lower electrical resistance than the (fresh) water in which it is swimming. When a fish swims over an arrangement of electrodes, the conductivity between electrode pairs will dip for a moment. The number of fish and the swimming direction is registered by a step-counter. The information is limited, and a resistivity counter may sometimes be used to activate a camera or video system to secure an image of fish that pass over the electrodes (e.g. Smith *et al*., 1996). The principle of conductivity for counting fish is utilized in a large number of detection systems in Canada, the UK, and the USA. A fairly recent evaluation of a system of this kind was made by Forbes *et al*. (1990).

There are several acoustic systems for counting fish that do not depend on visual information, and new ones are being developed (Menin and Paulus, 2003; Holmes *et al*., 2006). Even so, visual systems are often used for confirmation of performance (Holmes *et al*., 2006).

A comprehensive review of optic, resistive, and hydroacoustic fish counters in Scotland was recently published by Eatherley *et al*. (2005).

3.4.2 Plankton counters

Several different principles are used for plankton counting and species identification. Roff and Hopcroft (1986) published a description of a semi-automatic system consisting of a microscope, microscope drawing tube, and digitizer. They describe their motive as follows.

> It is now commonplace to derive weight estimates of organisms from their linear dimensions by some power function (e.g. McCauley, 1984). Because length–weight relationships are power functions, small deviations in length measurements produce considerable changes or variance in the dependant weight estimates. Dimensions of individuals must be measured with the highest possible accuracy and precision, and preferably repeated, or several body measurements should be made (McCauley, 1984).

The special advantage of their system was that a light spot on the digitizer cursor was projected backwards through the drawing tube and microscope objective onto the organism to be measured instead of measuring a screen image with a cursor. This method avoided most of the problems of potential measurement errors caused by distortion and bias in the camera and/or screen display.

A more advanced and automated system is the FlowCAM system designed by Sieracki *et al*. (1998), which combines particle counting triggered by either light scattering or fluorescence, imaging of the triggering particles, and automatic analysis of the particle images, giving particle properties and identification of particles

according to pre-prepared particle-property categories determined by, for example, taxonomy experts. The block diagram of the present version of the FlowCAM system from Fluid Imaging Technologies is shown in Figure 3.9.

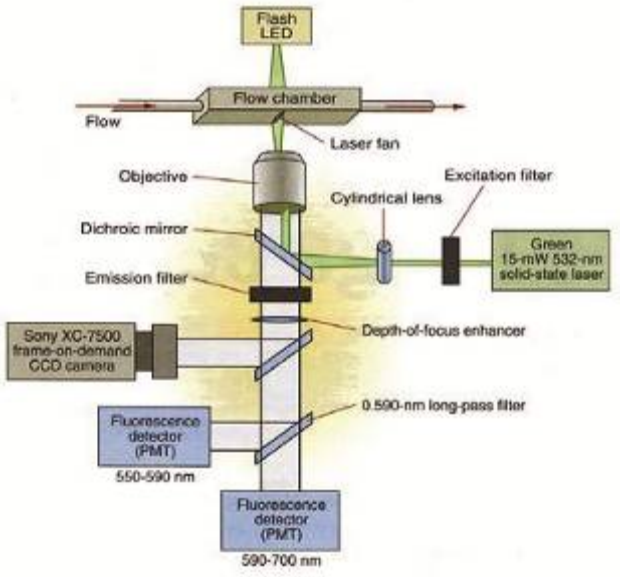

Figure 3.9. Block diagram of FlowCAM particle counter.

The liquid to be analysed is drawn into the flow chamber at a constant speed by a peristaltic pump, which means that the length of long particles can be estimated by the temporal length of the fluorescence signal. Flow chambers of different sizes can be mounted, and microscope objectives with different magnifications can be used to accommodate measurements of various particle-size ranges. The system has been used for recognition and enumeration of harmful algae, such as the red-tide dinoflagellate (*Karenina brevis*; Buskey and Hyatt, 2006), or to give early warning of algal blooms in a drinking-water reservoir (Reilley-Matthews, 2007). DTU Aqua (the National Institute of Aquatic Resources, Technical University of Denmark) uses a field-adapted version of the instrument for different investigations, such as estimating seasonal variations and possible food limitations in the compositions of plankton communities in an estuary, and laboratory experiments looking at the effect of various scenarios of ocean acidification on plankton species composition (Nielsen *et al*., 2010). Furthermore, the FlowCAM has been used in experiments demonstrating that the cell count drops drastically for some plankton species, when the samples are treated with Lugol's fixative solution.

A system for *in situ* plankton counting is the laser optical plankton counter (LOPC) described by Herman *et al*. (2004), which is an enhanced version of the original optical plankton counter (Herman, 1988, 1992). The principle of this instrument is shown in Figure 3.10.

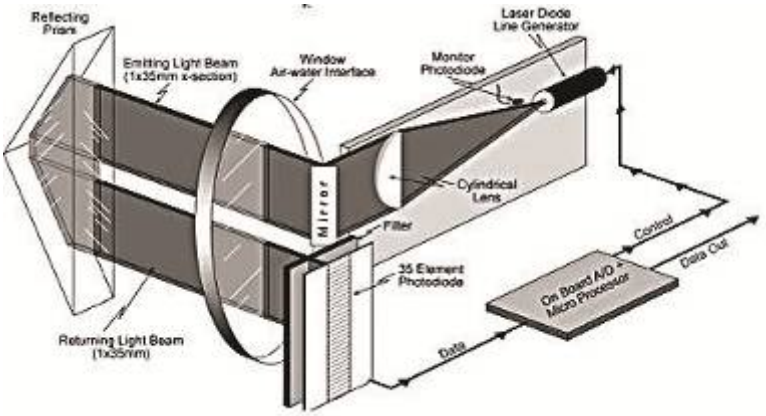

Figure 3.10. The operating principle of the LOPC, showing the formation of a ribbon-like laser beam of cross section 1 × 35 mm. The region between the window and prism (left) represents the sampling volume. Doubling back the beam via a prism eliminates the need for a second receiver-pressure case. (Source: Herman *et al.*, 2004.)

The main advantage of the new system is that, owing to a flatter beam and a larger number of detectors, the resolution has radically reduced the risk of particle coincidence, i.e. measuring two or more particles as one. This means that much higher particle concentrations can be measured than before. The instrument makes it possible to count both small and large particles in the range of ca. 100–35 000 μm and to carry out shape analysis on particles larger than ca. 1500 μm, as well as some identification of the larger particles.

There was a proliferation of *in situ* imaging systems during the late 1990s and early 2000s (Benfield *et al.*, 2007). One of the major advantages of imaging systems is that they are able to collect images of organisms without physically contacting them, which is an effective way of sampling fragile organisms, such as gelatinous zooplankton species. In addition to underwater systems, laboratory packages that can process preserved samples have been developed to speed up processing of current or historical samples (Grosjean *et al.*, 2004). Of course, sampling is only part of the battle. These systems can collect gigabytes of data, and the images need to be processed in order to provide taxonomically explicit estimates of abundance and size. This is an area of intense interest and combines the fields of biology, machine vision, pattern recognition, and statistics to generate spatial and temporal maps of taxon- and size-based zooplankton distributions accurately and efficiently. Some of the issues in the grand challenge of identification are: (i) plankton are morphologically heterogeneous (i.e. one technique will not work for all plankton); (ii) the medium has a variety of non-living targets that are similar in size and density (e.g. marine snow, bubbles); (iii) plankton vary in size by orders of magnitude; (iv) morphology changes during ontogenetic development; (v) because plankton are three-dimensional objects, taxonomic features may not always be visible, owing to optical resolution and/or orientation; and (vi) several different organisms may be present or collocated in space, so that they must be separated before being identified (Benfield *et al.*, 2007). The basic steps for image processing are importing the data (importation), feature selection and extraction, training-set production, classification, training, and error analysis, and there are numerous methods and software packages for each of these steps (Benfield *et al.*, 2007). Finally, the information must be shared with the broader community through web-based applications and databases such as OBIS (Ocean Biogeographic Information System) and IOOS (Integrated Ocean Observing System), or other partners in the Global Ocean Observing System (GOOS).

3.5 Laser line scanning

Laser line scanning (LLS) sweeps a narrow beam of light (laser) back and forth to make images of objects in the water column and the ocean bottom (synchronous scan; Figure 3.11). Because LLS uses light, the useable range of the system can be inhibited by attenuation and backscatter, so the instrument needs to be towed near where the observations are required. For most fisheries or environmental applications, the LLS system is housed in a towed vehicle, towed near the seabed. The most common configuration is to sweep the laser perpendicular to the vehicle's direction of travel so that the resulting swathe is much wider than the dimensions of the towed body. The total swathe width depends on the angular range of the sweep and the height of the instrument above the seabed, so the greater the altitude above the bottom, the greater the swathe width. However, the maximum range is ultimately limited by attenuation of the light (laser beam). Kocak *et al*. (2008) showed that viable images can be obtained at up to six attenuation lengths in turbid water.

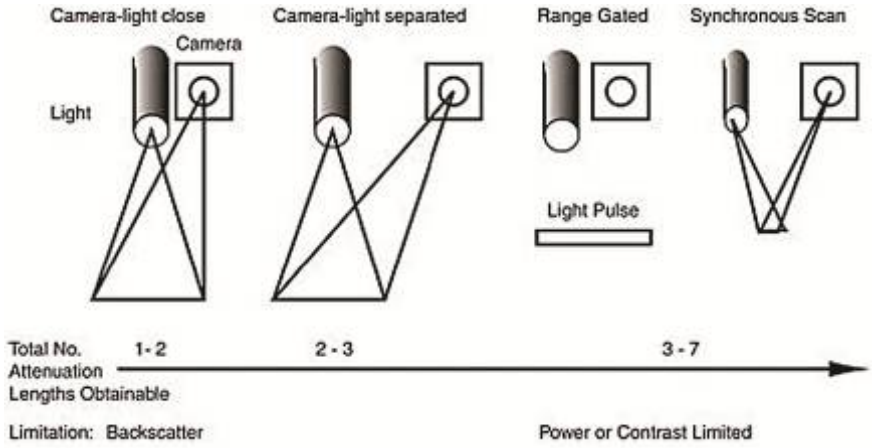

Figure 3.11. Classification of underwater image collection systems. LLS is an example of a synchronous scan. (Reprinted from Jaffe *et al*., 2001.)

As with any instrument that forms a "swathe" to be surveyed, there is a trade-off between maximizing swathe width (increasing sample area and minimizing sampling effort) and getting the highest resolution. As the distance from the instrument increases, the beam size increases; thus the footprint, or area illuminated, increases and, hence, the resolution decreases (larger footprint = lower resolution). The resolution can be increased by decreasing the beam width or by towing the instrument closer to the seabed. Decreasing the beam width is the best option because the LLS can be towed farther from the bottom, but technological limitations do not permit the formation of very narrow beams. Monochromatic light with wavelengths in the range of 450–550 nm has the least attenuation in seawater, and LLS systems utilize this by generating laser beams with wavelengths (blue–green) in this range (Rhoads *et al*., 1997). For a system with an angular sweep range of 70°, as in the Northrop Grumman SM-2000 Laser Line Scanner (blue–green laser, Nd:YAG @ 532 nm), a typical altitude is 45 m, which in clear water results in a swathe width of ca. 63 m and a resolution of 3 cm. However, as turbidity increases, the maximum altitude needs to decrease in order to compensate for greater attenuation; the swathe width decreases proportionally, which is detrimental to coverage, but can be advantageous for resolution. For example, the SM-2000 LLS system has a resolution of 0.2 cm at a range of 3 m (Yoklavich *et al*., 2003).

The most common application of LLS in fisheries is mapping and classification of the seabed. This information is often used in characterizing the demersal and benthic habitat of fish and invertebrates that live in, on, or near the ocean bottom. For example, the SM-2000 LLS system imaged biogenic objects at sufficient resolution to identify organisms, such as sea anemones, sea pens, and drift kelp (Figures 3.12 and 3.13; Yoklavich *et al*., 2003). This level of taxonomic detail is difficult to achieve with acoustic instrumentation. An advantage of LLS systems over camera or video imagery is that the swathe width is often 1–2 orders of magnitude wider for the LLS. Although the resolution is good, it is not as fine as that obtained with camera or video technology, and this limits the ability to identify small organisms, and many fish or macroinvertebrates, to species. However, cameras need to be very close to the subject if they are to make full use of the available resolution in even moderately turbid water. The combination of stand-off distance, swathe width, and resolution of an LLS system cannot be matched by other underwater imaging systems.

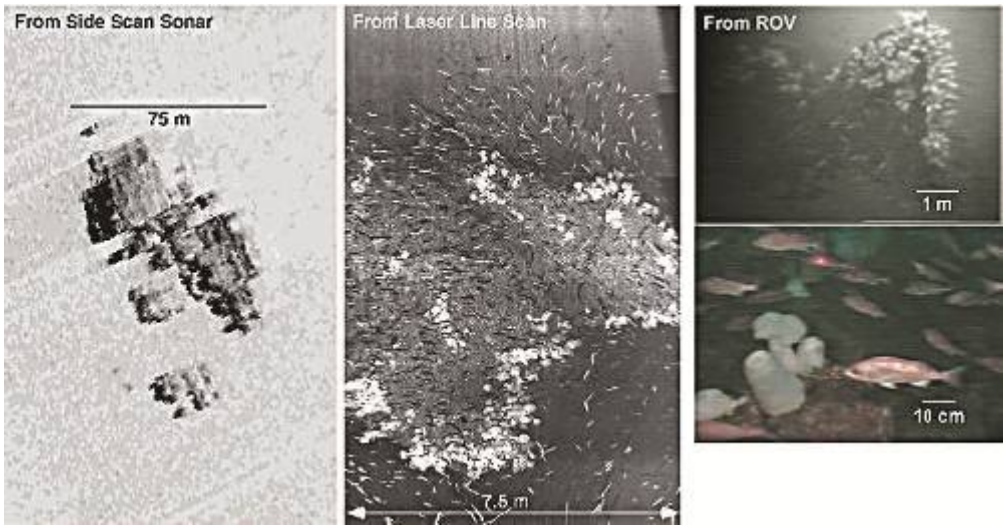

Figure 3.12. (Left) Sidescan sonar image of a large isolated rock outcrop outside the Big Creek Ecological Reserve at ca. 100 m water depth; (centre) Laser-line scan image of a large group of fish around an isolated rock outcrop covered with white sea anemones inside the Reserve at 60 m water depth; outcrop is estimated to be 4 m high; (right) ROV video images of a large group of young bocaccio (*Sebastes paucispinis*) and widow rockfish (*Sebastes entomelas*) around an isolated rock outcrop inside the Reserve at 60 m water depth; outcrop is estimated to be 5 m high. (Images reprinted from Yoklavich *et al*., 2003.)

Using monochromatic light is advantageous for data acquisition and image processing, but black-and-white images lack additional information that could be useful for target classification and identification. A multispectral LLS system was developed in the late 1990s to provide multispectral scans, and showed promise for improving identification of targets (Coles *et al*., 1998). In addition to these instruments, a four-channel LLS with an added fluorescence channel (fluorescent imaging laser line scanning, or FILLS) has been useful for mapping corals (Jaffe *et al*., 2001; Mazel *et al*., 2003). These monochromatic, multispectral, and FILLS systems have not been utilized to their full potential, but with renewed interest in ecosystem monitoring and essential fish habitat, they may gain more popularity and find increasing use in research and development.

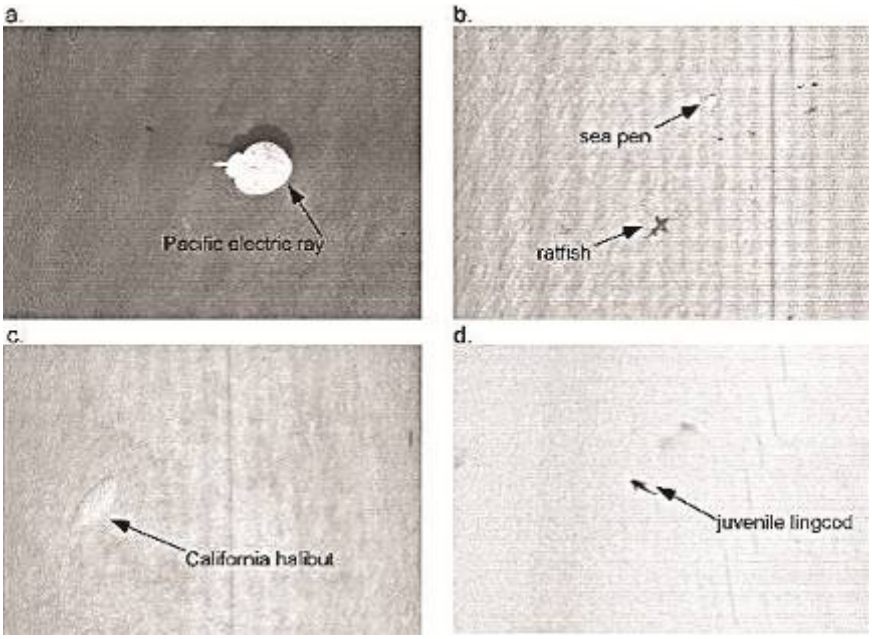

Figure 3.13. Laser-line scan images of: (a) Pacific electric ray (*Torpedo californica*), swathe width 4.0 m; (b) sea pen (order Pennatulacea) and ratfish (*Hydrolagus colliei*) in water depth 90 m (based on swathe width, fish is ca. 40 cm in length); (c) California halibut (*Paralichthys californicus*), swathe width 4.3 m; and (d) juvenile lingcod (*Ophiodon elongatus*) over sand bottom (based on swathe width, fish is ca. 20 cm in length). Fish identification is based on LLS image profile and fish observed or collected in the vicinity. (Images reprinted from Yoklavich *et al.*, 2003.)

3.6 Range-gated lasers

One of the difficulties in imaging objects in the ocean is that seawater tends to be full of small particles, and scattering from these particles between the camera and the object obscures the image of the object. As early as 1967, less than 10 years after the first laser demonstration, improved image quality was demonstrated using a range-gated laser to view an underwater target (Heckman and Hodgson, 1967). The basic principle is that a short laser pulse is used to illuminate the object. A camera with a very fast shutter (typically an ICCD) is timed so that the shutter does not open until the object is illuminated. Thus, the scattering from particles in front of the object do not affect the image. This type of system has been used for both underwater (Fournier *et al.*, 1993; He and Seet, 2001) and airborne (Ulich *et al.*, 1997; Cadalli *et al.*, 2002) imaging of fixed objects. In a variation, the shutter is timed to open after the pulse has passed the object, so that the object appears as a shadow against the light scattered by particles beyond it.

Three-dimensional images are possible by using sequential range-gated images (He and Seet, 2004; Busck, 2005). Another approach uses a streak camera to map the time of the laser-pulse return onto one axis of an imaging array and the position perpendicular to the flight track onto the other axis (McLean, 1999; Osofsky, 2001). Thus, each image from the array is a vertical slice through the water, and successive images along the flight track build up a full-volume image, rather than a simple two-dimensional image. Another way to obtain three-dimensional information is to scan an area with a lidar system that provides return as a function of distance. The three-dimensional approaches tend to be more expensive to implement, both in terms of initial cost and efficiency with which the laser energy is used.

The primary application of airborne imaging of underwater objects has been the detection of mines; however, attempts have also been made to use both ICCD (Oliver and Edwards, 1996) and streak-camera (Griffis, 2000) imaging systems for the detection of tuna (*Thunnus* spp.). There was even an attempt to market a range-gated imager to the tuna industry for detection of fish that were not associated with dolphins.

An ICCD system has also been used to capture images of adult salmon (Churnside and Wilson, 2004). Figure 3.14 is an example from the salmon study. The NOAA FLOE (a profiling backscatter lidar) was equipped with a gated ICCD camera with a second-generation, micro-channel plate intensifier and a P20 phosphor. Using the surface return from the backscatter lidar as a reference, the exposure depth was maintained at a constant 3 m, despite aircraft altitude fluctuations. The CCD element has a usable array of 756 × 485 pixels, which produced a resolution on the surface of 0.59 cm at the nominal aircraft altitude of 150 m. The contrast-to-noise ratio in this image is ca. 3.4, which was increased to 16.4 with matched-filter image processing.

Figure 3.14. Range-gated-laser image of adult pink salmon (*Oncorhynchus gorbuscha*) near Kodiak Island, Alaska. Imaged area is ca. 3.8 × 2.8 m.

Range-gated-laser imaging systems operating in the water generally operate in a direct-illumination mode to obtain images of the seabed (Fournier *et al*., 1993; Busck, 2005). This means that the image contains information about the distribution of reflectivity across the scene, not just object silhouettes. It is possible because the distance from the camera to the object is known. An example of the improvement over ambient-light imaging is shown in Figure 3.14. One difference between underwater and airborne images is that multiple laser pulses can be averaged in a slow-moving underwater camera to reduce the laser speckle noise that is evident in Figure 3.15. Aircraft motion precludes this type of averaging.

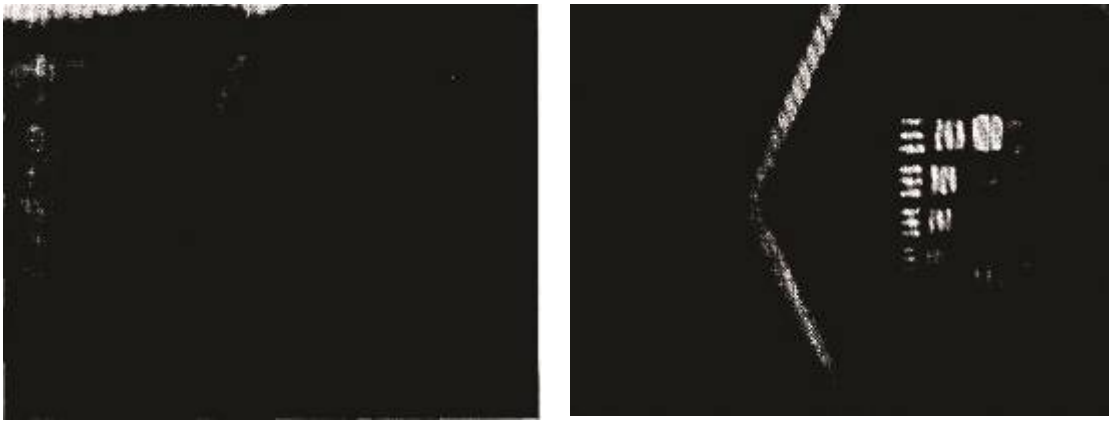

Figure 3.15. Underwater image of a target at a distance of 5 m: (left) ambient illumination; (right) range-gated-laser illumination. (Source: Fournier *et al.*, 1993.)

Airborne applications of range-gated-laser imaging can be useful for relatively large fish located very close to the surface. In this case, information about the size and type of fish is readily available. As depth increases, the contrast-to-noise ratio and quality of the images decrease dramatically. Various simulations (McLean and Freeman, 1996; DeWeert *et al.*, 1999; Zege *et al.*, 1999, 2001) suggest that the simpler range-gated-laser approach is probably the best for airborne applications. As the depth of fish is generally not known, the shadow mode is recommended. In this mode, any fish above the selected range gate are detected, and the only requirement is to set the range gate deeper than any expected fish. An attempt to use the direct-illumination mode will fail to detect fish that are deeper than expected.

3.7 Holography

Holographic cameras have been used primarily for plankton studies, first in the laboratory (Knox, 1966) and then *in situ* (Katz *et al.*, 1999; Malkiel *et al.*, 1999). This technology is most suitable for capturing images of organisms measuring a few micrometres to a few hundred micrometres in size, so it is not used to study fish directly.

The principles of holography are straightforward. Laser light scattered from an object and unscattered light from the same laser are allowed to fall on a recording medium. The interference between them produces an intensity pattern that is related to the optical field in the plane of the recording medium. If that medium is film, laser illumination of the film will produce a diffraction pattern that is the same as the pattern of light originally scattered by the object. Thus, the reconstructed hologram looks like the original three-dimensional object within the field of view subtended by the film. More recently, film has been replaced by digital imaging (Malkiel *et al.*, 2003; Sun *et al.*, 2007, 2008), and the reconstructed hologram is calculated from the recorded intensity pattern.

For underwater holographic cameras, in-line geometry is preferred for its simplicity. A collimated laser beam is propagated through the water to the digital image array. Light scattered by objects in the water between the laser and the detector array interferes with the unscattered light to form the hologram. In practice, a lens system in front of the detector array can be used to match the beam to the array size, but this is set to recollimate the light and not form an image on the array.

The primary advantage of holography over direct imaging is the ability to simultaneously image small objects over a relatively large volume. Malkiel *et al*. (1999) provide the following numerical example:

> A planar imaging system which can resolve 20 μm can do so over a depth of field, D, equal to d^2/λ, where d is the resolution and λ is the wavelength of the light. For $\lambda = 694$ nm (the wavelength in our present system), and $d = 20$ μm, the depth of field is 0.6 mm. In comparison, a hologram providing similar resolution can have a depth of field over a 100 times larger and, unlike a scanning planar system, it can record it instantaneously, which is a necessity for three-dimensional velocity measurements.

The digitally recorded hologram can be reconstructed numerically to provide the image that would have been seen with a monochromatic imaging system focused at any distance within the volume, i.e. require coherent illumination (lasers); Sheng *et al*., 2007. This processing can require a significant amount of time, but the power of portable computers is increasing rapidly.

3.8 Hyperspectral imaging

Hyperspectral cameras generate images with much more spectral information than the three spectral bands of red, green, and blue employed in the human visual system. There is no standard regarding how much spectral information is required to be considered hyperspectral, but approximately tenfold more, or 30 spectral bands, is a reasonable definition. The data comprise a three-dimensional array, with two spatial and one spectral dimension, often called a "hyper-cube". Spectral resolution is typically ≤10 nm. Most of the hyperspectral cameras in use, like the portable hyperspectral imager for low-light spectroscopy (PHILLS; Davis *et al*., 2002), were developed by the users. Most are airborne, although an orbiting imager, Hyperion (Pearlman *et al*., 2003), with a 30 m surface resolution, has been operating since 2000.

In a typical hyperspectral imager, a scene is imaged onto a narrow slit, which selects a narrow slice across the scene. A dispersive element behind the slit spreads the light into its spectral components in the plane normal to the slit. A detector array, commonly a CCD array, detects the light. Each column of the image then represents the spectrum from a single pixel in the final image. Each row represents a pixel along one axis of the image. Pixels along the other axis of the image are obtained sequentially, either in "pushbroom" fashion, as the platform moves, or by scanning the image of the scene across the slit.

The primary applications for hyperspectral imaging have been terrestrial (Kalacska *et al*., 2006; Oppelt and Mauser, 2007). These include: characterization of land use, identification of plant type and condition, and identification of mineral characteristics. Commonly, the spectrum measured by each pixel is compared with a spectral library. A spectrum or linear combination of a few spectra from the library is chosen that most closely matches the measured spectrum. Terrestrial applications have the advantage of relatively high reflectance compared with the ocean and a relatively broad spectrum. Conversely, marine applications must deal with low reflected light levels and a narrow spectral band centred in the blue–green.

Despite the limitations, hyperspectral imaging has found application, especially in relatively shallow water. Dierssen *et al*. (2003) used airborne hyperspectral imaging to simultaneously obtain the distribution of seagrass and the water depth in the Bahamas banks. This type of simultaneous inversion is typically necessary because

the observed spectrum is a combination of the reflectance spectrum of the bottom and the spectral absorption through the water path. Figure 3.16 presents an example of a colour image and the spectra at three pixels. The effects of bottom type and water depth are both clearly seen in this example.

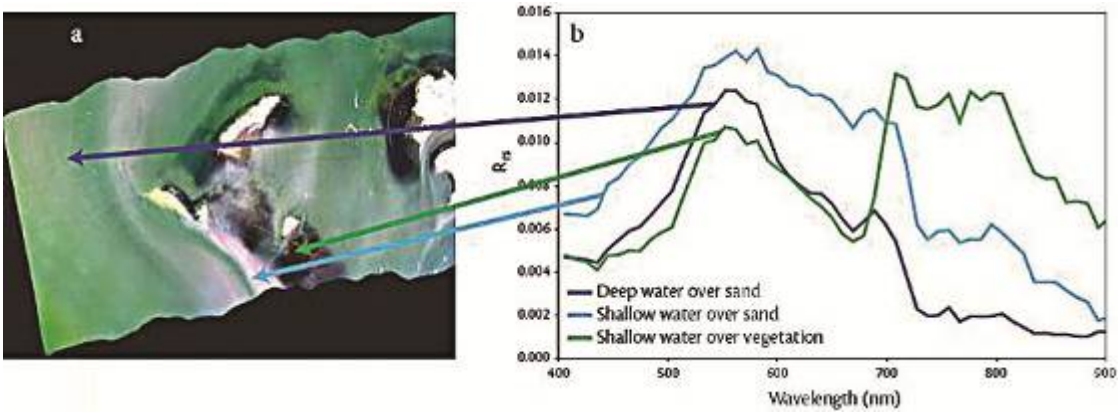

Figure 3.16. (a) A portion of PHILLS^{-1} image of an area in Barnegat Bay, New Jersey, collected on 23 August 2001, and illustrating a variety of spectrally different bottom types. (b) Remote-sensing reflectance (R_{rs}) spectra at the water surface for selected points in (a) derived from the portable hyperspectral imager for low-light spectroscopy (PHILLS) data. (Source: Philpot *et al.*, 2004.)

In-water hyperspectral measurements are still affected by depth-dependent spectral characteristics of the illumination that can be measured directly (Joyce and Phinn, 2003). Mishra *et al*. (2007) have used a similar approach to map bottom type in a coral-reef environment.

Hyperspectral imaging on a global scale has been realized with the Hyperion instrument launched in November 2000, on NASA's Earth Observing-1 (EO-1) satellite. Less than a year later, the European Space Agency (ESA) launched the compact high resolution imaging spectrometer (CHRIS) on the PROBA (Project for On-Board Autonomy) satellite.

4 Integration

James Churnside, Pierre M. Clement, Michael Jech, Mark R. Shortis, and Stephen J. Smith

Most factors involved when integrating and deploying optical systems are common to a wide variety of instruments, and will not be discussed here. There are a couple that deserve mention, however, because of the rather special requirements of optical systems, particularly underwater imaging systems.

4.1 Platforms

There are two general categories of platform for the optical systems discussed in this report: aircraft and in-water platforms. In both cases, unmanned systems are becoming more capable and are likely to find wider use in future.

It is difficult to imagine a type of aircraft that has not carried an optical system of one sort or another. The most common system is a camera of some type. At one extreme is a tiny camera on an unmanned aerial vehicle that is small enough to be launched by hand. At the other is a complex, multi-instrument system on a large surveillance aircraft. The factors that affect the choice of aircraft and flight operations are relatively straightforward and will not be considered further.

Similarly, there is a wide variety of in-water platforms that have been fitted with optical systems. These include surface vessels, towed vehicles (Dalen and Bodholt, 1991; Dalen *et al*., 2000, 2003), platforms fixed to the bottom, moorings, packages that are lowered on a cable (Strong and Lawton, 2004; Vandermeulen, 2007), drifters, manned submersibles, and autonomous underwater vehicles (AUVs). The number and variety of systems are far too extensive to cover here, but one example will be provided.

TowCam is a commonly used name for a towed-camera system (see also Rosenkranz *et al*., 2008, for description of HabCam towed-camera system). The TowCam developed by the Canadian Department of Fisheries and Oceans (Figure 4.1) is a towed, bottom-following, video and still photographic system for benthic and geological surveys (Gordon *et al*., 2007). It is towed at a speed of ca. 1 m s^{-1} at an altitude (controlled by the winch) ca. 2 m off the seabed. The maximum working depth at present is 200 m. Real-time video imagery is displayed in the ship's laboratory and on the bridge. Video imagery and navigation data are recorded for later analysis.

This system consists of a simple towed body containing a high-resolution, digital still camera and flash, a colour video camera and incandescent lamps, an acoustic altimeter, and an electronic module containing pitch, roll, and depth sensors. The unit is towed on a ¾ in, double-armoured cable (a fibre-optic cable package is being developed). A software package that was developed in-house monitors, displays, and logs the vehicle flight characteristics and sends control signals to the hydraulic system on the winch, causing it to adjust the cable length to maintain the towed body at a constant altitude above the bottom.

Figure 4.1. Canadian TowCam.

TowCam has proven to be an excellent tool for conducting general reconnaissance surveys. Major habitat features, such as sediment type, bedforms, fish, and large epibenthic organisms, including crabs, sea cucumbers, scallops, starfish, and sand dollars (greater than ca. 10 cm) can be discerned from the video imagery. TowCam does not damage the seabed and has the potential to carry other sensors. It can be used over any kind of seabed (e.g. mud, sand, gravel, cobble, boulder, bedrock), provided that the relief is relatively low. TowCam can become an excellent stock assessment tool for commercial fisheries such as scallops.

In addition to towed platforms, remotely operated vehicles (ROVs) and AUVs are becoming common for surveying localized areas. A number of applications for these vehicles, which can be used for habitat characterization and management, are related to seabed, benthic, and demersal characterization. There are a number of ROV and AUV manufacturers worldwide, and the models and capabilities are constantly improving. One of the greatest advantages of AUVs is also one of their greatest limitations: power. Vehicles tethered to a ship have essentially unlimited power, but the surface vessel must be in proximity to the vehicle. Although AUVs have much greater freedom, they must be powered by batteries or by solar or wave energy. Batteries are the most common source of power, and a variety of types are used, according to the application (e.g. Bradley *et al*., 2001). One of the largest energy sinks on an AUV is the lighting, which explains the interest in LED technology. AUVs come in a variety of sizes and shapes (Figure 4.2) and offer a variety of optical and acoustic configurations.

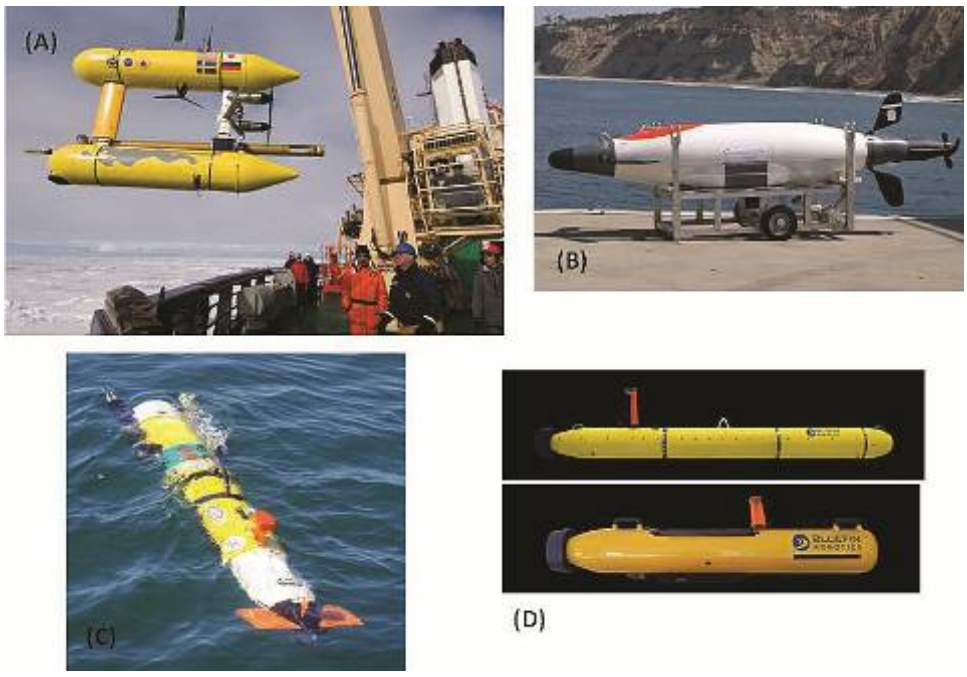

Figure 4.2. (A) SeaBed AUV (www.whoi.edu/page.do?pid=21138; image courtesy of H. Singh, Woods Hole Oceanographic Institution). (B) Fetch AUV (image courtesy of D. Demer, NOAA Southeast Fisheries Science Center). (C) Remus AUV (image courtesy of Kongsberg-Hydroid website, www.km.kongsberg.com/hydroid). (D) Bluefin Robotics AUVs (image courtesy of Bluefin Robotics website, www.bluefinrobotics.com).

4.2 Geolocation

Geolocation is the process by which the position of an instrumented vehicle system is estimated or measured in order to allow instrument data values to be attributed to parameters that define their location in a real-world geographic system. For airborne systems, the standard solution is a global position system (GPS) receiver, which is generally accurate to within 10–20 m. Differential GPS uses an additional receiver nearby to correct for some of the errors and thus to achieve an accuracy of 3–5 m. The Wide Area Augmentation System (USA) and Euro Geostationary Navigation Overlay Service (Europe) use an array of ground stations to provide correction data to an accuracy of 1–3 m. If highly accurate geolocation is required for airborne data, aircraft attitude is also needed. This is typically obtained with a gyroscopic system that measures angular acceleration in all three axes and calculates the pitch, roll, and yaw of the optical system. Angles and altitude provide the difference between the aircraft position and the footprint of the optical system on the surface.

These technologies are generally not viable for underwater systems because electromagnetic energy does not penetrate past the first few metres of the ocean surface nor propagate through the water for more than a few tens of metres. Hence, precise geolocation of underwater vehicle systems presents a unique set of challenges, particularly for autonomous or semi-autonomous vehicles (such as AUVs or ROVs) to track and/or navigate themselves. Most vehicle systems use a combination of relative positioning methods (e.g. dead reckoning, bottom tracking with Doppler, and inertial navigation systems) and absolute positioning methods (e.g. acoustic baseline systems and surfacing) to track their movement and locate the vehicle. The required degree of spatial accuracy and precision depends on the nature of the study, the instruments being used, and any associated practical constraints with obtaining the geolocation data. Budgetary and logistic constraints may

determine which tracking system (if any) is used. For example, blue-water national research vessels typically have acoustic geolocation systems, but smaller vessels or vessels of opportunity are less likely to offer this capability, and fitting of temporary systems may be cost-prohibitive or impractical. Typically, studies with a seabed focus, particularly those attempting to produce maps, may warrant the highest possible geolocation accuracy. Conversely, studies of mobile biota in the water column may only require very rudimentary geolocation information (e.g. the name of the waterbody being surveyed and instrument depth). The types of vehicle systems that can require accurate geolocation include vertically lowered and transect-towed, cable-attached systems, ROVs, AUVs, and gliders.

Dead reckoning is simply using information on the bearing and speed of the vehicle to calculate distance and direction travelled. In calm water with no currents, this method can be adequate (within approximately 10% of the distance travelled; Bahr and Leonard, 2006) for generating a cruise track and positioning the vehicle. As the seas are usually not calm and free of currents, dead reckoning alone is inadequate for applications that require highly accurate geolocation, but it is used as a first-order approximation for locating the vehicle.

For cable-attached vehicles towed along straight transects, a simple trigonometric model of the cable layback that combines heading (from vessel GPS), wire out, and vehicle depth can be used to estimate the position if more accurate geolocation systems are not available. Relative changes in position should be quite accurate as the vehicle is coupled directly via the cable to the ship, whose location is accurately determined by GPS. Factors that will determine absolute positional accuracy, include the accuracy of the wire-out measure or estimate, accuracy of the vessel's GPS position, deviation of the cable shape from an assumed straight line, and movement of the vehicle away from the transect line by currents. If operating on sloping ground, where a high-resolution, digital-elevation map (DEM) is available and the depth under the vehicle is recorded by an altimeter or echosounder, accuracy can be improved by constraining the estimate of vehicle location by matching the total measured depth (vehicle depth + depth under the vehicle) to depth values in the DEM (Anderson *et al*., 2008).

Bottom tracking is commonly achieved using an acoustic Doppler system – most commonly a Doppler velocimeter log (DVL). Acoustic Doppler systems (e.g. acoustic Doppler current profiler, or ADCP) are most commonly used to track currents in the water column but, for AUV applications, the Doppler can be used to track the direction and speed along the bottom as well as altitude above the bottom. Tracking errors are ca. 1% of the distance travelled (Bahr and Leonard, 2006), which is an order of magnitude improvement over dead reckoning. Doppler sounders are now standard on most AUVs and are used for internal navigation of the vehicle.

Inertial navigation systems (INS) combine compass and gyroscope technology in microelectronics (microelectromechanical systems, or MEMS) to track the vessel's motion. The error of these systems is ca. 0.2%, but many of these systems suffer from drift – primarily electronic drift of the sensors (Bahr and Leonard, 2006). When an INS is combined with a DVL, and when the DVL maintains a bottom lock, the position error growth can be less than 0.05% (McEwen *et al*., 2003). The primary difficulty in relative positioning or tracking systems is that errors compound and can increase significantly over time; therefore, unless there is communication between the vehicle and surface vessel, the *in situ* track or location of the vehicle is not known until the vehicle is retrieved.

Absolute positioning methods have the advantage of establishing where the vehicle is *in situ* during remote operations. State-of-the-art for absolute positioning of remote vehicles is triangulation from navigation buoys at known locations (long baseline, or LBL, systems) and/or for the vehicle to surface at regular intervals to obtain GPS fixes. Surfacing for GPS fixes provides an accurate position and time, and can be used to communicate with satellites or land-based receivers; it can also be used by the vehicle to adjust course and speed to maintain the survey track. However, surfacing requires energy and time, which can be limiting for self-propelled AUVs, but is usually of lesser concern for autonomous gliders during extended deployments.

Acoustic baseline systems consist of transponders and receivers that communicate acoustically to provide a location relative to the surface vessel or fixed array. Ultra-short baseline (USBL) and short baseline (SBL) systems have transceivers on or near the hull of the vessel and a transponder on the vehicle to monitor location relative to the surface vessel. USBL systems have a single transceiver that is able to determine angle and range to the vehicle, whereas SBL systems have a minimum of three receivers to triangulate three-dimensional location. Generally, hull-mounted USBL transceivers are omnidirectional and will detect transponders in any direction and angle from the vessel, provided they are within range and far enough below the surface to ensure good acoustic transmission. Transponders on the other hand can often be directional in order to provide higher signal level in the direction of the hull transceiver, thus improving range performance. This is advantageous for towed systems where directional stability is inherent. For ROVs and AUVs, omnidirectional transponders may be more appropriate, except when the vehicle strays outside the beams and locating the vehicle can be very difficult. For example, the Trackpoint 3 system (ORE Offshore, West Wareham, MA, USA) asserts system performance of ±0.5% RMS (root mean squared) of slant range for accuracy in the horizontal position, 0.1° azimuth resolution, and ±0.3 m RMS.

The accuracy of acoustic positioning systems is determined by a number of factors, including speed of sound determination, motion reference unit performance, and gyro-compass accuracy. For example, errors of several metres can easily exist for slant ranges in the order of 1000 m, and 0.2 m slant-range resolution from inaccurate measurements of sound speed and correction data, derived from auxiliary sensors used in determining transponder position, can be affected significantly by vessel motion. LBL systems utilize an array of transponders in a grid pattern to significantly improve the accuracy and precision of locating the vehicle. For example, Kongsberg asserts accuracy of 0.05 m for its combination USBL and LBL (high-precision acoustic positioning, or HiPaP) system. These accuracies are for the vehicle relative to the baseline, not for the vehicle relative to the surrounding area. In order to extrapolate from the baseline to the area being surveyed, the baseline hydrophones must be accurately surveyed to the area. This is most often achieved by locating the hydrophones using the GPS from a surface ship, and additionally by using the hydrophones to generate relative locations (Anderson and Smalley, 2008).

Underwater communication is improving (e.g. interAUV, AUV–surface vessel), and low baud rate (<1 kb s^{-1}) transfers are possible for distances of less than 2 km. All baseline systems are useful over a small area (a few km^2), but are not suitable for wide-area surveys. In addition, whereas the accuracy of underwater navigation systems is within the order of ≥10 cm, this is insufficient for the subcentimetre resolution required for video mosaicing (Pizarro and Singh, 2003; Rzhanov, 2005).

4.3 Data processing

4.3.1 Stereo cameras

Although underwater photography has been available for more than 150 years, the first scientific uses of underwater images were for seabed-mapping applications, as well as for commercial oil and gas exploration in the 1960s. Sony released the first portable camcorder in 1983, and it was quickly utilized for underwater video imaging. The next major milestone was the advent of digital camera and video technology, which has greatly improved the utility, reliability (fewer moving parts and no complications from using film), efficiency (digital data can be directly stored and analysed), and accuracy (CCD and CMOS sensitivity is continually improving) of acquiring and processing underwater images. Current technologies allow high-resolution images suitable for measuring and monitoring benthic organisms (e.g. Abdo *et al*., 2006), seabed mapping (e.g. Edwards *et al*., 2003), and other applications, including measurements of fish (e.g. Somerton and Gledhill, 2005).

Individual cameras provide a wealth of information and can be used in all instances where stereo cameras are employed. Images from a single camera can be used to detect, locate, enumerate, identify, and measure objects in the water column and on or near the seabed. The primary limitation of using a single camera is not being able to measure range (distance from the camera), which can complicate size measurements. Without a reference guide, such as a metred rod or grid, size measurements from a single camera are difficult. A convenient technique for measuring sizes of objects using a single camera has been the use of pairs of underwater lasers (e.g. Chen and Lee, 2000). The lasers are usually oriented parallel with the optical axis and parallel with each other. Laser beams are visible on the seabed or targets, and are often visible in the water column because they reflect off objects in the water; the measured distance between the two lasers is used to measure the size of the imaged objects. This works well when the objects are relatively flat and perpendicular (i.e. broadside incidence) to the optical axis. When the objects are bent or oriented at angles off-broadside incidence, stereo cameras can provide significant improvement to the measurements.

Underwater stereo-video measurement remains a narrow speciality; consequently, there are few off-the-shelf stereo camera systems available. Such systems have a limited market, and manufacturers either find a niche or produce very flexible systems that can be applied to a range of measurement tasks. Perhaps the most widely known off-the-shelf system is VICASS (video image capturing and sizing system), which is used extensively in the aquaculture industry to measure the biomass of fish in a cage or tank. VICASS is based on broadcast-quality NTSC cameras on a fixed base and is calibrated by the manufacturer (AKVA Group). The system is designed for non-specialist operators who require biomass based on species-specific, length–weight regressions (Pienaar and Thomson, 1969). AQ1 Systems manufactures a similar system, also using a fixed base and calibrated cameras. The AM100 system has the advantage of higher resolution, progressive scan cameras, and the fully digital Gigabit Ethernet (GigE) interface to improve accuracy of measurement and allow use with fast-swimming species such as southern bluefin tuna (*Thunnus maccoyii*; e.g. Harvey *et al*., 2003b).

At the opposite end of the spectrum are manufacturers who provide flexible building blocks for stereo-image systems. The Australian company SeaGIS supplies frames and housings to allow a variety of cameras to be used in a stereo configuration. Video or digital still cameras can be used with neutrally buoyant, diver-swimmable systems

or larger frames used in drop-camera mode. In both cases, the housings are high-pressure sewer pipe combined with acrylic ports, permitting use to depths of up to 150 m.

Beyond the off-the-shelf systems are many purpose-built systems manufactured for scientific research or as one-off solutions, such as those described by Klimley and Brown (1983), Harvey and Shortis (1996), Harvey *et al*. (2003a), Chong and Stratford (2002), Stokesbury *et al*. (2004, 2007), Abdo *et al*. (2006), Costa *et al*. (2006), Shortis *et al*. (2009a), and various articles in Somerton and Gledhill (2005). Some of the first applications of stereo imagery in fisheries were to provide fishery-independent abundance data for reef fish (Ellis and DeMartini, 1995; Okamoto *et al*., 2000) and to monitor and measure fish in the wild (Cullen *et al*., 1965), in aquaculture pens, tanks, and ponds (Ruff *et al*., 1995; Petrell *et al*., 1997; Shieh and Petrell, 1998), or in controlled environments (Huse and Skiftesvik, 1990; Hughes and Kelly, 1996; Lundgren and Nielsen, 2008). For aquaculture pens, packing densities of the fish are often too high for acoustic measurements of individuals, but holding pens or tanks are often small enough for coverage of all or most of the pen by optical technology (Ruff *et al*., 1995). In each case, the system has been designed for a particular measurement task, so characteristics such as the type of imager, the camera housings, and the base separation between the cameras are specific to the circumstance. Harvey and Shortis (1996) used video camcorders in sewer-pipe housings to carry out transect surveys, Abdo *et al*. (2006) used digital still cameras in acrylic housings to measure the volumes of sponges, whereas Shortis *et al*. (2009a) used video cameras in aluminium housings for deep-water habitat surveys.

Stereo camera systems can, of course, be constructed using pairs of single off-the-shelf cameras. Major manufacturers, such as Canon and Sony, offer underwater housings that are capable of deployment to depths of up to 10 m. Canon provides underwater housings for more than 40 digital still cameras, and Sony offers a waterproof housing that is compatible with more than 20 camcorder models. To access greater depths, specialized housings are required from independent manufacturers, such as Ikelite and Sealux. The housings are composed of polycarbonate or aluminium and are rated to 50−100 m.

There are three substantive issues that must be resolved for stereo camera systems constructed as one-off solutions (Shortis *et al*., 2009b). First, the cameras must be synchronized in order to avoid systematic errors in the measurements. Ideally, the cameras should be electronically synchronized to fire exposures simultaneously. This is possible for systems based on digital interfaces used with digital video cameras, and is feasible for digital still cameras. For other types of cameras, especially video camcorders, electronic synchronization is not feasible and other techniques must be adopted. Harvey and Shortis (1996) were the first to use a system of flashing LEDs within the fields of view of both cameras in order to visually synchronize video camcorders to the nearest frame. This level of synchronization is sufficient in most circumstances, but may lead to systematic errors for fast-swimming species or rapid movement of the camera system.

The second fundamental requirement is that the system be geometrically stable. Clearly, the camera housings must be rigidly connected to a base bar so that the separation and relative orientation of the housings are fixed. Any change to the geometry will invalidate the calibration of the system. Similarly, the total optical path from the camera sensor to the external interface with the water must also be stable. Any change in the integrity of the optical path can also invalidate the calibration,

depending on the type of calibration strategy. To avoid changes in geometry, it is often the case that lenses with a fixed focal length, rather than zoom lenses, are used with digital video or digital still cameras. The focus setting is selected so that it is physically recoverable, usually at infinity, or the focus ring is locked at a particular setting. Camcorders require that the zoom and focus settings are recoverable, and usually set to infinity and the widest field of view. Furthermore, extensive testing with a range of cameras and housings across many deployments has revealed that the geometric relationship between the camera lens and the housing port is also important (Shortis *et al*., 2000). Stability of the system is maximized if there are rigid connections between the cameras and their ports in order to ensure that the total optical path is not a weakness in the calibration.

The final consideration is the base-to-distance ratio, known in classical aerial photogrammetry as the base–height ratio. The precision of photogrammetric measurements in the plane parallel with the photographs and in the direction perpendicular to the base deteriorate in proportion to the distance from the cameras and the square of the distance from the cameras, respectively. Precision in the direction perpendicular to the base improves in proportion to the length of the base between the cameras. Accordingly, the precision of measurements of three-dimensional positions to determine a length, such as those at the snout and tail of a fish, are influenced negatively by distance and positively by base length.

Although many factors need to be considered, from well-established experience in stereo photogrammetry, the base-to-distance ratio should ideally be within the range of 1:1 to 1:5. A ratio more than 1:1 results in large changes in perspective that will affect the accuracy of stereo measurement, as well as the limitation of stereo coverage in positions close to the cameras, whereas a ratio less than 1:10 will lead to a rapid deterioration in precision. Accordingly, the base between the cameras should be designed to be appropriate to the expected range of distances between the cameras and the fauna or flora to be measured. Sensible limits on the physical size of the base restrict the potential range at which measurements can be captured, so inevitably the design of stereo camera systems is a compromise between portability and optimal precision of measurement.

As digital technology improves, it allows the acquisition of vast amounts of data in ever-decreasing amounts of time. However, the ability to analyse and manage these data is not developing at the same rate. The current bottlenecks for fully utilizing underwater imagery are: (i) event-logging software that directly accesses the recording medium; (ii) database software for quick and efficient management, search, and retrieval of images; (iii) software that can correct for camera altitude (for seabed applications); and (iv) automated processing algorithms (Somerton and Gledhill, 2005).

Stereo information can also be retrieved from a single moving camera, provided that successive images are overlapping (Hartley and Zisserman, 2004). This technique, known as structure-from-motion, requires accurate information about the motion of the camera. It has the advantage over two-camera stereo systems that multiple images can provide observations of an object from more than two angles. For quantitative uses, the camera needs to be calibrated (Scaramuzza *et al*., 2006). As images need to be overlapping, lenses with wide fields of view are preferred, such as omnidirectional, spherical, and fisheye (Terabayashi *et al*., 2009). The choice of lens depends on the application. As cameras on AUVs become more prevalent, obtaining

as much information from the optical systems as possible will be the challenge for data processing and analysis.

4.3.2 Image analysis

Image processing and analysis is a huge field with many scientific, commercial, and personal applications. Indeed, it is so ubiquitous that the name of one software package, "Photoshop", is commonly used as a verb. It is impossible to cover the full range of what can be done but some of the general categories are discussed briefly below. Commercial or open-source software is available to do all of the tasks that are described. The categories are:

- **Image enhancement**, which covers most of the personal applications. Brightness, contrast, sharpness, and colour balance can be adjusted. Beyond this, the three channels of colour photographs can be manipulated individually or combined in any fashion. For example, the red channel of a red–green–blue aerial image will not pick up features much deeper than a few metres in the ocean, because of the high absorption of red wavelengths by seawater. The blue channel, on the other hand, will penetrate to a few tens of metres in clear waters.
- **Automatic target recognition**, which requires some information about the target, but what information to use depends on the target. For example, when trying to detect seagrass against a sandy bottom from aerial photographs, comparing the brightness of each pixel with a threshold value may be sufficient. Identifying different types of seagrass may require recognizing subtle differences in colour. Pattern-recognition techniques use information from multiple pixels to make a determination. For example, object shape can be used to identify individual fish or plankton in an image (Culverhouse *et al.*, 1996; 2003) or schools in a lidar return.
- **Target tracking**, which requires the capability to identify the same object in successive images, generally acquired at video-frame rates of 25 or 30 fps. As the camera measures the two-dimensional angle between the optical axis of the camera and the object, additional information is required to find the position. This can be done by using a second camera to obtain two additional angles or an acoustic rangefinder to obtain the distance to the object. Once the position of the object is measured in a succession of images, its trajectory can be calculated. An example would be the behaviour of fish in a net from video.

4.4 Metadata

Whatever the data source, metadata are a critical component. For fishery applications, this generally includes at least time and position.

The most common format for digital-camera metadata is EXIF (exchangeable image file format), which is a feature of JPEG (joint photographic experts group) image files. EXIF information can be viewed and edited in most image-processing programs. It generally includes camera settings and can also include GPS position, copyright status, artist, artist's comments, and more. In fact, there are over 100 fields in this format.

More specific metadata formats are also available. As an example, the Habitat Ecology Data Management Group at the Bedford Institute of Oceanography in Canada has been providing services to a variety of research programmes using

metadata-capture tools for at-sea collection, post-processing, and archival. A great deal of this work in the past few years has included metadata associated with image collection. To meet this requirement, protocols and practices were developed to ensure that these metadata can be linked to the image.

As standard practice, all of the available navigation data are captured and saved. The minimum requirements are GPS position, time, sounding and gyro heading. An audio-encode device (e.g. GeoStamp, Intuitive Circuits) is used to write the GPS time to the audio track of any digital tape that is recorded. Event-data are captured and annotation of event (e.g. species seen), class (e.g. substrate character), and station-keeping information are performed at sea using an in-house software package called CAROL.

CAROL is a Delphi 6.0 digital logbook that accepts serial-feed National Marine Electronics Association (NMEA) strings and writes out flagged events with a concatenated consecutive day and GPS time-string (GPSTime). The user can preset many of the features (COM port number, class–event fields, mission ID, etc.) using an initialization, or "ini", file. The program is a graphical user interface (GUI) with programmed buttons that can be pressed to capture the GPSTime from the serial feed and write out to an ASCII text file.

The opening page provides entry points for station-keeping information, and there are buttons to prompt for specifically designed capture-device pages. The page also has colour-coded status "lights" that flash green to show that data feeds are functioning. Each of these device pages has a set of buttons that allow the user to annotate the important points during the data-capture sequence. Blue areas are filled in by the programme, and white fields are user-updateable and flag comments with GPSTime on the adjacent button-press.

These device pages allow the user to manage all of the station-keeping information, and there is also another level of metadata control for at-sea data collection, allowing initial interpretation of the images being recorded. This is the class–event page. For this page, the user can preset the button values and quick keys in the "ini" file so that the programme is set for the type of research being conducted. For the events button- or key-presses, CAROL writes flagged times into a text-output file. The class flags are different in that they are used for timed coverage of substrate classification. Each key-press starts the collection of GPSTime stamps, at whatever the serial-feed rate is, for a predetermined length of time. The time-length is defined in the "ini" file, and in the middle of the interval, a reminder window indicates that the substrate flag will be turned off and gives the user the option of continuing.

There are two output files: "D" and "R". Both are ASCII text containing all of the captured metadata using proprietary NMEA strings. The "D" file contains only the flagged CAROL strings, and the "R" file contains these strings interspersed with the raw NMEA from the serial-port navigation stream.

The text files are processed into tables using Microsoft Access 2002 database scripts for easy data processing and extraction. Some of the processing is still done by manual manipulation, and the products generally end up being presented as geographic information system (GIS) layers with hyperlinked stills (if taken) or graphs, etc. Microsoft Windows XP shared-drive environment is used to allow secure access to the products.

4.5 Calibration

4.5.1 Stereo cameras

There are many approaches to the total calibration of stereo camera systems. One approach is an integrated process in which the camera's internal characteristics (such as principal distance and lens distortions) and the relative orientation (base separation and relative pointing directions) of the cameras are determined simultaneously (King, 1995; Harvey and Shortis, 1996). Other approaches to calibration follow a two- or three-step approach that determines groups of parameters sequentially for convenience or for operational reasons (Leatherdale and Turner, 1983; Li *et al.*, 1997). In the multistep approach, the first phase determines the internal characteristics independently for each camera. In the second phase, the relative orientations of the calibrated cameras are determined using stereo-image measurements. In the absence of an external reference, all locations determined from correlating left and right images are computed with respect to (typically) the centre of the base between the cameras and the mean-pointing direction. If an absolute reference is required (e.g. in longitudinal studies of seabed habitats), an absolute orientation is required. This final step of locating and orienting the camera pair with respect to the external datum is discussed in other subsections of this section (e.g. Section 4.2).

Most underwater film cameras are one of two types: (i) semi-metric, which have relatively low and stable lens distortion and may contain fiducial or reseau marks to model film distortion; or (ii) non-metric, which can have high and unstable lens distortion and do not contain fiducial or reseau marks (Osborn, 1997). Although the quality of cameras, especially digital cameras, is continually improving and the CCD and CMOS sensors are much more reliable than film, these systems must be calibrated, and depending on the stability of the camera body, lens, and mounting systems, they must be calibrated at regular intervals.

For quantitative use, photographic systems must be geometrically calibrated for accurate measurements (Harvey and Shortis, 1998). There are intrinsic and extrinsic parameters for camera calibration. The reconstruction of an object from stereo imagery requires three orientations: (i) interior (within the cameras), (ii) relative (between the cameras), and (iii) absolute (between cameras and object space; Osborn, 1997). Interior orientation references four types of physical parameters: (i) principal distance, (ii) principal point, (iii) lens distortion (e.g. radial and decentring), and (iv) image distortion. The principal distance is the separation between the perspective centre of the lens and the focal plane, and it varies with the focus of the lens. When the lens is focused at infinity, the principal distance is approximately equal to the nominal focal length of the lens. The principal point is the intersection of the optical axis with the focal plane. Radial lens distortion results from the preference in lens design for image quality over image geometry for mass-produced lenses, whereas decentring distortion is caused by coaxial misalignment of the lens elements. Other distortions in the lens arise from non-uniformities in the shape (i.e. curvature) or in homogeneity of the lens material, which affect the refractive properties of the lens. If the focus of the lens is adjustable, then the principal point and distance must be calibrated for each focus setting.

In an ideal lens, all perspective centres, image points, and the objects depicted in the images should be collinear (Figure 4.3). This means that, for every point, there is a straight line that connects that point with the perspective centre (Osborn, 1997). Deviations in the straight line are distortions in the image. In addition to lens

distortions, image distortions may be caused by imperfections in the receiver (e.g. CCD or CMOS sensor) or irregularities in the positioning or orientation of the sensor relative to the lens. Geometric errors result from lens distortion, non-perpendicularity of the image plane and camera's optical axis, and the limited spatial resolution of the pixel array and distortions resulting from the analogue-to-digital conversion.

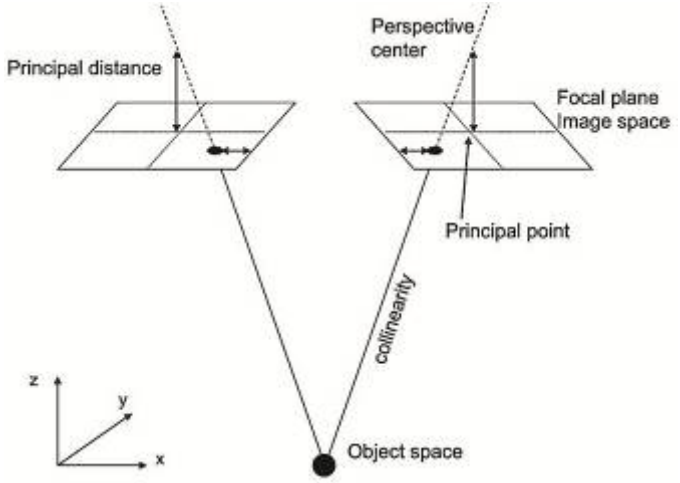

Figure 4.3. Stereo camera geometry. (Redrawn from Osborn, 1997.)

Extrinsic parameters define the relative geometries between paired (stereo) cameras and to the absolute orientation of the camera pair in free space. Relative geometries include the separation of the perspective centres of each lens, the pointing angles of the two optical axes, and the rotations of the sensors (CCD or CMOS sensors in digital cameras; Harvey and Shortis, 1996). Once the relative orientations of the two cameras have been established, their orientation with respect to the landscape can be determined. This is done by comparing objects with known location and orientation (e.g. vertical and horizontal orientation and location with respect to direction) in an image or by incorporating tilt, angle, gyroscope, or other instruments on the mounting apparatus. The absolute geometry can then be incorporated in the image analyses if the images and sensors are synchronized.

There has been a steady development of calibration methods, including: (i) the use of grids at a specified range (Adams, 1982; Snow *et al.*, 1993), which has the disadvantage of the calibration being valid at only the calibration range; (ii) the use of checkerboard patterns (e.g. Ruff *et al.*, 1995); (iii) the use of three-dimensional objects, such as cubes (Shortis *et al.*, 2003), grids, and targets in two-stage calibrations (Li *et al.*, 1997); and (iv) *in situ*, free-network, self-calibrations (Harvey and Shortis, 1996). The calibration of intrinsic and relative parameters can be done in air, but the refractive properties of the water and lens must be incorporated. If the calibration is done in air or in different environmental conditions than the images were acquired, the refractive properties can be incorporated using explicit ray tracing. Ray tracing is a rigorous solution, but is only as good as the model used and the range of conditions anticipated. If the environmental conditions change, the correction may not be valid. In general, radial distortion is the primary component of image distortion caused by the refractive interfaces and is difficult to model accurately (Harvey and Shortis, 1998). The alternative is to allow the effects of refraction, radial distortion, and asymmetry to be implicitly absorbed in the intrinsic and extrinsic calibration parameters. This method is widely adopted and utilized by most calibration procedures.

All calibration methods utilize a calibration object that is two-dimensional (e.g. checkerboard) or three-dimensional (e.g. frame or grid) with measurement points. If the locations of the calibration object and measurement points are predetermined, the calibration is externally constrained (Baldwin and Newton, 1982). Although this method is used and appears advantageous, the positioning of the calibration object must be accurately and precisely known, and the object must be rigid. In order to meet these conditions, a free-network self-calibration based on a self-calibrating, multistation bundle solution of Granshaw (1980) has been used and is a convenient method of calibrating cameras (Harvey and Shortis, 1998). A disadvantage to self-calibrations is that there are potential correlations among the principal point location, decentring lens distortion, lens locations, and orientation of the cameras. Furthermore, the calibrations are effectively empirical and are unlikely to be optimal when applied to different conditions or different camera-to-object distances. Additionally, many images must be acquired in order to maximize the confidence with which the calibration parameters are determined. However, the convenience and quality (accuracy and precision) of these types of calibrations have been shown to be sufficient and beneficial for fishery applications when the camera system is stable, environmental conditions are similar, and the objects to be measured are at the same range of distances.

In recent years, computer-vision applications have rekindled interest in calibration techniques (Remondino and Fraser, 2006). The computer-vision applications have developed separate calibration methods, which are not necessarily based on photogrammetry. The accuracy, precision, and application will dictate which of two underlying functional models should be used: (i) a camera model based on perspective projection; or (ii) a projective camera model supporting projective rather than Euclidean-scene reconstruction. For example, photogrammetric methods often support measurement accuracy of 1:20 000, whereas computer-vision applications may only require 5% (camera-to-object distance) accuracy. These methods can be further categorized into linear techniques, non-linear techniques, and a combination of linear and non-linear. Linear techniques are quick and simple, but cannot accommodate lens distortion and are the least accurate. Non-linear techniques, which form the basis of self-calibrating bundle adjustments, are founded in photogrammetry. Combination methods use a two-phase approach, where the linear parameters are determined first and then the non-linear parameters are configured. Calibration models for machine and computer vision (Heikkila and Silven, 1997; Zhang, 2000) employ reference grids (e.g. checkerboard pattern) and are mostly based on the method of Tsai (1986, 1987).

Two commonly used software packages for stereo calibration and stereo-image analysis are the Vision Measurement System (VMS), which is part of Geometric Software (www.geomsoft.com), and a calibration toolbox (http://www.vision.caltech.edu/bouguetj/calib_doc/) developed in Matlab (The Mathworks, Inc., Natick, MA, USA). The VMS system utilizes the free-network self-calibration with images from a three-dimensional cube. The calibration toolbox uses images from a two-dimensional checkerboard for calibration.

For colour cameras, the above calibrations are still required, but additional effects must be considered. One issue is chromatic aberration in the lens, which is usually separated into longitudinal (axial) and lateral (oblique) aberrations (Remondino and Fraser, 2006). Longitudinal aberrations cause blurring of the image, which is difficult to rectify. Oblique aberrations cause a degree of misregistration of the colour channels and offer the possibility of correction in post-processing.

The calibration of stereo cameras is a straightforward and rapid process that can take place in an on-board tank on the vessel or, conditions permitting, adjacent to, or beneath, the vessel. The calibration fixture can either be secured in position while the cameras are manoeuvred around it, or manipulated while the cameras are secured in position; a combination of both approaches can also be used. For example, a small two-dimensional checkerboard may be manipulated in front of an ROV stereo camera system held in a tank. For a diver-controlled stereo camera system, a large three-dimensional calibration fixture may be tethered underneath the vessel and the cameras moved around it. In either case, the outcome is a convergent network of many exposures of the calibration fixture, with the fixture filling the image frame and incorporating multiple rolls about the optical axis of the cameras. This network geometry and frame coverage are necessary to ensure that the camera calibration parameters are recovered both reliably and precisely (Shortis *et al*., 2009b). Rapid measurement and processing of the captured images are afforded by the automatic recognition of the checkerboard pattern (Zhang, 2000) or the use of coded targets (Shortis *et al*., 2003).

4.5.2 Hyperspectral imager

Two factors need to be addressed in the calibration of a hyperspectral imager: (i) spectral calibration of the dispersive element and the detector array, and (ii) radiometric calibration of the receiver. The approach to the former is similar to that for non-imaging spectrometers, and the approach to the latter is similar to that for other radiometers. Davis *et al*. (2002) provide a good description of calibration of the ocean portable hyperspectral imager for low-light spectroscopy (Ocean PHILLS), based on a technique of Bowles *et al*. (1998).

In spectral calibration of the Ocean PHILLS, a diffuse surface is illuminated by oxygen, mercury, argon, and helium gas-emission lamps, one at a time. The diffuse surface allows a uniform spectral illumination across the system. The known positions of the emission lines are matched to the position of the line in the detector array. Despite the care with which this is done, the authors note small (1–3 nm) discrepancies between the laboratory calibration and the spectral position of strong atmospheric spectral features, such as the Fraunhofer line at 431 nm and the oxygen absorption peak at 762 nm. The laboratory calibration is adjusted, if necessary, to match these features in field measurements.

Radiometric calibration of the Ocean PHILLS is done with a 1 m integrating sphere coated with Spectraflect and illuminated with up to 10 halogen lamps. A colour filter is placed in front of the instrument to obtain a spectral input that is whiter than the spectrum from the sphere. A decade of dynamic range is obtained by illuminating the sphere with 1–10 of the halogen lamps, and the quadratic response of each pixel to incident radiance is obtained. This response function is used as the calibration for each pixel in the array. The authors found that the response of this system was very linear, with the non-linear term in the calibration typically accounting for less than 0.1% of the total irradiance at each detector element.

4.5.3 Lidar

In principle, radiometric calibration of a backscatter lidar is simple: a flat target of known optical properties is illuminated with the lidar, and the receiver response is measured. For convenience, a diffuse target with reflectivity R is chosen. The reflectivity of a diffuse target can be related to the equivalent volume-backscatter coefficient of scatterers in the water by the relationship

$$R = 0.5\pi c\tau\beta(\pi),$$

where c is the speed of light in water, τ is the laser pulse length, and $\beta(\pi)$ is the volume scattering coefficient at a scattering angle of π radians, or volume-backscatter coefficient. $\beta(\pi)$ is the fundamental optical measurement of a profiling lidar and can be related to the density of fish or other scatterers if the optical TS is known.

In practice, this calibration procedure, like many others, is difficult to do precisely. The main problem is the difficulty in obtaining a well-calibrated reflectance target that provides a signal level similar to that obtained in the ocean; reflectance values of available standards are much too high. Thus, it is necessary to make the calibration measurement at much higher signal levels and carefully measure the non-linearities in the receiver, or to attenuate the transmitted beam and carefully measure the attenuation. Attempts have also been made to do *in situ* calibration by flying the lidar over a calibration target suspended in the ocean, an approach that requires extraordinary piloting skills.

4.6 Measurement uncertainty

The accuracy, precision, and time-based stability of photographic measurements have been investigated for many years. This attention to detail comes from the use of photographs and digital images in photogrammetry. Measurement uncertainty has been investigated as two general components: (i) the precision and time-based stability of the camera system; and (ii) the accuracy of the measures, such as length, compared with the true dimensions of the object of interest.

The accuracy of stereo analysis depends primarily on three components of the system: (i) the spatial sampling of the sensors; (ii) the accuracy to which the image can be identified and distinguished in the image; and (iii) the spatial separation of the cameras (Ruff *et al*., 1995). The stability of the measurements over time (as opposed to short-term jitter of the camera) is affected by physical handling (e.g. during deployments, charging batteries, and replacing the memory of the camera either in or out of the mounting apparatus) and by changing environmental conditions that can alter the optical properties of the water. Accuracy and/or uncertainty are difficult to evaluate except under very controlled conditions.

Typically, airborne calibrations have higher precision than calibrations done in water. Harvey and Shortis (1998) demonstrated the precision of underwater measurements over repeated calibrations of approximately one-half the dimension of a pixel. This is a reduction in precision from airborne calibrations that commonly have precisions of 0.1- to 0.2-fold the pixel dimension, with best-case precisions of 0.02–0.03 pixels using discrete targets in optimal conditions (Shortis *et al*., 1995, 2001). Measurement variability was found to be less when calibrations were performed in a "clean" environment than when calibrated *in situ*. For example, Harvey and Shortis (1998) found that calibrations done in open water were almost three times as variable as those done in a pool. Handling of the cameras appears to be the most common source of introducing variability in camera calibrations. Zoom lenses are less accurate than fixed lenses, for which a 72% degradation in internal precision and a decrease of 44% in external accuracy have been reported (Shortis *et al*., 2006).

Measurement accuracy, especially *in situ* on mobile species such as fish, is difficult to quantify and evaluate. Stereo video measurements have been compared with visual estimates by divers, where the divers' estimates were considered as the standard, but these comparisons raised questions about the accuracy of the visual estimates

(Harvey *et al*., 2001b, 2002). For example, Harvey *et al*. (2001a) demonstrated considerable improvement in the coefficient of variation (*CV*) for stereo video measurements (<5%) as opposed to visual estimates by novice and experienced divers (10–30%) when measuring lengths of plastic silhouettes. Camera angles of greater than 50° relative to the target can result in significant degradation in measurement accuracy (Harvey and Shortis, 1996).

Whether a calibration is done using a three-dimensional cube or a two-dimensional checkerboard does not appear to affect the stability of calibrations. Ruff *et al*. (1995) found a 1–1.5% error in length measurements of range using the checkerboard, and ca. 3.6% in length measurements of real fish (two fish). Hughes and Kelly (1996) found a mean error of 0.47 cm (0.27 cm s.d.) in locating grid points using orthogonally located cameras (i.e. not stereo video). Petrell *et al*. (1997) obtained 0.5% error in measurements of fish mass (fish length was ±2.1% and height was ±5.8% from stereo); precision was ±3% for fork length and ±4.5% for width. These measurements were done on stationary and dead fish. Swimming fish were within ±5% (Petrell *et al*., 1997; Shieh and Petrell, 1998). Li *et al*. (1997) demonstrated accuracies of 0.8 cm in lateral directions and 1.2 cm along depth direction for objects within a 2–3 m range (0.3% lateral and 0.4% depth). Wang *et al*. (2008) used a three-dimensional checkerboard cube for calibration and found errors of approximately 2 mm in the *x*, *y*, and *z* directions and error in fork-length estimation of approximately 1 cm.

Improvements in camera technology and post-processing methods appear to be improving stereo measurements. Harvey *et al*. (2003b) report errors associated with estimating southern bluefin tuna lengths of less than 0.6% and body depths (dorsal to ventral distance) of less than 1.4% in an aquaculture setting. For reef fish, Harvey *et al*. (2004) revealed errors associated with estimating range (distance of the object from the camera) of less than 1%, and interestingly, this error did not significantly increase with increasing distance. Harvey *et al*. (2003a, 2003b) also reported differences in calibration settings between salt water and freshwater, indicating that care must be taken when using cameras in salt water that were calibrated in freshwater, and vice versa. They recommend using

$$significance = \frac{\left|\text{parameter}_{t} - \text{parameter}_{t-1}\right|}{\sqrt{\text{variance}_{t} + \text{variance}_{t-1}}}$$

to compare parameters over time (t).

5 Applications

James Churnside, Richard O'Driscoll, Michael Jech, Emma Jones, Gavin J. Macaulay, Howard McElderry, Stephen J. Smith, and Eirik Tenningen

There are many applications of fishery optical technologies, and their number is growing rapidly. Several examples are presented here as illustrations, but the list is by no means exhaustive.

5.1 Video and still camera surveys

One of the most obvious applications for video or imaging surveys is the study of coral reefs. The water is typically shallow and clear, so very high-quality images can be obtained by a video or still camera carried by a diver. Corals can often be identified to species level (Cruz *et al*., 2008). Surveys similar to those of Cruz *et al*. (2008) and Kikuchi *et al*. (2003a, 2003b) in Brazil, have been conducted at numerous other locations, including Australia (Carleton and Done, 1995), the Caribbean Sea (Aronson *et al*., 1994; Rogers and Miller, 2001), the Philippines (Alcala and Vogt, 1997), and the Mariana Islands (Houk and van Woesik, 2006). The most complete evaluation compared results from six different techniques in the Red Sea (Leujak and Ormond, 2007). They concluded that video transects provided the most cost-effective technique for detecting changes in reef structure, but high-resolution still cameras were better able to capture the more detailed information required to understand the processes behind these changes.

Coral reefs can also be surveyed from above the surface of the water, although the level of detail is reduced. Figure 5.1, for example, is a satellite image of a segment of the Great Barrier Reef in Australia. Satellite data can be used to detect coral bleaching on large spatial scales (Yamano and Tamura, 2004; Kutser and Jupp, 2006), but coral types cannot be distinguished (Kutser and Jupp, 2006). More detail is available in aerial imagery (Berkelmans and Oliver, 1999), so more information can be obtained. As with any imaging system, the trade-off is between the ability to resolve fine-scale details and the ability to cover large areas quickly. With readily available image arrays, the swathe width will vary by a factor of ca. 500 to a few thousand times the resolution.

Figure 5.1. True-colour image of section of the Great Barrier Reef off the coast of Australia, taken with the multi-angle imaging spectroradiometer (MISR). Image width is about 360 km, with a resolution of 240 m. (Image courtesy of the NASA/GSFC/LaRC/JPL, MISR Team.)

Where the bottom topography is smoother than that found in coral reefs, it is possible to perform in-water video surveys of the bottom without the need for a diver to hold the camera. ROVs have been used to study groundfish (Adams *et al*., 1995) and juvenile flatfish (Norcross and Mueter, 1999). Towed vehicles have been used to study the abundance of rockfish (*Sebastes* spp.; Martin and Yamanaka, 2004) and the association of lobsters (*Homarus americanus*) with bottom type (Tremblay *et al*., 2009). A towed sled was used to survey scallops (*Patinopecten caurinus*) in the Gulf of Alaska (Rosenkranz and Byersdorfer, 2004). AUVs have been used to survey groundfish (Clarke *et al*., 2009) and other fish (Auster *et al*., 2005). These are just a few examples in a field that is expanding rapidly.

Recently, aerial surveys of sardines have been undertaken in the Northeast Pacific. A high-resolution digital camera was flown at an altitude of 1300 m. Sardines were identified by inspection of the images, and the area of each school in the image was measured. Selected schools were captured after the aerial image was obtained, and the biomass was obtained at the processing plant. The schools were selected to cover the range of sizes observed. A linear regression of biomass against school area from the captured schools was used for the entire survey. This technique was not intended to be an accurate estimate of total biomass, because it was clear that not all schools would be visible. Instead, it was used as a minimum estimate to constrain population models.

5.2 Trawl cameras

The use of trawls for verifying the species composition of backscatter dates back to the first fishery applications of underwater acoustics. The combination of trawling and acoustics has been successful for fishery management and will continue to be a very useful tool for managing fisheries. The downsides of trawls are that: they are lethal to the organisms that are captured; fragile organisms can be destroyed to the extent that identification is problematic; and, in most cases, only a subset of the fish caught is actually used for biological measurements (e.g. length, weight, sex, maturity, age, and diet). In addition, although acoustic data provide high-resolution information on the spatial distribution of organisms, trawls tend to spatially integrate over larger volumes than do acoustic measurements. A solution to this problem is to position cameras near the aft-end of the trawl in order to optically "capture" the

organisms as they pass through the net (K. Williams *et al*., 2010). Although cameras have been placed on nets for years in order to study the behaviour of fish within and outside nets, and to address catchability and selectivity (see Section 5.5), in this case the purpose of these cameras is to provide species and length information without the need to physically capture the individuals.

Stereo cameras, LED strobes, computer, microcontroller, sensors, and a battery power supply make up the system used by NOAA's Alaska Fisheries Science Center (Figure 5.2; K. Williams *et al*., 2010). The machine-vision cameras are Joint Architectural Intelligence (JAI; www.jai.com) high-resolution, high-sensitivity cameras capable of capturing multimegapixel images at up to 15 fps. Machine-vision camera systems are more complex than consumer systems, but provide greater control over image acquisition. The cameras have stereographic-projection lenses that provide 80° field of view with little distortion (Figure 5.2). LED lamps were chosen for their lower power consumption, and the entire system is housed in a frame designed to withstand the rigours of trawling. Current efforts are directed at automated processing of the images for species identification and organism length.

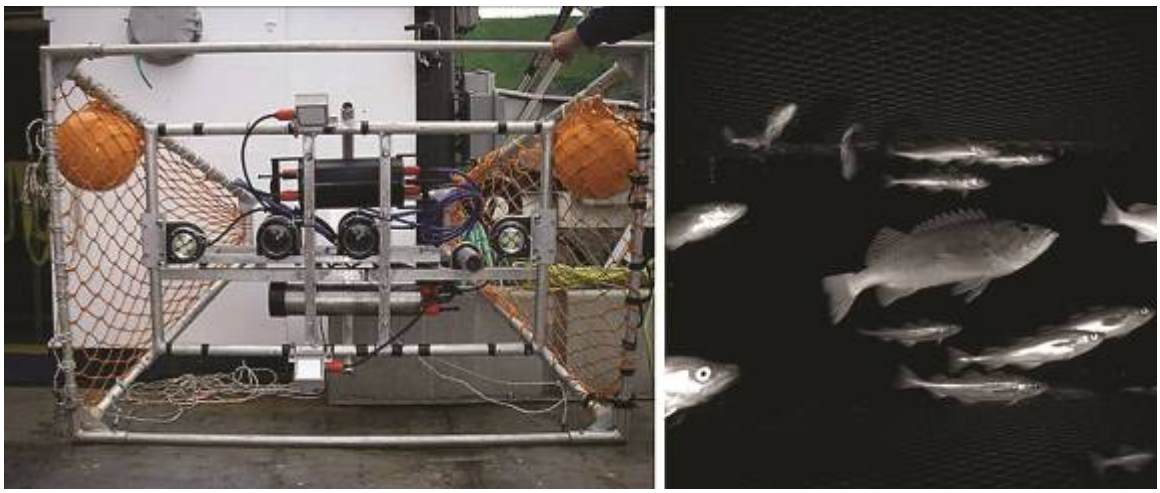

Figure 5.2. (Left) Cam-Trawl system showing the stereo cameras, LED lamps, electronic housings for power and data storage, and frame before it is mounted in a midwater trawl. (Right) Walleye pollock (*Theragra chalcogramma*) and Pacific rockfish (*Sebastes* spp.) inside a midwater trawl. (Images courtesy of K. Williams and R. Towler, NOAA Alaska Fisheries Science Center.)

5.3 Lidar surveys

Detection of fish schools by airborne lidar was demonstrated originally by Squire and Krumboltz (1981). More recently, comparisons of lidar and echosounder measurements of capelin (*Mallotus villosus*) and herring (*Clupea harengus*; Brown *et al*., 2002), mullet (family Mugilidae) and baitfish (Churnside *et al*., 2003), zooplankton (Churnside and Thorne, 2005), and epipelagic juvenile fish (Carrera *et al*., 2006) have demonstrated good agreement, provided that the measurements were made within a few days, and that both lidar and acoustic data were appropriately filtered to remove unwanted signals.

Recently, Churnside *et al*. (2011a) compared airborne lidar and photography for surveys of menhaden (*Brevoortia tyrannus*). Lidar was more reliable, with fewer missed schools, fewer false detections, and less variability in repeated surveys of the same area. The photographs detected more schools, because of the wider swathe. The main conclusion of this study was that the combination of lidar and photography was

very powerful, because the photographs provided important school identification information and the lidar detected schools deeper in the water.

Between 1997 and 2005, the Polar Research Institute of Marine Fisheries and Oceanography (PINRO) carried out annual surveys on feeding mackerel in the Norwegian Sea (Figure 5.3). All of these surveys were carried out within the framework of ecosystem surveys that were also collecting oceanographic data, which described current conditions and phenomena at the sea surface and subsurface layers (sea surface temperature (SST), transparency, pycnocline depth, chlorophyll *a* concentration, hydrodynamics special structure, and distribution). Calibration and confirmation of fish concentrations were carried out by Russian and Norwegian research and commercial vessels. The large variability in the extent of the area surveyed and in the location of fish is clear from these maps. Although most of the data analysis was done manually, some progress has been made in automating lidar processing in this region (Churnside *et al*., 2009c).

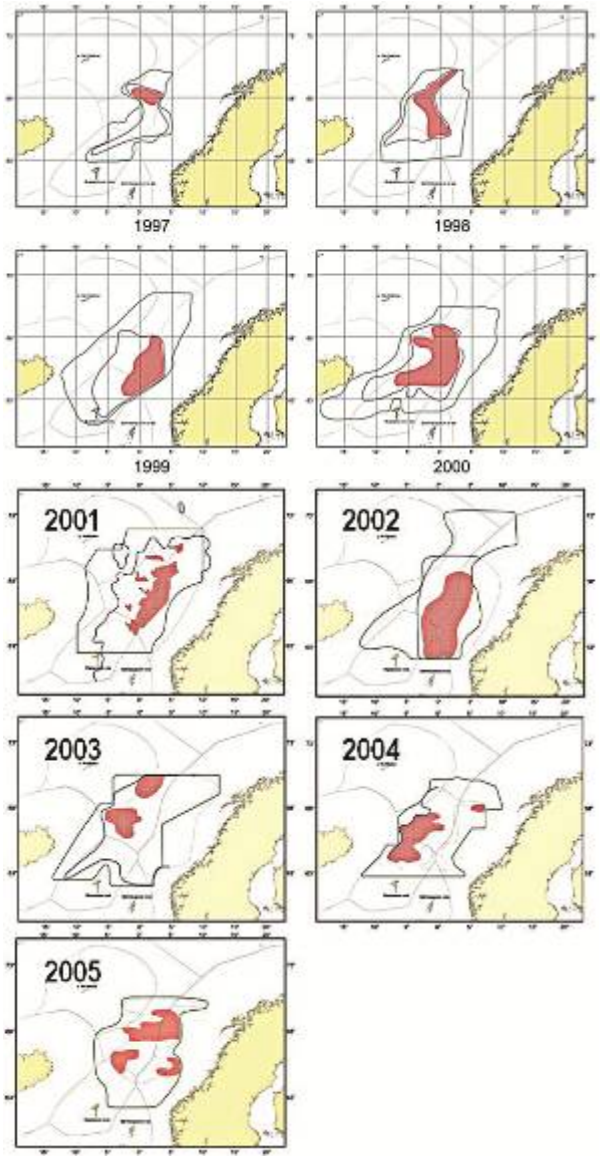

Figure 5.3. Spatial distribution of mackerel in the Norwegian Sea between 1997 and 2005. Outer green line = boundary of aerial surveys, inner blue line = total area of mackerel, pink shaded region = area of highest concentrations.

One of the most promising applications for airborne lidar is as a component of adaptive surveys. A broad-area airborne survey with lidar and photography could be used to direct an acoustic and trawl component so that the surface vessel is used most effectively. In a study of sardines in the Northeast Pacific (Churnside *et al*., 2009a), the aircraft and surface vessel covered the same areas in order to allow "what if" investigations for different assumptions about the vessel time available. In one case, vessel time was reduced to 60% of that in the original survey, but 90% of the original acoustic energy would still have been detected. With a further reduction to 30% of the original vessel time, 70% of the original acoustic energy would still have been detected. Of course, an adaptive survey with the full amount of vessel time would have produced a much more accurate survey, because more time would have been spent on the higher concentrations of fish. More studies of this type are recommended in order to improve the design of optimal adaptive surveys.

5.4 Supporting acoustic measurements

Optical observations and measurements in fishery acoustics are generally used to monitor behaviour with respect to variability in TS, and for species identification. As the acoustic TS is a fundamental measure in fishery acoustics (MacLennan and Simmonds, 1992; Sawada *et al*., 2002) and is highly dependent on fish behaviour (Nakken and Olsen, 1977; Towler *et al*., 2003), there has been considerable interest in relating the behaviour of fish (Sawada *et al*., 2009) and zooplankton (Benfield *et al*., 1998; Jaffe *et al*., 1998) to TS. Measurements have been made *in situ* (Sawada *et al*., 2004; Takahashi *et al*., 2004; Doray *et al*., 2007) and *ex situ* (Van Long *et al*., 1985; Lundgren and Nielsen, 2008; Gurshin *et al*., 2009; Kang *et al*., 2009).

Although these types of measurements have been beneficial for relating behaviour to acoustic variability, obtaining them is not a trivial matter.

Difficulties with merging acoustic and optical data include the following.

1) Synchronizing the data streams, e.g. synchronizing the acoustic data with the camera data. The acoustic system and the camera are often controlled by separate computers, and synchronizing these computers to the necessary resolution can be difficult, especially for video data. One method of alleviating the synchronicity issue is to use a still camera that is triggered by the acoustic system (Lundgren *et al*., 2001).

2) The time and effort required to process the optical data, e.g. processing the video data for behavioural measurements. These measurements (e.g. angle of orientation or activity) are commonly done manually, which is time-consuming relative to processing the acoustic data.

3) The disparity in detection ranges between acoustics and optics. Acoustic systems can detect organisms tens to hundreds of metres away, whereas optical systems require the targets to be within metres. At the optimal ranges for optical measurements, the targets can be within the nearfield of the acoustic transducer, where nearfield measurements are not reliable.

4) The potential for avoidance. Optical measurements often require artificial light, which can strongly affect fish behaviour. Fish often avoid light sources directly, or lamps may illuminate the vehicle, which can cause fish to flee. Conversely, fish may be attracted to a light source, but this would not be considered as altered behaviour. Infrared illumination reduces the behavioural effects of light, but increases the potential response to the instrument platform because of the short working distance required in the

infrared. All of these issues can be overcome, but a commercial solution is not currently available.

Acoustic techniques are well suited to imaging the aquatic environment, but suffer from poor imaging resolution when compared with optical techniques. It is in this area that optical techniques can enhance acoustic measurements, for example, by providing species, size, shape, and attitude to add to the acoustic measurements from a scattering object.

Determining the species of an organism that generates an acoustic echo is useful, and sometimes essential, in many aspects of fishery acoustics. Examples include *in situ* TS measurements and species composition of acoustic marks or layers for echo integration and partitioning.

In situ TS measurements typically involve ensonifying individual organisms and measuring their backscatter. The TS varies with many attributes, including species, size, life-stage, behaviour, and tilt-and-roll relative to the acoustic beam. Most of these attributes cannot be measured with acoustic techniques to any degree of precision. Appropriate optical techniques (e.g. photographic images and video) can help: a single optical image can provide species identification, whereas stereo images can provide information on the tilt-and-roll angle and size. Successive images (e.g. from video) can provide information on behaviour and additional context to assist with fish identification (e.g. swimming behaviour).

The acoustic and optical instruments can be mounted on one platform and attempts made to collect simultaneous acoustic and optical measurements of individual organisms. Alternatively, the optical instruments can be used separately in time and space to collect supporting information. Which of these techniques is the most appropriate depends on many factors, including operational requirements, equipment characteristics, and study constraints.

Simultaneous recording of acoustic and optical data from fish is a common technique, particularly for *in situ* and *ex situ* TS studies (Nielsen and Lundgren, 1999; Ryan *et al*., 2009). The use of optical techniques to assist acoustic seabed classification is discussed in detail by Anderson *et al*. (2007).

If the acoustic and optical sensors are mounted on one platform, matching the sampling volumes of the instruments should be considered. This involves consideration of the effective ranges and field-of-view. Field-of-view of an acoustic sensor is usually narrow (a commonly used 38 kHz acoustic transducer has a beam angle of 7°), with an effective range of about 3 m to several hundreds of metres, whereas that of a still camera or video is wide (often more than 50°), with an effective range of 1 m or less to approximately 10 m. The volume of overlap can often be very small, with the minimum range determined by transducer-nearfield considerations and the maximum range by penetration of light for the optical sensor. Another consideration is the imaging resolution of an optical sensor, which decreases with range to the point where even large objects can be difficult to identify. It is useful to have optical sensors with a wider field-of-view so that more images of each organism are captured. This helps by providing additional visual information about an organism, such as behaviour, length, and size. An alternative approach to matching sampling volumes is to physically separate the optical and acoustic sensors so that they image the same volume of water at their respective optimal ranges.

To provide the most value, optical and acoustic measurements can be taken simultaneously, with the aim of obtaining paired measurements of the same

organism; this requires some form of synchronization between sensors. If the optic and acoustic systems are able to record timestamps in, or associated with, their data, synchronization can be accomplished in one of several ways.

1) Prior to deployment, an optical image of a timer display can be collected on the acoustic equipment. The offset in times then allows the estimation of any offset between the optical timestamp and the acoustic timestamp. This relies on the timestamps in either system not drifting or drifting in a linear manner (for which a similar record of the offset would be required at the end of a deployment).

2) A timestamp signal can be fed into the optical equipment, which then records the time with the optical data (for video, this can be achieved via a video overlay device). Information can also be encoded into the audio track of video recordings using appropriate devices. The opposite is also possible: provide a timestamp from the optical system to the acoustic system. The effect of any timing delays in the generation, transmission, and storing of the timestamps should be considered.

3) The taking of images or video can be synchronized with the pinging of the echosounder, or vice versa. Most scientific acoustic equipment has the facility to produce an electronic ping trigger, or to operate from an external electronic ping trigger.

Unsynchronized target identification for TS is also useful, for example, lowering an optical sensor into an aggregation of fish can provide a measure of target identification for TS studies.

Optical and acoustic sensors saturate at different organism densities. For example, fish densities observed during *in situ* TS studies can be too high to resolve single acoustic targets well before the optic sensors can no longer resolve single targets. Similarly, the relatively short range of optical sensors compared with acoustic sensors can lead to situations where many acoustic targets are observed, but few are within the range of the optical sensors. One approach to overcome this limitation, and also to allow comparison with previous swept-area trawls is to remove the codend from a net and replace it with a video system that can record the passage of fish through the opening (Bonacci and Wakefield, 2009; K. Williams *et al*., 2010). This technique is particularly useful in protected areas where fishing is not allowed.

5.5 Behaviour

5.5.1 Behaviour towards trawls

Most of the current understanding of how fish respond to fishing gear has been gained by observation in the field, either directly by divers or through the use of underwater cameras. The earliest observations were on Danish seinenets and demersal trawls by divers *in situ*, either hanging onto the trawl itself or using a towed underwater vehicle, who noted the variability in swimming behaviour at different towing speeds and the reactions to different components of a trawl (Parrish *et al*., 1962, 1964; Hemmings, 1969, 1973; Korotkow and Martyschewski, 1977; Main and Sangster, 1981a, 1981b; Albert *et al*., 2003). The development of the underwater SIT camera that could be operated remotely, mounted either onto a towed vehicle beside the trawl or directly onto the net, allowed observations at greater depths and towing speeds, and in much lower light conditions. These observations, although mainly qualitative, revealed characteristic avoidance reactions to the doors, herding

behaviour in front of the sweeps and in the trawl mouth, and escape behaviour once inside the trawl (Wardle, 1983).

Tank-based video studies have also enhanced the understanding of behaviour during the catching process (Blaxter *et al*., 1964; Blaxter and Parrish, 1966; Glass and Wardle, 1995; Glass *et al*., 1993, 1995). The reactions of fish to mesh panels of different colours and contrasts demonstrated that fish will tend to stay clear of netting panels if they can see an escape route (Glass *et al*., 1993), but they can learn to swim through meshes (Özbilgin and Glass, 2004). Other examples include: comparison of behaviour at different light levels using infrared illumination (Ryer and Olla, 2000; Gabr *et al*., 2007); how water temperature affects swimming ability and escape behaviour (Özbilgin and Wardle, 2002); and the limits of swimming endurance for different species (He and Wardle, 1988; Yanase *et al*., 2007). In all of these cases, the use of video to record reactions and replay them at slow speeds allows a more detailed analysis, such as counting and timing of tail-beat frequencies, and the quantification of behavioural events.

The same analysis can be applied to footage collected *in situ*, although it is less easy to control ambient conditions, such as light level and water clarity. Quantification of behaviour can be done in terms of orientation, swimming speed/gait, and different short-scale events, such as turning to swim in a different direction, collision with another fish, or burst-swim to attempt escape. These data can be used to build simple echograms (Castro *et al*., 1992) and to characterize the behaviour of different species (Piasente *et al*., 2004) or behaviour under different conditions, such as fish-escape behaviour under the influence of fish density (Godø *et al*., 1999), codend pulsing (O'Neill *et al*., 2003), towing speed and density (Jones *et al*., 2008), and mesh type (Engås *et al*., 1988). Basic quantitative observations from video can also be used to parametrize models. Kim and Wardle (2003) used swimming speed, acceleration, and angular velocity to classify behaviour as "optomotor" or "erratic". These observations were then used in a model based on chaos theory in a neural network to predict fish responses in the mouth of a trawl (Kim and Wardle, 2005). Reid *et al*. (2007) used video footage of monkfish (*Lophius piscatorius*) responses to sweeps, wing tips, and groundgear to produce quantitative information for an individual-based, particle-tracking model of behaviour ahead of a survey trawl. Information such as the initial state of the fish, different response behaviours and angle of movement, and distance moved in response to sweeps, allowed estimation of probability of escape over multiple interactions (Reid *et al*., 2007).

Understanding the differences in behaviour of different species provides the basis for the development of modifications to fishing gear in order to mitigate bycatch and discarding. Observations of differences in swimming behaviour between haddock (*Melanogrammus aeglefinus*) and whiting (*Merlangius merlangus*), which tend to rise towards the top sheet of the net as they fall back, and cod (*Gadus morhua*), which enter the net much lower down, formed the basis of the horizontal-separator panel. Other examples where video observations of behaviour have been used in the development of such tools include the separation of squid (*Loligo pealeii*) and scup (*Stenotomus chrysops*) in the inshore squid fishery of Massachusetts (Glass *et al*., 2001), and the separation of halibut (*Hippoglossus stenolepis*), cod (*Gadus macrocephalus*), and sole in the North Pacific groundfish fishery (Rose, 1995; Gauvin, 2008). The development of successful bycatch reduction devices (BRDs) is often an iterative process, and video observation alongside selectivity experiments can reveal valuable information, such as reactions to differences in water flow near BRDs (Engås *et al*., 1999), where and when fish escape from a grid or panel (Grimaldo *et al*., 2008), and

differences in behavioural responses to "fluttering" as opposed to tense netting panels (Grimaldo *et al*., 2007).

Behaviour can be very different at low light levels, and flash photography, ICCD cameras, and infrared illumination have revealed the lack of ordered orientation, avoidance, and escape behaviour in various species (Glass and Wardle, 1989; Walsh and Hickey, 1993; Matsuoka *et al*., 1997; Olla *et al*., 1997, 2000). There is still a lack of sufficient knowledge of behaviour in low light conditions that may be best addressed by the use of observation tools that do not require light, such as the Didson acoustic camera.

5.5.2 Behaviour towards stationary gear (pots and longlines)

Video, particularly stereo video, has been used extensively to study schooling behaviour (Dill *et al*., 1981; van Long *et al*., 1985). Pitcher *et al*. (1985) used a pair of 35 mm synchronized still cameras to collect three-dimensional information on fish in schools and determined that mackerel and herring choose neighbours of a similar size. The structure of fish schools, including nearest-neighbour distance and external shape, has been studied using annular-tank and shadow methods (Partridge *et al*., 1980). More recently, the study of schooling behaviour in relation to fishery surveys has used multibeam sonars, but observations of individuals from larger-scale studies are still required. Stereo video is also useful for studying fish swimming *in situ* (Klimley and Brown, 1983; Long and Aoyama, 1985; van Rooij and Videler, 1996) and for length measurements in aquaculture (McFarlane and Tillet, 1997; Shieh and Petrell, 1998; Steeves *et al*., 1998; Lines *et al*., 2001).

Tank-based observations using surveillance video with multiple cameras installed above a tank capturing 1 fps have been used to assess the reactions of fish to underwater noise, such as that of a wind turbine. The video allowed the position of fish to be quantified in relation to the noise source over periods of days (Müller, 2007). Other work investigating the reaction of elasmobranchs to electric fields (Stoner and Kaimmer, 2008) looked at magnetic deterrents for spiny dogfish (*Squalus acanthias*), using tank experiments and video.

5.6 Video-based electronic monitoring of fishing operations

Howard McElderry

5.6.1 Introduction

Video-based electronic monitoring (EM) is becoming a key part of the fishery monitoring toolbox, particularly in situations where traditional observer-based alternatives would be logistically or financially impractical.

Over the past decade Archipelago Marine Research Ltd. ("Archipelago") has pioneered the development of video-based electronic monitoring technology for monitoring commercial fishing activities. A number of pilot studies have been carried out to test the efficacy of this technology. Table 5.1 lists more than 25 studies spanning diverse geographies, fisheries, fishing vessels, gear types, and fishery monitoring challenges. This work, summarized in McElderry (2008), demonstrates its suitability across a range of monitoring issues, including fishing location, catch, catch handling, fishing methods, quota management, protected species interactions, and use of mitigation measures.

Although appropriate to monitoring in situations that are unsuitable for observers, EM is also useful in placements on vessels with observers, recognizing that it may be impossible for an observer to simultaneously monitor different parts of a fishing vessel. A significant advance resulting from EM technology is the ability to audit the accuracy of "self-reported data", or fishing information provided by vessel personnel. This capability, widely used in British Columbia groundfish fisheries, encourages industry involvement in data-collection activities, provides veracity to self-sample data, and allows the creation of fully documented fisheries more efficiently than possible with an observer programme.

5.6.2 Technology overview

A typical EM system, shown schematically in Figure 5.4, consists of up to eight closed circuit television (CCTV) cameras, a GPS receiver, a hydraulic pressure sensor, winch sensors, and a control centre with user interface (keyboard and monitor). In some cases, a satellite modem may be included to send hourly system health and activity updates to the fishery or monitoring agency. Ancillary sensors used in some applications may include radio frequency identification (RFID) tag readers and net pinger hydrophones.

The control centre is usually located on the bridge with wiring to all sensors, cameras, and to the ship's electrical power (DC or AC). The control centre monitors system performance, records time-stamped sensor and video data alongside GPS coordinates, and provides a continuous display of EM system status and on-deck activity for the wheelhouse crew. All data are recorded on a high-capacity hard drive that is retrieved when the fishing vessel returns to port. Wireless transmission of EM data has not been employed (with the exception of brief satellite updates) because data volumes are very large, and therefore not suitable for real-time reporting.

Table 5.1. Summary of electronic monitoring (EM) studies by Archipelago Marine Research Ltd. (Source: McElderry, 2008.) Monitoring application: EM = Effort Monitoring; CM = Catch Monitoring; DM = Discard Monitoring; CH = Catch Handling; PS = Protected Species; MP = Mitigation Practices.

Year	Region	Fishery/species	Gear	Client	Monitoring application	Vessels	Days	Status
1999	Canada	BC Area A Crab Trap	Trap	Area A Crab Association	EM, CM, DM, CH, PS, MP	50	2500	Adopted
2002	Canada	BC Salmon Seine	Seine	Fisheries and Oceans Canada	EM	1	19	Pilot
2003	Canada	BC Halibut Longline	Longline	Fisheries and Oceans Canada/Pacific Halibut Management Association	EM, DM, CH, PS, MP	19	459	Pilot
2003	Canada	BC Salmon Troll	Troll	Fisheries and Oceans Canada	EM, CM, DM, PS	4	60	Pilot
2003	Canada	BC Prawn Trap	Trap	Fisheries and Oceans Canada/Pacific Prawn Fishermen's Association	EM, CM	1	60	Pilot
2005	Canada	BC Groundfish Longline	Longline	Fisheries and Oceans Canada/BC Commercial Integ. Groundfish Society	EM	230	12 000	Adopted
2006	Canada	BC Midwater Trawl (hake)	Trawl	Fisheries and Oceans Canada	EM, CM	35	2500	Adopted
2007	Canada	BC Inshore Trawl (groundfish)	Trawl	Fisheries and Oceans Canada/ BC Commercial Integ. Groundfish Society	EM, DM	12	1000	Adopted
2002, 2009	USA (Alaska)	Alaska Halibut Longline	Demersal Longline	International Pacific Halibut Commission	EM, CM, DM	2	120	Pilot
2003	USA (Alaska)	Alaska Groundfish Factory Trawl	Trawl	National Marine Fisheries Service (NMFS)	EM, CM, DM, PS, MP	5	200	Pilot
2005, 2007	USA (Alaska)	Alaska Rockfish Trawl	Trawl	Groundfish Data Bank	EM, PS, MP	10	40	Pilot
2006–11	USA (Alaska)	Alaska Groundfish Factory Trawl	Factory Trawl	US Seafoods	EM, DM	8	1600	Adopted
2006–07	USA (California)	California Drift Gillnet (swordfish)	Drift Gillnet	National Marine Fisheries Service (NMFS)	EM, CM	5	58	Pilot
2007–10	USA (California)	California Groundfish Fixed Gear	Longline/Trap	The Nature Conservancy	EM, CM, DM, PS, MP	4	200	Pilot
2007–11	USA (Florida)	Gulf of Mexico Snapper/Grouper Longline	Demersal Longline	National Marine Fisheries Service (NMFS)	EM, CM, DM, PS	6	250	Pilot
2008	USA (Hawaii)	Hawaii Pelagic Longline (tuna/swordfish)	Pelagic Longline	Western Pacific Regional Fishery Management Council	EM, CM, DM, PS	4	250	Pilot
2010	USA (N. Carolina)	South Atlantic Snapper/Grouper	Longline/Bandit	University of North Carolina	EM, CM, PS, MP	6	250	Pilot
2004, 2007	USA (New England)	New England Fixed Gear (cod, haddock)	Longline	Cape Cod Hook Fishermen's Association (CCCHFA)	EM, CM, DM	4	50	Pilot
2007	USA (New England)	New England Herring	Small Mesh Trawl	Cape Cod Hook Fishermen's Association (CCCHFA)	EM, CM, DM	1	10	Pilot
2010, 2011	USA (New England)	New England Groundfish	Trawl/Gillnet/Longline	National Oceanic and Atmospheric Administration (NOAA)	EM, CM, DM, PS	10	800	Pilot
2002, 2005–2010	USA (WA/OR)	WOC Midwater Trawl Shorebased Hake	Midwater Trawl	National Oceanic and Atmospheric Administration (NOAA)	EM, CM, DM, PS	30	1500	Adopted
2008	EU (Denmark)	North Sea Groundfish	Trawl/Seine/Gillnet	National Institute for Aquatic Resources (DTU Aqua)	EM, DM	20	3000	Adopted
2010	EU (England)	North Sea Groundfish	Trawl/Seine	Centre for Environment, Fisheries and Aquaculture Science (CEFAS)	EM, DM	12	1800	Adopted
2010	EU (England)	Irish Sea Groundfish	Trawl	Centre for Environment, Fisheries and Aquaculture Science (CEFAS)	EM, DM	5	500	Adopted
2011	EU (Germany)	North Sea Groundfish	Trawl/Gillnet	VTI Baltic, Kutterfisch/ WWF Germany	EM, DM	6	600	Pilot
2011	EU (Netherlands)	North Sea Groundfish	Trawl/Seine	IMARES/VisNed	EM, DM	2	300	Pilot

Year	Region	Fishery/species	Gear	Client	Monitoring application	Vessels	Days	Status
2009	EU (Scotland)	North Sea Groundfish	Trawl/Seine/Gillnet	The Scottish Government	EM, DM	25	4000	Adopted
2008	EU (Sweden)	North Sea Groundfish	Trawl/Seine/Gillnet	Swedish Board of Fisheries	EM, DM	2	250	Pilot
2005	Australia	South Australia Shark	Gillnet	Australian Fisheries Management Authority (AFMA)	EM, DM	1	16	Pilot
2005	Australia	HIMI Toothfish	Longline	Australian Fisheries Management Authority (AFMA)	EM, PS	1	48	Pilot
2005	Australia	Eastern Tuna Billfish	Longline	Australian Fisheries Management Authority (AFMA)	EM, PS	1	40	Pilot
2005	Australia	Tasmania Small Pelagics (redbait, mackerel)	Midwater Trawl	Australian Fisheries Management Authority (AFMA)	EM	1	42	Pilot
2009	Australia	Eastern Tuna Billfish	Pelagic Longline	Australian Fisheries Management Authority (AFMA)	EM, PS	10	1500	Pilot
2010	Australia	Northern Prawn Fishery	Trawl	Australian Fisheries Management Authority (AFMA)	EM, CM, DM, PS	1	50	Pilot
2010	Australia	Pilbara (West Australia) Trawl (snapper)	Trawl	Australian Fisheries Management Authority (AFMA)	EM, PS	1	70	Pilot
2011	Australia	South Australia Shark	Gillnet	Australian Fisheries Management Authority (AFMA)	EM	10	In progress	Pilot
2003	New Zealand	Inshore Groundfish Setnet	Gillnet	Seafood Industry Council (SeaFIC)	EM, PS	5	82	Pilot
2003	New Zealand	Hoki Midwater Trawl	Midwater Trawl	Hoki/Squid Fishery Management Company Ltd.	EM, CM, PS, MP	1	31	Pilot
2007	New Zealand	Pelagic Longline (tuna)	Longline	Ministry of Fisheries/Department of Conservation	EM, PS, MP	2	60	Pilot
2007	New Zealand	Demersal Longline (groundfish)	Longline	Ministry of Fisheries/Department of Conservation	EM, CM, DM, PS, MP	2	50	Pilot
2008	New Zealand	Inshore Trawl (groundfish)	Trawl	New Zealand Department of Conservation	EM, CM, PS, MP	2	800	Pilot
2011	New Zealand	Inshore Snapper	Demersal Longline	New Zealand Department of Conservation	EM, CM, PS, MP	4	In progress	Pilot

Monitoring application: EM = Effort Monitoring; CM = Catch Monitoring; DM = Discard Monitoring; CH = Catch Handling; PS = Protected Species; MP = Mitigation Practices.

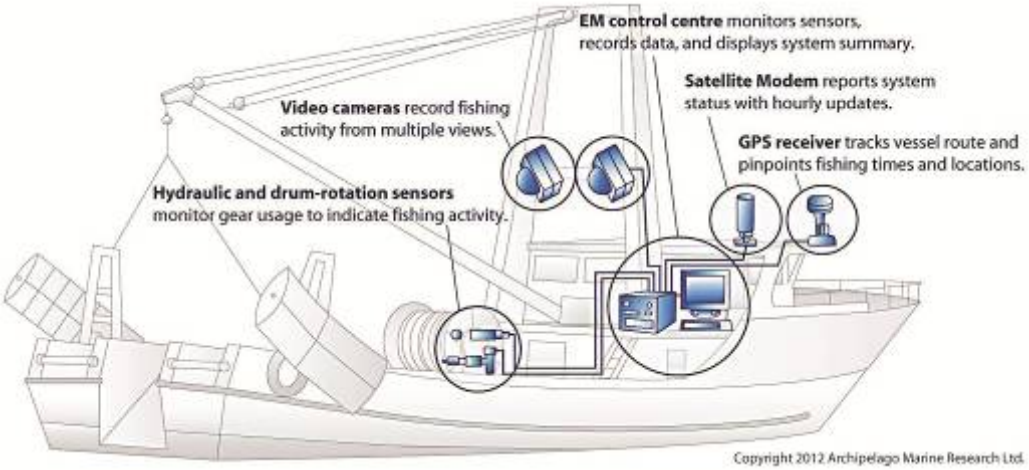

Figure 5.4. Schematic of an electronic monitoring system illustrates the main components and typical placement on a fishing vessel.

The GPS receiver is mounted in the vessel rigging or on a cabin ceiling away from other electronics, where it can provide independent information on vessel position, speed, heading, and time. The electronic pressure transducer is installed on the supply side of the hydraulic system and indicates when hydraulic equipment (winches, pumps, lifts, etc.) is operating. An optical sensor is mounted on winches to detect their activity. CCTV cameras are mounted to the vessel standing structure in locations that provide unobstructed views of key fishing activities, such as hauling, sorting, processing, and discards. Some cameras may be configured to provide a wide overview of deck activity, whereas others provide a close-up view of key areas or activities (for example, to aid in species identification at the discard chute).

The EM system is designed to operate continuously throughout the fishing trip, starting automatically when powered, resuming functions after a power interruption, and restarting itself in the event of a software lockup. EM sensor data are recorded continuously for the entire fishing trip, with a typical frequency of one data line per 10 s interval. The data storage requirement for sensor data is about 0.5 Mb per day.

Image data are generally recorded according to various selectable criteria. Common configurations include continuous recording while the vessel is not in port, recording only during fishing operations (as sensed by hydraulic or winch sensor activity), or recording from the start of the first fishing event until the vessel returns to port. The EM system records imagery from up to four cameras at selectable recording rates, ranging from 1 to 30 fps (frames per second). All recorded images include a text overlay indicating vessel name, date, time, and position.

Data capacity requirements for image files vary according to frame rates, the number of active cameras, recording specifications, and image compression (Codec) settings. Image files are much larger than sensor data files, ranging from 100 to more than 1000 Mb per camera per hour. The commercial availability of inexpensive high capacity (500 Gb) hard drives allows sufficient data storage for most monitoring applications.

The EM system provides a comprehensive sensor and image data record of the fishing trip. Data analysis is primarily concerned with integrity and quality of the data, then with the specific monitoring objectives. Sensor data are interpreted using a temporal and spatial display (Figure 5.5) to determine the time and location of fishing

and other vessel activities during the fishing trip. Next, image data are interpreted to make specific observations on a range of issues, as explained in Section 5.6.2).

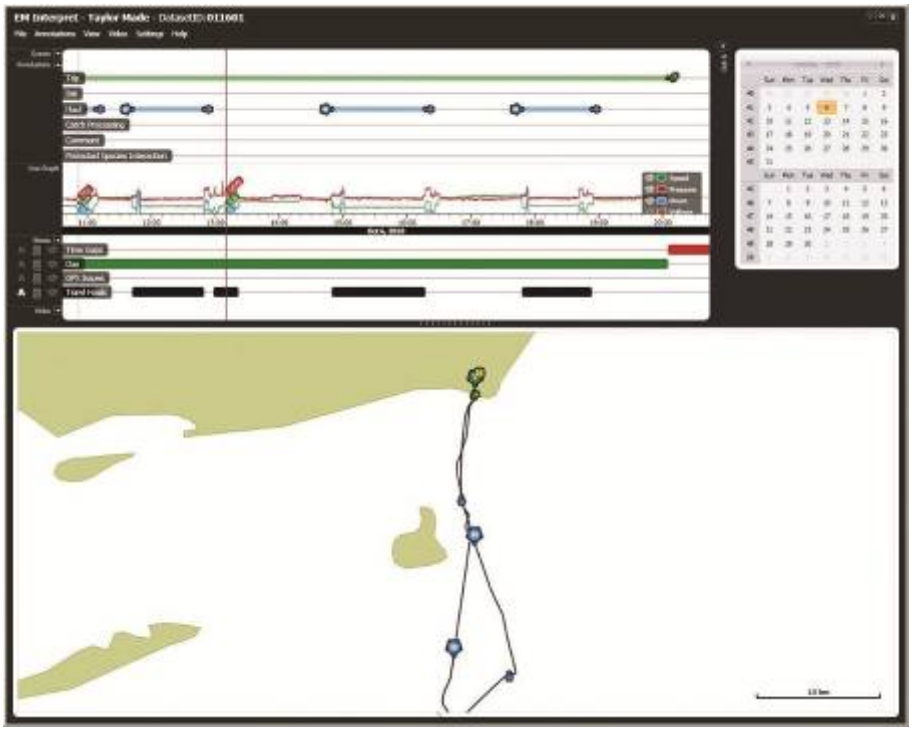

Figure 5.5. Plot showing setting and hauling activities on a groundfish longline vessel. The time-series (top) depicts vessel speed, drum (winch) rotations, and hydraulic pressure. The map (bottom) displays a GPS plot indicating the vessel cruise track, and the location of gear setting and hauling activities.

The EM data analysis varies according to the fishery monitoring objectives, image quality, and quantity of data. Sensor data are usually interpreted rapidly, typically requiring only a few hours to review an entire two-week fishing trip. Image interpretation is more complex to process, but can generally be performed at rates much lower than the actual elapsed time. EM image files can be readily played on most standard Microsoft Windows-based media player software products. The complexity lies with multiple camera views that must be played synchronously for a reviewer to fully interpret vessel activities. Using catch census on the British Columbia groundfish longline fishery as an example, image processing can be done at ca. 60% of real time, whereas monitoring deployment of seabird mitigation devices can take less than 10% of real time.

5.6.3 EM and suitability for fisheries monitoring

5.6.3.1 Pros and cons of EM

The advantages and disadvantages of electronic monitoring need to be compared with observer programmes – the only other method that provides credible and trustworthy data. Table 5.2 outlines the pros and cons of EM against the observer alternative in terms of operational issues and monitoring efficacy. It offers a compelling advantage in terms of cost and labour requirements; for example, observer costs are more than three times the cost of EM in British Columbia groundfish fisheries; the methods require 14 h vs. 2.5 h of program labour per sea day, respectively (McElderry, 2008).

Table 5.2. Electronic Monitoring vs. Observers–Pros and Cons (from McElderry and Gislason (in press)).

Operational Issues	EM Pros/Cons Relative to Observers	
1. Vessel suitability	Pro	• EM on-vessel space requirement is much less (observers require ample accommodation and workspace)
2. Intrusiveness	Pro	• EM is less intrusive than observers; does not disrupt crew dynamics • EM does not slow on-board handling and processing
3. Equipment reliability	Con	• EM equipment can break down
4. Equipment tampering	Con	• EM equipment can be made tamper-resistant and tamper-evident, but not tamper-proof • Regulatory system needs to recognize and penalize tampering
5. Data credibility	Pro	• 100% observer coverage is required to prevent "observer bias" (i.e. strategic behaviour of skippers on observed trips), but there also are logistical issues to getting observers on board scheduled trips (e.g. weather-related events) • EM offers more precise recording of time and location
6. Observer reliability	Pro	• Unlike a person, an EM camera does not get sick
7. Viewscape	Pro	• EM provides multiple views of a vessel simultaneously, whereas an observer can only be in one place at a time and requires rest periods
Monitoring efficacy		
8. Continuous, permanent record	Pro	• Fishing event imagery can be sampled or reviewed in full • Reviewers have a range of playback controls, such as speed, replay, frame capture, etc., to optimize viewing conditions • An observer has one chance to record a fishing event
9. Species identification	Con	• Observers are better positioned to distinguish hard-to-identify species, but EM is good for most species • Number of cameras and quality of camera placement affects EM resolution • EM performs better when catch is landed in a serial manner (e.g. groundfish trawl can present challenges)
10. Catch volumes	Con	• EM can only record catch in pieces, not weight • Observers have a better opportunity to weigh the catch
11. Real-time capability	Con	• Observer data can be in real time, EM cannot
Cost		
12. Cost-effective	Pro	• EM is 1/3 or less the cost of 100% observer programme in most applications • An EM programme requires less labour
Other		
13. Health and safety	Pro	• EM can alleviate health and safety concerns tied to an observer being aboard a fishing vessel
14. Biosampling	Con	• Observers can do biosampling, EM cannot

Often, catch monitoring is the most important information objective in a fishery monitoring programme. At-sea monitoring programmes generally document catch by species and quantity, including both retained and discarded catch. The use of EM for catch monitoring has been examined in a number of studies, and its efficacy depends on several factors. Catch quantities, species distinctiveness, fishing method, and on-board handling practices determine whether or not catch can be reliably determined from EM image data. Further, the number of cameras and their placement affect image resolution and complexity, and consequently the ease with which the imagery can be interpreted.

Fishing gears such as longline and gillnet receive their catch aboard in a serial manner, and multiple cameras can be set up to observe catch as it moves through the retrieval process. Retrieval rates are generally slow, with crew removing catch items from the gear. Demersal longline fishing usually uses short (<0.5 m) branch lines, and

nearly all catch items are brought to or over the rail (Figure 5.6). Gillnet gear is similarly conducive to monitoring by EM, because catch items can be counted and identified as they are disentangled from the gear. Pelagic longline fishing, which employs much longer branch lines (3–5 m) and a more involved landing process, is more complicated to monitor, with the possibility of certain species being released before coming into camera view.

Figure 5.6. Example EM camera view from a longline vessel showing each individual fish as it is hauled from the water and onto the vessel, allowing for rapid identification of the species.

The use of EM to monitor catch with trap fishing may also be complex. In some cases, trap contents are emptied into a hopper from which it is sorted and processed. If the hopper is not cleared between trap hauls, it may be difficult to count catch contents on a trap-by-trap basis. The best solution is to position a camera over the point where catch is removed from the hopper and to census catch from this control point. This method may require a change in crew behaviour to ensure that all trap contents are placed in the hopper and all catch pass by the control point. An example of trap fishing is shown in Figure 5.7.

Figure 5.7. Example EM camera views from a BC sablefish trap vessel showing (upper left) trap hauling and fish hopper, (lower left) census control point where a crew member removes fish from hopper, and (right), a close-up view of the discard chute.

Fishing gears such as seines and trawlnets bring catch aboard *en masse*, making it difficult to determine catch composition, unless the catch can be directed past a specific control point, for example, a fish chute or conveyor, where individual catch items can be recognized; however, in many instances, the quantities of fish are too large for this to be practical. Camera positions on trawlers generally provide wide-angle views of the entire fishing deck, making it difficult to recognize specific elements of the catch. Generally, EM is not used to completely census catch in trawl fisheries because of the large quantities associated with each fishing event.

When cameras are positioned so that they provide close-up views of catch items, EM generally provides sufficient resolution to identify catch species, although observers are better able to identify catch to species level, particularly species that are uncommon or closely resemble each other. For catch quantification, EM probably does the better job, because retrieval events are easier to observe from images where viewing speed can be adjusted as necessary, halted to provide the viewer with rest breaks, or replayed to double-check interpretations. The permanent data record also allows images from the same events to be examined more than once.

EM can be reliable for monitoring catch utilization, provided that fish handling operations occur within the camera's field of view. Receiving fish under camera but discarding them over the other side of the vessel, or later when the cameras are switched off, would not be detected, whereas observers can more easily monitor these events.

5.6.4 Catch handling

Some fisheries prescribe particular methods for on-board catch handling to ensure bycatch viability and proper catch accounting. EM has been tested successfully in a variety of instances, such as seine fisheries involving special brailing requirements; longline and trawl fisheries requiring measurement of catch prior to release (Figure 5.8); and factory trawl fisheries, where the observer requires assurance that catch is not sorted prior to sampling. EM provides multiple simultaneous views that make it easier to monitor large, complex operations. The main shortcoming of EM is the difficulty of providing camera coverage of all areas on a fishing vessel where catch handling occurs (although newer EM systems address this by supporting additional cameras). Also, some catch-handling requirements may be very subtle, and may be difficult or time consuming to detect.

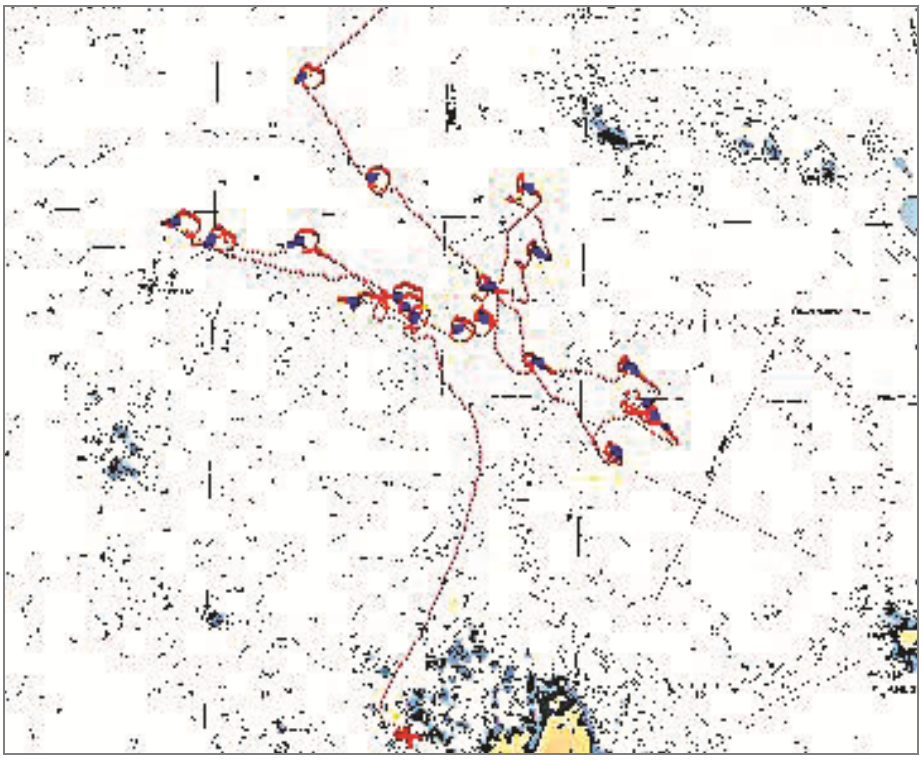

Figure 5.8. A spatial plot showing vessel cruise track from a salmon seine fishing trip. The cruise track is shown in red; hydraulic pressure spikes corresponding to net retrieval are shown in blue.

5.6.5 Fishing methods

Vessel activity determined from sensor data and confirmed by camera images can be used to accurately position fishing activities and monitor compliance with area closures, marine protected areas, and other area restrictions (Figure 5.9). The same information can be applied to gear-control measures, such as the amount of gear, soak limits, temporal and spatial gear restrictions, deployment of mitigation devices, and other applications. The incorporation of RFID technology provides an effective approach to monitoring the use of trap and other fishing gear.

Figure 5.9. Example EM camera views from a trawl vessel showing (left) close-up view of the discard chute and (right) complete view of the fishing deck.

5.6.6 Protected-species interaction

Protected species include threatened or endangered species of marine mammals, seabirds, and sea turtles. Protected species interact with fisheries in a variety of ways, including directly as catch, or simply being in the vicinity of fishing operations where they may be harmed. Many at-sea monitoring programmes concentrate on monitoring protected-species interaction, and fishery coverage can be problematic because encounter rates are often low. The use of EM for protected-species monitoring has been proposed as a more cost-effective way of achieving desired coverage levels. Catch interaction of protected species can often be easily detected using EM, if the species are brought within camera view. As these items are often distinct from the target catch, image-review times may be very fast, particularly if the only purpose of catch monitoring is to monitor protected-species captures.

The use of EM for non-catch-related protected-species interaction is less clear. Seabird interaction with trawl warps can be characterized but are difficult to quantify. More general monitoring of protected-species presence in the vicinity of fishing vessels can be difficult because image resolution is poor. The combined motion of the vessel and water, and the lack of a fixed visual reference (i.e. a horizon), create viewing conditions in which it is difficult to resolve animals. EM would also not be very useful for monitoring deck landings of seabirds because of the number of cameras required to monitor areas where seabirds could board.

5.6.7 Mitigation measures

Mitigation measures are designed to limit protected-species interaction with fishing vessels. These measures may include specific devices such as net pingers, seabird streamer lines, and escape panels. EM is particularly useful with devices such as streamer lines because their effectiveness can be easily assessed from images played back much faster than real time. Similarly, a hydrophone can be used to monitor acoustic effectiveness of marine-mammal-deterring net pingers. In contrast, trawl escape grids may be more difficult because EM can confirm placement (prior to deployment) but not performance.

Mitigation measures may also include procedures such as restrictions on the discharge of offal, or where and when fishing gear may be operated. Mitigation through restrictions on fishing gear has been covered previously.

5.6.8 Conclusion

Video-based electronic monitoring has proven to be a practical and cost-effective alternative to traditional observer-based methods for a wide range of fisheries and gear types. At approximately one-third the cost of an observer, an EM programme can be used in place of an at-sea observer programme or as part of an integrated fishery monitoring initiative in conjunction with at-sea observers, dockside observers, logbooks, and hail programs. A large vessel now has the option of implementing a multicamera system, or combining an at-sea observer with EM, in which the EM system would assume catch reporting duties, freeing the observer for more specialized tasks such as biological sampling, weighing, analysis, and interpretation.

As a compact, automated solution, electronic monitoring is proving to be a particularly attractive alternative for smaller to mid-sized vessels where observer-based monitoring can be too costly or impractical owing to space restrictions, limited resources, or other logistical concerns. As the technology evolves, EM users can expect to benefit from enhanced reliability, sharper imagery, and greater data storage.

By providing an efficient and affordable means to gather and analyse fishing activity data, video-based electronic monitoring is providing progressive fisheries with the tools to ensure a level playing field across all vessels, and to support sustainable resource-management initiatives on a fleet-wide basis.

5.7 Habitat classification

5.7.1 Benthic

The application of optics to seabed classification has largely been a matter of collecting images of the seabed and using them for classification. The number of classifications and their descriptions depend on the location and purpose of the classification. One purpose that is becoming more important is monitoring to observe any long-term changes, especially for critical habitat, such as coral reefs and seagrass beds.

The advantage of underwater cameras is that the high resolution that can be obtained provides very detailed information (Figures 5.10 and 5.11), and they can be used at any depth. They have been used in studies of coral reefs (I. Williams *et al.*, 2001; Edmunds, 2002; Lirman *et al.*, 2007), and for all habitat types (Rosenkranz *et al.*, 2008). For shallow corals, nearly the same level of detail can be obtained at higher speed from a surface vessel (Riegl *et al.*, 2001). Larger areas can also be classified quickly using a combination of acoustics and underwater video (Rooper and Zimmermann, 2007; Holmes *et al.*, 2008). Under the right conditions, LLS imagers can provide more detailed information than simple underwater cameras (Amend *et al.*, 2007).

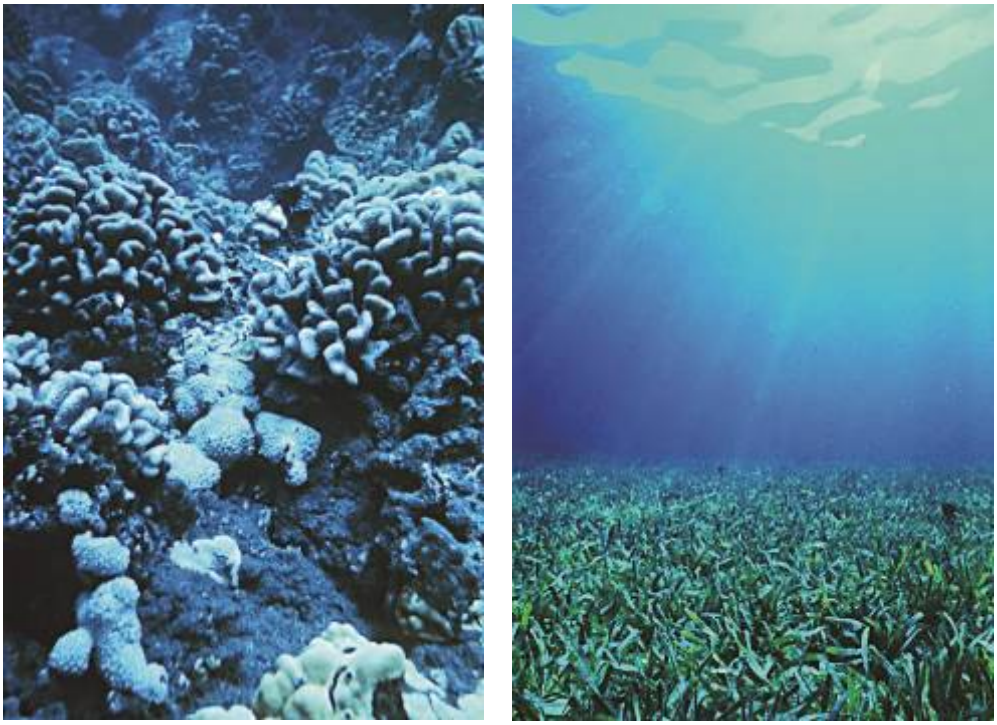

Figure 5.10. Underwater images of coral and seagrass. (Images courtesy of the NOAA Online Photo Library.)

Figure 5.11. Underwater image of organisms on a rocky reef. (Image courtesy of H. Singh, Woods Hole Oceanographic Institution.)

One example is the Mareano programme, in which the seabed of northern Norway was explored using video and multibeam surveys to assess the distribution of megafauna and examine associations of benthic organisms with their physical environment (Buhl-Mortensen *et al.*, 2009). The study area was initially divided into ten marine landscapes, based on seabed morphology and general water-mass distribution. In total, 195 taxa were observed during video recordings. The largest number of taxa was found within fjord/coast and upper-slope landscapes.

Multivariate statistical methods were used to relate bottom environment and taxonomic composition and to find the relation between faunal groups and landscapes.

For shallow-water habitats, airborne and satellite images can provide information over large areas. The resolution that can be achieved, of course, is generally less than that of in-water images. This technique has been used for shallow coral reefs (Mumby *et al*., 1998; Cuevas-Jimenez *et al*., 2002; Armstrong *et al*., 2006) and seagrass beds (Dierssen *et al*., 2003; Holmes *et al*., 2007). To cover even larger areas, satellite images have been used for both corals (Palandro *et al*., 2003; Benfield *et al*., 2007) and seagrass (Ferguson and Korfmacher, 1997; Mumby and Edwards, 2002). Hyperspectral images are able to provide even more information about water depth and type of vegetation than standard three-colour images (Alberotonza *et al*., 1999).

5.7.2 Pelagic

The pelagic habitat is characterized by water temperature, salinity, nutrient levels, light levels, and productivity. Several of these can be estimated remotely by passive optical methods. The primary application of these methods has been global mapping of the pelagic habitat from space using two types of imaging radiometers. The first uses mid- or far-infrared to measure SST. The second uses a combination of visible and near-infrared to measure ocean colour and derived quantities. Examples of routinely measured parameters from orbiting optical imagers are listed in Table 5.3. These are mainly products from the moderate resolution imaging spectroradiometer (MODIS) on the Aqua satellite, although one example is from the Sea-viewing Wide Field-of-view Sensor (SeaWIFS) on OrbView-2.

Table 5.3. Examples of ocean parameters routinely measured from satellite-based optical radiometers (http://oceancolour.gsfc.nasa.gov/PRODUCTS/).

Parameter	Optical wavelengths (nm)	Instrument
Sea surface temperature (SST)	4000, 11 000	MODIS
Normalized water-leaving radiance	412, 443, 488, 531, 551, 667	MODIS
Chlorophyll *a*	Various combinations of water-leaving radiance wavelengths	MODIS
Diffuse-attenuation coefficient	490	MODIS
Photosynthetically active radiation (PAR)	400–700	SeaWIFS
Primary productivity	Those for SST, Chl *a*, and PAR	MODIS

Although temperature profiles cannot be obtained from space, SST estimates are routinely produced from infrared radiometers in orbit. Figure 5.12 shows an example of global SST from the 11 μm imaging radiometer that is part of MODIS. These images are 2007 seasonal averages with spatial resolution of 4 km. Shorter averages begin to develop data gaps, depending on orbital characteristics and cloud cover.

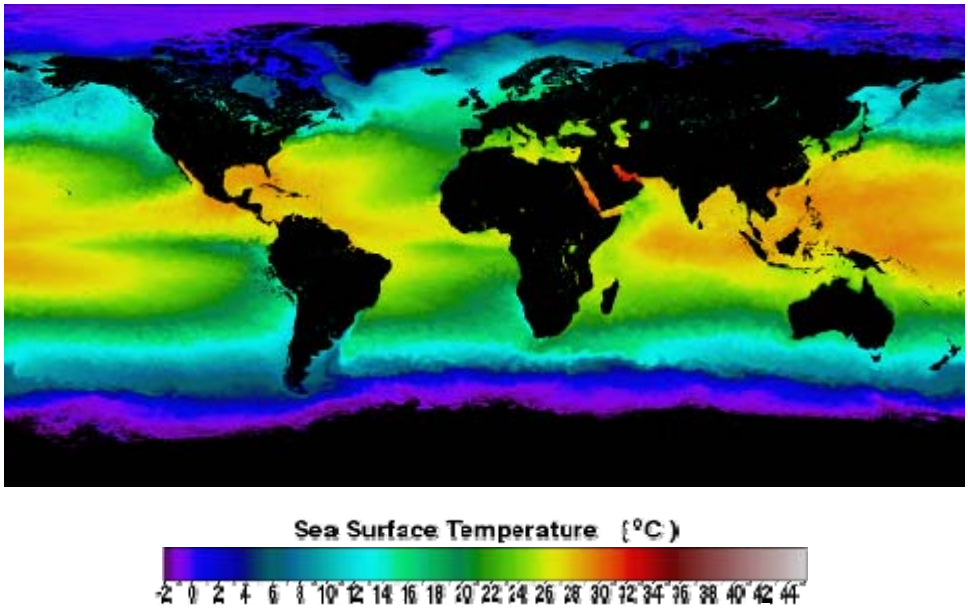

Figure 5.12. Sea surface temperature (SST) averaged over summer 2007. (Source: Aqua MODIS 11 μm data.)

The first orbiting ocean-colour sensor was the Coastal Zone Colour Scanner launched in 1978. This was very successful, and a host of other instruments followed. There are currently nine operational sensors. The primary product of these instruments is the water-leaving radiance at a variety of wavelengths across the visible and near-infrared. From these data, products like those listed in Table 5.3 can be derived. More information on sensors and products is available from the International Ocean Colour Coordinating Group (http://www.ioccg.org/), together with an extensive database of ocean-colour publications.

One of the most robust products of the ocean-colour imagers is the chlorophyll *a* concentration in surface waters. Figure 5.13 presents an example of a seasonal average from the MODIS imager on the Aqua satellite. Plankton blooms are clear in the northern summer. Although chlorophyll concentration is a useful tool for understanding the spatial and temporal distribution of productivity in the ocean, it is not the only factor. Quantitative estimates of primary productivity are obtained from remotely sensed estimates of chlorophyll, irradiance, and temperature (Campbell *et al.*, 2002).

Salinity cannot be measured by remote optical techniques. However, some indication can be obtained where there is a strong correlation between salinity and some other quantifiable factor. An example would be the observation of fresh river plumes using optical estimates of suspended sediments, which are available from orbiting ocean-colour imagers like MODIS. The same applies to the remote measurement of nutrient levels in the water.

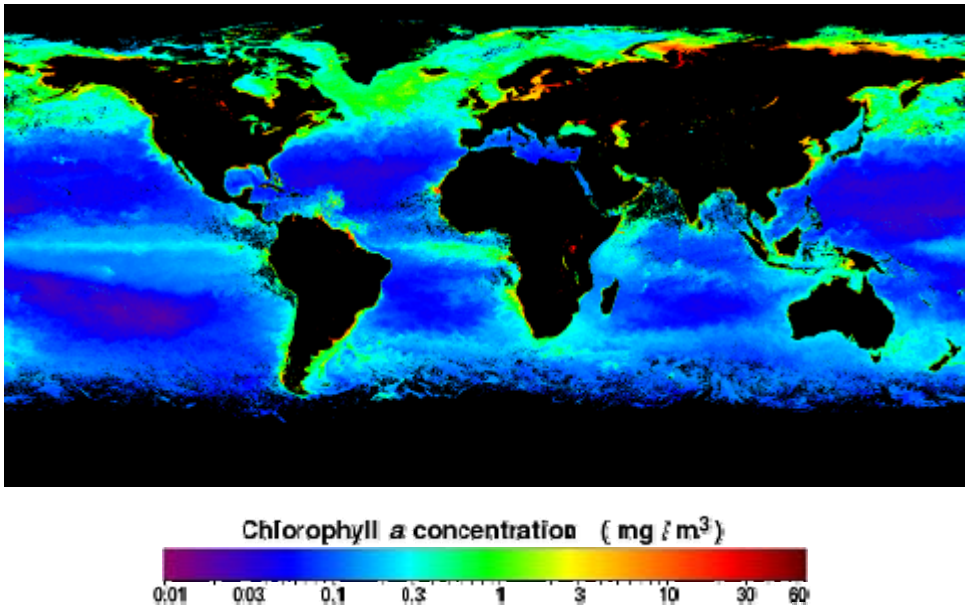

Figure 5.13. Chlorophyll *a* concentrations averaged over summer 2007. (Source: Aqua MODIS ocean-colour data.)

6 Recommendations

We do not recommend the establishment of an ICES working group on optical technologies at this time. Many optical techniques that have been developed for other applications can be applied directly to fisheries and to fishery–oceanography problems with little modification. Continued development in optical techniques will benefit fishery applications without direction from the fishery community.

We do recommend a larger involvement of the optics community in the Working Group on Fishery Acoustics Science and Technology (WGFAST). The combined power of acoustics and optics has been demonstrated in a number of areas, and we expect more combined studies in future. There are two areas combining acoustics and optics that are particularly promising:

1) A remotely located camera system (e.g. towed, AUV, ROV) combined with acoustic surveys. In principle, this could provide species identification and information about fish length and orientation needed to estimate TS while underway. With this information, few, if any, trawls would be needed to support the acoustic survey.

2) An adaptive survey for epipelagic species that uses an aerial survey with lidar and photography to direct an acoustic survey so that the surface vessel time is concentrated in the most important regions. This technique would provide a survey with lower overall cost and greater precision than an acoustic survey alone. How well this will work for any particular species will depend on the depth distribution of that species (Lo *et al*., 2000).

7 References

Abdo, D. A., Seager, J. W., Harvey, E. S., McDonald, J. I., Kendrick, G. G., and Shortis, M. R. 2006. Efficiently measuring complex sessile epibenthic organisms using a novel photogrammetric technique. Journal of Experimental Biology and Ecology, 339: 120–133.

Adams, L. P. 1982. Underwater analytical photogrammetry using non-metric cameras. International Archives of Photogrammetry, 24(5): 12–22.

Adams, P. B., Butler, J. L., Baxter, C. E., Laidig, T. E., Dahlin, K. A., and Wakefield, W. W. 1995. Population estimates of Pacific coast groundfishes from video transects and swept-area trawls. Fishery Bulletin US, 93: 446–455.

Ahlen, J., and Bengtsson, E. 2005. Evaluation of underwater spectral data for colour correction applications. Proceedings of the 14th Scandinavian Conference on Image Analysis (SCIA 2005), 19–22 June 2005, Joensuu, Finland. Lecture Notes in Computer Science, 3540: 1148–1156.

Alberotanza, L., Brando, V. E., Ravagnan, C., and Zandonella, A. 1999. Hyperspectral aerial images. A valuable tool for submerged vegetation recognition in the Orbetello Lagoons, Italy. International Journal of Remote Sensing, 20: 52–33.

Albert, O. T., Harbitz, A., and Hoines, A. S. 2003. Greenland halibut observed by video in front of survey trawl: behaviour, escapement, and spatial pattern. Journal of Sea Research, 50: 117–127.

Alcala, M. L. R., and Vogt, H. 1997. Approximation of coral reef surfaces using standardized growth forms and video counts, *In* Proceedings of the 8th International Coral Reef Symposium, 4–29 June 1996, Panama, Vol. 2, pp. 1453–1458. Ed. by H. A. Lessios and I. G. Macintyre. Smithsonian Tropical Research Institute, Panama.

Amend, M., Yoklavich, M. M., Rzhanov, Y., Grimes, C. B., and Wakefield, W. W. 2007. Mosaics of benthic habitats using laser line scan technology: it's in the details. *In* Mapping the Seafloor for Habitat Characterization, pp. 61–70. Ed. by B. Todd and H. G. Greene. Geological Association of Canada. Special Paper 47.

Anderson, J. T., Holliday, V., Kloser, R., Reid, D., and Simard, Y. 2007. Acoustic seabed classification of marine physical and biological landscapes. ICES Cooperative Research Report No. 286. 198 pp.

Anderson, J. T., Holliday, D. V., Kloser, R., Reid, D. G., and Simard, Y. 2008. Acoustic seabed classification: current practice and future directions. ICES Journal of Marine Science, 65: 1004–1011.

Anderson, L. A., and Smalley, J. K. 2008. Dependable and accurate surveying of hydrophones. Sea Technology, 49: 15–20.

Armstrong, R. A., Singh, H., Torres, J., Nemeth, R. S., Can, A., Roman, C., Eustice, R., *et al.* 2006. Characterizing the deep insular shelf coral reef habitat of the Hind Bank marine conservation district (US Virgin Islands) using the Seabed autonomous underwater vehicle. Continental Shelf Research, 26: 194–205.

Aronson, R. B., Edmunds, P. J., Precht, W. F., Swanson, D. W., and Levitan, D. R. 1994. Large-scale long-term monitoring of the Caribbean coral reefs: simple, quick, inexpensive techniques. Atoll Research Bulletin, 421: 1–19.

Auster, P. J., Lindholm, J., Plourde, M., Barber, K., and Singh, H. 2005. Camera configuration and use of AUVs to census mobile fauna. Marine Technology Society Journal, 41: 49–52.

Austin, R. W., and Petzold, T. J. 1986. Spectral dependence of the diffuse attenuation coefficient of light in ocean waters. Optical Engineering, 25: 471–479.

Bahr, A., and Leonard, J. J. 2006. Cooperative localization for autonomous underwater vehicles. *In* Proceedings of the 10th International Symposium on Experimental Robotics (ISER '06), 6–10 July 2006, Rio de Janeiro, Brazil. Springer Tracts in Advanced Robotics, 39: 387–395. Springer 2008. ISBN 978-3-540-77456-3.

Baldwin, R. A., and Newton, I. 1982. A proposed system for underwater photogrammetry from a manned submersible camera platform. International Archives of Photogrammetry, 24(5): 39–52.

Bazeille, S., Quidu, I., and Jaulin, L. 2007. Identification of underwater man-made objects using colour. Proceedings of the Institute of Acoustics, 29: 45–52.

Benfield, M. C., Wiebe, P. H., Stanton, T. K., Davis, C. S., Gallager, S. M., and Green, C. H. 1998. Estimating the spatial distribution of zooplankton biomass by combining Video Plankton Recorder and single-frequency acoustic data. Deep-Sea Research II, 45: 1175–1199.

Benfield, M. C., Grosjean, P., Culverhouse, P. F., Irigoien, X., Sieracki, M. E., Lopez-Urrutia, A., Dam, H. G., *et al.* 2007. RAPID: Research on Automated Plankton Identification. Oceanography, 20: 172–187.

Berkelmans, R., and Oliver, J. K. 1999. Large-scale bleaching of corals on the Great Barrier Reef. Coral Reefs, 18: 55–60.

Blaxter, J. H. S., and Parrish, B. B. 1966. The reaction of marine fish to moving netting and other devices in tanks. Marine Research, 1966(1): 15 pp.

Blaxter, J. H. S., Parrish, B. B., and Dickson, W. 1964. The importance of vision in the reaction of fish to drift nets and trawls. *In* Modern Fishing Gear of the World, Vol. 2, pp. 529–536. Ed. by H. Kristjonsson. Fishing News Ltd, London.

Bonacci, L. A., and Wakefield, W. W. 2009. Pilot work using a codend video camera for improved acoustic interpretation of backscatter observed during fisheries acoustic surveys. Journal of the Acoustical Society of America, 125: 2551–2551.

Bowles, J., Kappus, M., Antoniades, J., Baumback, M., Czarnaski, M., Davis, C. O., and Grossmann, J. 1998. Calibration of inexpensive pushbroom imaging spectrometers. Metrologia, 35: 657–661.

Bradley, A. M., Feezor, M. D., Singh, H., and Sorrell, F. Y. 2001. Power systems for autonomous underwater vehicles. IEEE Journal of Oceanic Engineering, 26(4): 526–538.

Brown, E. D., Churnside, J. H., Collins, R. L., Veenstra, T., Wilson, J. J., and Abnett, K. 2002. Remote sensing of capelin and other biological features in the North Pacific using lidar and video technology. ICES Journal of Marine Science, 59: 1120–1130.

Buhl-Mortensen, P., Buhl-Mortensen, L., Dolan, M., Dannheim, J. and Kröger, K. 2009. Megafaunal diversity associated with marine landscapes of northern Norway: a preliminary assessment. Norwegian Journal of Geology, 89: 163–171.

Busck, J. 2005. Underwater 3-D optical imaging with a gated viewing laser radar. Optical Engineering, 44: 116001-1–116001-7.

Buskey, E. J., and Hyatt, C. J. 2006. Use of the FlowCAM for semi-automated recognition and enumeration of red tide cells (*Karenia brevis*) in natural plankton samples. Harmful Algae, 5: 685–692.

Cadalli, N., Munson, D. C., and Singer, A. C. 2002. Bistatic receiver model for airborne lidar returns incident on an imaging array from underwater objects. Applied Optics, 41: 3638–3649.

Campbell, J., Antoine, D., Armstrong, R., Arrigo, K., Balch, W., Barber, R., Behrenfeld, M., *et al.* 2002. Comparison of algorithms for estimating ocean primary production from surface chlorophyll, temperature, and irradiance. Global Biogeochemical Cycles, 16: 74–75.

Carleton, J. H., and Done, T. J. 1995. Quantitative video sampling of coral reef benthos: large-scale application. Coral Reefs, 14: 35–46.

Carrera, P., Churnside, J. H., Boyra, G., Marques, V., Scalabrin, C., and Uriarte, A. 2006. Comparison of airborne lidar with echosounders: a case study in the coastal Atlantic waters of southern Europe. ICES Journal of Marine Science, 63: 1736–1750.

Castro, K. M., DeAlteris, J. T., and Milliken, H. O. 1992. The application of a methodology to quantify fish behaviour in the vicinity of demersal trawls in the Northwest Atlantic, USA. *In* Proceedings of the MTS '92 Conference on Global Ocean Partnership, 19–21 October 1992, Washington, DC, Vol. 1: 310–315. Marine Technology Society.

Chang, P. C. Y., Flitton, J. C., Hopcraft, K. I., Jakeman, E., Jordan, D. L., and Walker, J. G. 2003. Improving visibility depth in passive underwater imaging by use of polarization. Applied Optics, 42: 2794–2803.

Chen, H-H., and Lee, C-J. 2000. A simple underwater video system for laser tracking. *In* Oceans 2000: Where Marine Science and Technology Meet. Proceedings of the MTS/IEEE Oceans Conference, 11-14 September 2000, Providence, RI. Vol. 3: 1543–1548.

Chong, A. K., and Stratford, P., 2002. Underwater digital stereo-observation technique for red hydrocoral study. Photogrammetric Engineering and Remote Sensing, 68: 745–751.

Churnside, J. H., and Donaghay, P. L. 2009. Spatial characteristics of thin scattering layers observed by airborne LIDAR. ICES Journal of Marine Science, 66: 778–789.

Churnside, J. H., and Hunter, J. R. 1996. Laser remote sensing of epipelagic fishes. *In* Laser Remote Sensing of Natural Waters: From Theory to Practice, pp. 3–53. Ed. by V. I. Feigels and Y. I. Kopilevich. Proceedings of SPIE, 2964. 224 pp.

Churnside, J. H., and McGillivary, P. A. 1991. Optical properties of several Pacific fishes. Applied Optics, 30: 2925–2927.

Churnside, J. H., and Thorne, R. E. 2005. Comparison of airborne lidar measurements with 420 kHz echo-sounder measurements of zooplankton. Applied Optics, 44: 5504– 5511.

Churnside, J. H., and Wilson, J. J. 2004. Airborne lidar imaging of salmon. Applied Optics, 43: 1416–1424.

Churnside, J. H., Tatarskii, V. V., and Wilson, J. J. 1997. Lidar profiles of fish schools. Applied Optics, 36: 6011–6020.

Churnside, J. H., Wilson, J. J., and Tatarskii, V. V. 2001a. Airborne lidar for fisheries applications. Optical Engineering, 40: 406–414.

Churnside, J. H., Sawada, K., and Okumura, T. 2001b. A comparison of airborne lidar and echo sounder performance in fisheries. Journal of the Marine Acoustical Society of Japan, 28: 49–61.

Churnside, J. H., Demer, D. A., and Mahmoudi, B. 2003. A comparison of lidar and echo sounder measurements of fish schools in the Gulf of Mexico. ICES Journal of Marine Science, 60: 147–154.

Churnside, J. H., Demer, D. A., Griffith, D., Emmett, R. L., and Brodeur, R. D. 2009a. Comparisons of lidar, acoustic and trawl data on two scales in the northeast Pacific Ocean. CalCOFI Reports, 50: 118–122.

Churnside, J. H., Ostrovsky, L., and Veenstra, T. 2009b. Thermal footprints of whales. Oceanography, 22: 206–209.

Churnside, J. H., Tenningen, E., and Wilson, J. J. 2009c. Comparison of data-processing algorithms for fish lidar detection of mackerel in the Norwegian Sea. ICES Journal of Marine Science, 66: 1023–1028.

Churnside, J. H., Sharov, A. F., and Richter, R. A. 2011a. Aerial surveys of fish in estuaries: a case study in Chesapeake Bay. ICES Journal of Marine Science, 68: 239–244.

Churnside, J. H., Brown, E. D., Parker-Stetter, S., Horne, J. K., Hunt, G. L., Hillgruber, N., Sigler, M. F., *et al.* 2011b. Airborne remote sensing of a biological hot spot in the southeastern Bering Sea. Remote Sensing, 3: 621–637.

Clarke, M. E., Tolimieri, N., and Singh, H. 2009. Using the SeaBED AUV to assess populations of groundfish in untrawlable areas. *In* The Future of Fisheries Science in North America: Fish and Fisheries Series, Vol. 31, pp. 357–372. Ed. by R. Beamish and B. Rothschild. Springer, New York. 736 pp.

Coates, C. G., Denvir, D. J., McHale, N. G., Thornbury, K. D., and Hollywood, M. A. 2004. Optimizing low-light microscopy with back-illuminated electron multiplying charge-coupled device: enhanced sensitivity, speed, and resolution. Journal of Biomedical Optics, 9: 1244.

Coles, B. W., Radzelovage, W., Jean-Laurant, P. J., and Reihani, K. 1998. Processing techniques for multi-spectral laser line scan images. *In* Oceans '98: Engineering for Sustainable Use of the Oceans. Proceedings of the IEEE/OES Oceans Conference, 28 September–1 October 1998, Nice, France, 3: 1766–1179. IEEE Oceanic Engineering Society.

Costa, C., Loy, A., Cataudella, S., Davis, D., and Scardi, M. 2006. Extracting fish size using dual underwater cameras. Aquacultural Engineering, 35: 218–227.

Cruz, I. C. S., Kikuchi, R. K. P., and Leão, Z. M. A. N. 2008. Use of the video transect method for characterizing the Itacolomis Reefs, eastern Brazil. Brazilian Journal of Oceanography, 56: 271–280.

Cuevas-Jimenez, A., Ardisson, P-L., and Condal, A. R. 2002. Mapping of shallow coral reefs by colour aerial photography. International Journal of Remote Sensing, 23: 3697–3712.

Cullen, J. M., Shaw, E., and Baldwin, H. A. 1965. Methods for measuring the three-dimensional structure of fish schools. Animal Behaviour, 13: 534–543.

Culverhouse, P. F., Williams, R., Reguera, B., Ellis, R. E., and Parisini, T. 1996. Automatic categorisation of 23 species of dinoflagellate by artificial neural network. Marine Ecological Progress Series, 139: 281–287.

Culverhouse, P. F., Williams, R., Reguera, B., Herry, V., and González-Gil, S. 2003. Do experts make mistakes? Marine Ecological Progress Series, 247: 17–25.

Dalen, J., and Bodholt, H. 1991. Deep-towed vehicle for fish abundance estimation, concept and testing. ICES Document CM 1991/B:53. 13 pp.

Dalen, J., Totland, A., and Stenersen, E. 2000. Upgrading and rebuilding of a deep towed vehicle system for the EU project "REDFISH". Report to the "REDFISH" project QLRT-PL 1999–01222, Institute of Marine Research, Bergen, Norway, 29 September 2000. 18 pp.

Dalen, J., Nedreaas, K., and Pedersen, R. 2003. Comparative acoustic abundance estimation of pelagic redfish (*Sebastes mentella*) from hull mounted and deep towed acoustic systems. ICES Journal of Marine Science, 60: 472–479.

Davis, C. O., Bowles, J., Leathers, R. A., Korwan, D., Downes, T. V., Snyder, W. A.., Rhea, W. J., *et al.* 2002. Ocean PHILLS hyperspectral imager: design, characterization, and calibration. Optics Express, 10: 210–221.

DeWeert, M. J., Moran, S. E., Ulich, B. L., and Keeler, R. N. 1999. Numerical simulations of the relative performance of streak-tube, range-gated, and pmt-based airborne imaging lidar systems with realistic sea surfaces. *In* Airborne and In-Water Underwater Imaging, pp. 115–129. Ed. by G. D. Gilbert. Proceedings of SPIE, 3761: 198 pp.

Dierssen, H. M., Zimmerman, R. C., Leathers, R. A., Downes, T. V., and Davis, C. O. 2003. Ocean color remote sensing of seagrass and bathymetery in the Bahamas Banks by high-resolution airborne imagery. Limnology and Oceanography, 48: 444–455.

Dill, L. M., Dunbrack, R. L., and Major, P. F. 1981. A new stereographic technique for analyzing the three-dimensional structure of fish schools. Environmental Biology of Fishes, 6: 7–13.

Doray, M., Josse, E., Gervain, P., Reynal, L., and Chantrel, J. 2007. Joint use of echosounding, fishing and video techniques to assess the structure of fish aggregations around moored fish aggregating devices in Martinique (Lesser Antilles). Aquatic Living Resources, 20: 357–366.

Eatherley, D. M. R., Thorley, J. L., Stephen, A. B., Simpson, I., MacLean, J. C., and Youngson, A. F. 2005. Trends in Atlantic salmon: the role of automatic fish counter data in their recording. Scottish Natural Heritage Commissioned Report No. 100 (ROAME No. F01NB02). 55 pp.

Edmunds, P. J. 2002. Long-term dynamics of coral reefs in St John, US Virgin Islands. Coral Reefs, 21: 357–367.

Edwards, B. D., Dartnell, P., and Chezar, H. 2003. Characterizing benthic substrates of Santa Monica Bay with seafloor photography and multibeam sonar imagery. Marine Environmental Research, 56: 47–66.

Ellis, D. M., and DeMartini, E. E. 1995. Evaluation of a video camera technique for indexing abundances of juvenile pink snapper, *Pristipomoides filamentosus*, and other Hawaiian insular shelf fishes. Fishery Bulletin US, 93: 67–77.

Engås, A., Isaksen, B., and Valdemarsen, J. W. 1988. Escape behaviour of fish in codends in bottom trawls. *In* Proceedings of the Square Mesh Workshop, 25 November 1988, St John's, Newfoundland. Ed. by H. A. Carr. Massachusetts Division of Marine Fisheries, 2: 60–64.

Engås, A., Foster, D., Hataway, B. D., Watson, J. W., and Workman, I., 1999. The behavioural response of juvenile red snapper (*Lutjanus campechanus*) to shrimp trawls that utilize water flow modifications to induce escapement. Marine Technology Society Journal, 33: 43–50.

Ferguson, R., and Korfmacher, K. 1997. Remote sensing and GIS analysis of seagrass meadows in North Carolina, USA. Aquatic Botany, 58: 241–258.

Forbes, H. E., Smith, G. W., Johnstone, A. D. F., and Stephen, A. B. 1990. An assessment of the performance of the resistivity fish counter in the Borland lift fish pass at Dundreggan dam on the River Moriston. Fisheries Research Services Report No. 02/00, Fisheries Research Services, Marine Laboratory, Aberdeen. 13 pp.

Fournier, G. R., Bonnier, D., Forand, J. L., and Pace, P. W. 1993. Range-gated underwater imaging system. Optical Engineering, 32: 2185–2190.

Gabr, M., Fujimori, Y., Shimizu, S., and Miura, T. 2007. Behaviour analysis of undersized fish escaping through square meshes and separating grids in simulated trawling experiment. Fisheries Research, 85: 112–121.

Gallager, S. M., Singh, H., Tiwari, S., Howland, J., Rago, P., Overholtz, W., Taylor, R., *et al.* 2005. High resolution underwater imaging and image processing for identifying essential fish habitat, p. 50. *In* Report of the National Marine Fisheries Service Workshop on Underwater Video Analysis, August 4–6, 2004. Ed. by D. A. Somerton and C. T. Gledhill. US Department of Commerce, NOAA Technical Memorandum, NMFS-F/SPO-68. 69 pp.

Gauldie, R. W., Sharma, S. K., and Helsley, C. E. 1996. Lidar applications to fisheries monitoring problems. Canadian Journal of Fisheries and Aquatic Sciences, 53: 1459–1468.

Gauvin, J. R., 2008. Final Report on EFP 06–03 to Develop a Halibut Excluder for the Gulf of Alaska Shoreside Cod Trawl Fishery. Marine Conservation Alliance Foundation. 22 pp.

Gilbert, G. D., and Pernicka, J. C. 1967. Improvement of underwater visibility by reduction of backscatter with a circular polarization technique. Applied Optics, 6: 741–745.

Glass, C. W., and Wardle, C. S. 1989. Comparison of the reactions of fish to a trawl gear, at high and low light intensities. Fisheries Research, 7: 249–266.

Glass, C. W., and Wardle, C. S. 1995. Studies on the use of visual stimuli to control fish escape from codends. II. The effect of a black tunnel on the reaction behaviour of fish in otter trawl codends. Fisheries Research, 23: 165–174.

Glass, C. W., Wardle, C. S., and Gosden, S. J. 1993. Behavioural studies of the principles underlying mesh penetration by fish. ICES Marine Science Symposia, 196: 92–97.

Glass, C. W., Wardle, C. S., Gosden, S. J., and Racey, D. N. 1995. Studies on the use of visual stimuli to control fish escape from codends. I. Laboratory studies on the effect of a black tunnel on mesh penetration. Fisheries Research, 23: 157–164.

Glass, C. W., Carr, H. A., Sarno, B., Matsushita, Y., Morris, G. D., Feehan, T., and Pol, M. V. 2001. Bycatch, discard and impact reduction in Massachusetts inshore squid fishery. Paper presented at the ICES Working Group on Fisheries Technology and Fish Behaviour (FTFB), 23–27 April 2001, Seattle, WA, USA.

Godø, O. R., Walsh, S. J., and Engås, A. 1999. Investigating density-dependent catchability in bottom-trawl surveys. ICES Journal of Marine Science, 56: 292–298.

Gordon, D. C., McKeown, D. L., Steeves, G., Vass, W. P., Bentham, K., and Chin-Yee, M. 2007. Canadian imaging and sampling technology for studying benthic habitat and biological communities. *In* Mapping the Seafloor for Habitat Characterization, pp. 29–37. Ed. by B. J. Todd and H. G. Greene. Geological Association of Canada, Special Paper 47.

Granshaw, S. I. 1980. Bundle adjustment methods in engineering photogrammetry. The Photogrammetric Record, 10: 181–207.

Griffis, A. J. 2000. Demonstration and evaluation of the streak tube imaging LIDAR for use in bycatch reduction. Saltonstall Kennedy Grant NA77FD0045 Report 96-SWR-010. National Marine Fisheries Service, Southwest Region, Long Beach, CA, USA.

Grimaldo, E., Larsen, R. B., and Holst, R. 2007. Exit windows as an alternative selective system for the Barents Sea demersal fishery for cod and haddock. Fisheries Research, 85: 295–305.

Grimaldo, E., Sistiaga, M., and Larsen, R. B., 2008. Evaluation of codends with sorting grids, exit windows, and diamond meshes. Size selection and fish behaviour. Fisheries Research, 91: 271–280.

Grosjean, P., Picheral, M., Warembourg, C., and Gorsky, G. 2004. Enumeration, measurement, and identification of net zooplankton samples using the ZOOSCAN digital imaging system. ICES Journal of Marine Science, 61: 518–525.

Gruev, V., Ortu, A., Lazarus, N., Van der Spiegel, J., and Engheta, N. 2007. Fabrication of a dual-tier thin film micropolarization array. Optics Express, 15: 4994–5007.

Gurshin, C. W. D., Jech, J. M., Howell, W. H., Weber, T. C., and Mayer, L. A. 2009. Acoustic backscatter and density measurements of captive Atlantic cod using a 300-kHz multibeam sonar synchronized with a 120-kHz split-beam echosounder. ICES Journal of Marine Science, 66: 1303–1309.

Hartley, R., and Zisserman, A. 2004. Multiple View Geometry in Computer Vision., 2nd edn. Cambridge University Press, Cambridge, UK. 650 pp.

Harvey, E. S., and Shortis, M. R. 1996. A system for stereo-video measurement of sub-tidal organisms. Marine Technology Society Journal, 29: 10–22.

Harvey, E. S., and Shortis, M. R. 1998. Calibration stability of an underwater stereo-video system: Implications for measurement accuracy and precision. Marine Technology Society Journal, 32: 3–17.

Harvey, E., Fletcher, D., and Shortis, M. 2001a. A comparison of the precision and accuracy of estimates of reef-fish lengths determined visually by divers with estimates produced by a stereo-video system. Fishery Bulletin US, 99: 63–71.

Harvey, E., Fletcher, D., and Shortis, M. 2001b. Improving the statistical power of length estimates of reef fish: a comparison of estimates determined visually by divers with estimates produced by a stereo-video system. Fishery Bulletin US, 99: 72–80.

Harvey, E., Fletcher, D., and Shortis, M. 2002. Estimation of reef fish length by divers and by stereo-video. A first comparison of the accuracy and precision in the field on living fish under operational conditions. Fisheries Research, 57: 255–265.

Harvey, E., Shortis, M., Stadler, M., and Cappo, M. 2003a. A comparison of the accuracy and precision of measurements from single and stereo-video system. Marine Technology Society Journal, 36: 38–49.

Harvey, E., Cappo, M., Shortis, M., Robson, S., Buchanan, J., and Speare, P. 2003b. The accuracy and precision of underwater measurements of length and maximum body depth of southern bluefin tuna (*Thunnus maccoyii*) with a stereo-video camera system. Fisheries Research, 63: 315–326.

Harvey, E., Fletcher, D., Shortis, M. R., and Kendrick, G. A. 2004. A comparison of underwater visual distance estimates made by scuba divers and a stereo-video system: implications for underwater visual census of reef fish abundance. Marine and Freshwater Research, 55: 573–580.

He, D-M., and Seet, G. G. L. 2001. Underwater LIDAR imaging in highly turbid waters. *In* Ocean Optics: Remote Sensing and Underwater Imaging, pp. 71–81. Ed. by R. J. Frouin and G. D. Gilbert. Proceedings of SPIE, 4488: 280 pp.

He, D-M., and Seet, G. G. L. 2004. Underwater lidar imaging scaled by 22.5 cm/ns with serial targets. Optical Engineering, 433: 754–766.

He, P., and Wardle, C. S. 1988. Endurance at intermediate swimming speeds of Atlantic mackerel, *Scomber scombrus* L., herring, *Clupea harengus* L., and saithe, *Pollachius virens* L. Journal of Fish Biology, 33: 255–266.

Heckman, P. J., and Hodgson, R. T. 1967. Underwater optical range gating. IEEE Journal of Quantum Electronics, QE-3: 445–448.

Heger, A., Ieno, E. N., King, N. J., Morris, K. J., Bagley, P. M., and Priede, I. G. 2008. Deep-sea pelagic bioluminescence over the Mid-Atlantic Ridge. Deep-Sea Research II, 55: 126–136.

Heikkila, J., and Silven, O. 1997. A four-step camera calibration procedure with implicit image correction. Proceedings of the IEEE Computer Society Conference on Computer Vision and Pattern Recognition, 17–19 June 1997, San Juan, Puerto Rico (CVPR '97): 1106–1112.

Hemmings, C. C. 1969. Observations on the behaviour of fish during capture by the Danish seine net, and their relation to herding by trawl bridles. *In* FAO Conference on Fish Behaviour in Relation to Fishing Gear Techniques and Tactics, 19–27 October 1967, Bergen, pp. 645–655. Ed. by A. Ben-Tuvia and W. Dickson. FAO Fisheries Report No. 62(3).

Hemmings, C. C. 1973. Direct observation of the behaviour of fish in relation to fishing gear. Helgolander Wissenschaftliche Meeresuntersuchungen, 24: 348–360.

Herman, A. W. 1988. Simultaneous measurement of zooplankton and light attenuance with a new optical plankton counter. Continental Shelf Research, 8: 205–221.

Herman, A. W. 1992. Design and calibration of a new optical plankton counter capable of sizing small zooplankton. Deep-Sea Research, 39: 395–415.

Herman, A. W., Beanlands, B., and Phillips, E. F. 2004. The next generation of Optical Plankton Counter: the Laser-OPC. Journal of Plankton Research, 26: 1135–1145.

Holmes, J. A., Cronkite, G. M. W., Enzenhofer, H. J., and Mulligan, T. J. 2006. Accuracy and precision of fish-count data from a "dual-frequency identification sonar" (DIDSON) imaging system. ICES Journal of Marine Science, 63: 543–555.

Holmes, K. W., van Niel, K. P., Kendrick, G. A., and Radford, B. 2007. Probabilistic large-area mapping of seagrass species distributions. Aquatic Conservation: Marine and Freshwater Ecosystems, 17: 385–407.

Holmes, K. W., Van Niel, K. P., Radford, B., Kendrick, G. A., and Grove, S. L. 2008. Modelling distribution of marine benthos from hydroacoustics and underwater video. Continental Shelf Research, 28: 1800–1810.

Houk, P., and van Woesik, R. 2006. Coral reef benthic video surveys facilitate long-monitoring and the Commonwealth of the Northern Mariana Islands: toward an optimal sampling strategy. Pacific Science, 60: 177–189.

Hou, W., Lee, Z., and Weidemann, A. D. 2007. Why does the Secchi disk disappear? An imaging perspective. Optics Express, 15: 2791–2802.

Hughes, N. F., and Kelly, L. H. 1996. New techniques for 3-D video tracking of fish swimming movements in still or flowing water. Canadian Journal of Fisheries and Aquatic Sciences. 53: 2473–2483.

Huse, I., and Skiftesvik, A. B. 1990. A PC-aided video-based system for behaviour observation of fish larvae and small aquatic invertebrates. Aquacultural Engineering, 9: 131–142.

Jaffe, J. S., Ohman, M. D., and De Robertis, A. 1998. OASIS in the sea: measurement of the acoustic reflectivity of zooplankton with concurrent optical imaging. Deep-Sea Research II, 45: 1239–1253.

Jaffe, J. S., Moore, K. D., McLean, J., and Strand, M. P. 2001. Underwater optical imaging: status and prospects. Oceanography, 14: 66–76.

Jerlov, N. G. 1976. Marine Optics. Elsevier, Amsterdam. 231 pp.

Jones, E. G., Summerbell, K., and O'Neill, F. G. 2008. The influence of towing speed and fish density on the behaviour of haddock in a trawl cod-end. Fisheries Research, 94: 166–174.

Joyce, K. E., and Phinn, S. R. 2003. Hyperspectral analysis of chlorophyll content and photosynthetic capacity of coral reef substrates. Limnology and Oceanography, 48: 489–496.

Kalacska, M., Sanchez-Azofeifa, G. A., Rivard, B., Caelli, T., White, H. P., and Calvo-Alvarado, J. C. 2006. Ecological fingerprinting of ecosystem succession. Estimating secondary tropical dry forest structure and diversity using imaging spectroscopy. Remote Sensing of the Environment, 108: 82–96.

Kang, D., Cho, S., Lee, C., Myoung, J-G., and Na, J. 2009. *Ex situ* target-strength measurements of Japanese anchovy (*Engraulis japonicus*) in the coastal northwest Pacific. ICES Journal of Marine Science, 66: 1219–1224.

Katz, J., Donaghay, P. L., Zhang, J., King, S., and Russell, K. 1999. Submersible holocamera for detection of particle characteristics and motions in the ocean. Deep-Sea Research I, 46: 1455–1481.

Kikuchi, R. K. P, Leão, Z. M. A. N., Testa, V., Dutra, L. X. C., and Spanó, S. 2003a. Rapid assessment of the Abrolhos Reefs, eastern Brazil (Part 1: Stony corals and algae). Atoll Research Bulletin, 496: 172–187.

Kikuchi, R. K. P, Leão, Z. M. A. N., Sampaio, C. L. S., and Telles, M. D. 2003b. Rapid assessment of the Abrolhos Reefs, eastern Brazil (Part 2: Fish communities). Atoll Research Bulletin, 496: 189–204.

Kim, Y. H., and Wardle, C. S. 2003. Optomotor response and erratic response: quantitative analysis of fish reaction to towed fishing gears. Fisheries Research, 60: 455–470.

Kim, Y. H., and Wardle, C. S. 2005. Basic modelling of fish behaviour in a towed trawl based on chaos in decision-making. Fisheries Research, 73: 217–229.

King, B. R. 1995. Bundle adjustment of constrained stereopairs – mathematical models. Geomatics Research Australia, 63: 67–92.

Klimley, A. P., and Brown, S. T. 1983. Stereophotography for the field biologist: measurement of lengths and three-dimensional positions of free-swimming sharks. Marine Biology, 74: 175–185.

Knox, C. 1966. Holographic microscopy as a technique for recording dynamic microscopic subjects. Science, 153: 989–990.

Kocak, D. M., Dalgleish, F. R., Caimi, F. M., and Schechner, Y. Y. 2008. A focus on recent developments and trends in underwater imaging. Marine Technology Society Journal, 42: 52–67.

Korotkow, W. K., and Martyschewski, W. N. 1977. Results obtained by the use of the underwater device "Atalant" for the study on how fish behave and how trawl nets operate. Fischerei-Forschung Schriftenreihe, 15: 39–43.

Krekova, M. K., Krekov, G. M., Samokhvalov, I. V., and Shamanaev, V. S. 1994. Numerical evaluation of the possibilities of remote sensing of fish schools. Applied Optics, 33: 5715–5720.

Kutser, T., and Jupp, D. B. L. 2006. On the possibility of mapping between corals to the species level based on their optical signatures. Estuarine, Coastal and Shelf Science, 69: 607–614.

Lamberg, A., Fiske, P., and Hvidsten, N. A. 2001. Forsøk med videoregistrering av anadrom fisk i elv. Norwegian Institute for Nature Research, Trondheim, NINA Oppsdragsmedling, 715: 1–26.

Larsen, B. M., Lamberg, A., and Hvidsten, N. A. 1995. Metoder for overvåkning av gytebestander av anadrom laksefisk. Norwegian Institute for Nature Research, Trondheim, NINA Oppdragsmelding, 331: 1–36.

Lauver, E. D. 2006. Priest Rapids Project Video Fish-Counting Program Annual Report 2005, Prepared for The Public Utility District No. 2 of Grant County, Washington, USA.

Leatherdale, J. D., and Turner, J. 1983. Underwater photogrammetry in the North Sea. Photogrammetric Record, 11: 151–167.

Lethlean, N. G. 1953. An investigation into the design and performance of electric fish-screens and an electric fish-counter. Transactions of the Royal Society of Edinburgh, 62: 479–526.

Leujak, W., and Ormond, R. F. G. 2007. Comparative accuracy and efficiency of six coral community survey methods. Journal of Experimental Marine Biology and Ecology, 351: 168–187.

Li, R., Li, H., Zou, W., Smith, R. G., and Curran, T. A. 1997. Quantitative photogrammetric analysis of digital underwater video imagery. IEEE Journal of Oceanic Engineering, 22: 364–375.

Lines, J. A., Tillet, R. D., Ross, L. G., Chan, D., Hockaday, S., and McFarlane, N. J. B. 2001. An automatic image-based system for estimating the mass of free-swimming fish. Computers and Electronics in Agriculture, 31: 151–168.

Lirman, D., Gracias, N. R., Gintert, B. E., Gleason, A. C. R., Reid, R. P., Negahdaripour, S., and Kramer, P. 2007. Development and application of a video-mosaic survey technology to document the status of coral reef communities. Environmental Monitoring and Assessment, 125: 59–73.

Lo, N. C. H, Hunter, J. R., and Churnside, J. H. 2000. Modeling statistical performance of an airborne lidar survey for anchovy. Fishery Bulletin US, 98: 264–282.

Lundgren, B., and Nielsen, J. R. 2008. A method for the possible species discrimination of juvenile gadoids by broad-bandwidth backscattering spectra vs. angle of incidence. ICES Journal of Marine Science, 65: 581–593.

Lundgren, B., Nielsen, H., Nielsen, J. R., and Faber, P. 2001. Estimation of 3D position, angle of attitude, and orientation of free-swimming fish in a hydroacoustic beam field under variable lighting conditions. Proceedings of the 12th Scandinavian Conference of Image Analysis (SCIA 2001), 11–14 June 2001, Bergen: 382–390.

MacLennan, D. N., and Simmonds, E. J. 1992. Fisheries Acoustics. Chapman and Hall, London, UK. 325 pp.

Main, J., and Sangster, G. I. 1981a. A study of the fish capture process in a bottom trawl by direct observation from a towed underwater vehicle. Department of Agriculture and Fisheries for Scotland, Scottish Fisheries Research Report No. 23. 23 pp.

Main, J., and Sangster, G. I. 1981b. A study of the sand clouds produced by trawl boards and their possible effect on fish capture. Department of Agriculture and Fisheries for Scotland, Scottish Fisheries Research Report No. 20. 20 pp.

Malkiel, E., Alquaddoomi, O., and Katz, J. 1999. Measurements of plankton distribution in the ocean using submersible holography. Measurement Science and Technology, 10: 1142–1152.

Malkiel, E., Sheng, Katz, J., and Strickler, J. R. 2003. The three-dimensional flow field generated by a feeding calanoid copepod measured using digital holography. Journal of Experimental Biology, 206: 3657–3666.

Martin, J. C., and Yamanaka, K. L. 2004. A visual survey of inshore rockfish abundance and habitat in the southern Strait of Georgia using a shallow-water towed video system. Canadian Technical Report of Fisheries and Aquatic Sciences, 2566. 52 pp.

Matsuoka, T., Ishizuka, S., Anraju, K., and Nakano, M. 1997. Assessment by underwater infrared video of the selectivity of an experimental Danish seine for deep-water prawn. *In* Developing and Sustaining World Fisheries Resources: The State of Science and Management. Proceedings of the 2nd World Fisheries Congress, 28 July–2 August 1996, Brisbane, Australia. pp. 551–557. Ed. by D. A. Hancock, D. C. Smith, A. Grant, and D. Beumer. CSIRO Publishing, Collingwood, Australia. 797 pp.

Mazel, C. H., Strand, M. P., Lesser, M. P., Crosby, M. P., Coles, B., and Nevis, A. J. 2003. High-resolution determination of coral reef bottom cover from multispectral fluorescence laser line scan imagery. Limnology and Oceanography, 48: 522–534.

McCauley, E. 1984. The estimation of the abundance and biomass of zooplankton in samples. *In* A Manual on Methods for the Assessment of Secondary Productivity in Fresh Waters, 2nd edn, pp. 228–265. Ed. by J. A. Downing and F. H. Rigler. IBP Handbook No. 17, Blackwell Scientific Publications, Oxford, UK. 500 pp.

McElderry, H. 2008. At sea observing using video-based electronic monitoring. Background paper prepared by Archipelago Marine Research Ltd for the Electronic Monitoring Workshop July 29–30, 2008, Seattle, WA, held by the North Pacific Fishery Management Council, the National Marine Fisheries Service, and the North Pacific Research Board: The Efficacy of Video-based Monitoring for the Halibut Fishery. Available online at: http://www.fakr.noaa.gov/npfmc/misc_pub/EMproceedings.pdf.

McElderry, H., and Gislason, G. (In press). Video-based electronic monitoring of fishing operations. Marine and Coastal Fisheries.

McEwen, R., Thomas, H., Weber, D., and Psota, F. 2003. Performance of an AUV navigation system at Arctic latitudes. *In* Oceans 2003: Celebrating the Past, Teaming Toward the Future. Proceedings of the MTS/IEEE Oceans Conference, 22–26 September 2003, San Diego, CA, 2: 642–653.

McFarlane, N. J. B., and Tillet, R. D. 1997. Fitting 3D point distribution models to fish stereo images. *In* Proceedings of British Machine Vision Conference (BMVC), 8–11 September 1997, University of Essex, UK. Ed. by A. F. Clark. Vol. 1: 330–339.

McLean, J. W. 1999. High-resolution 3-D underwater imaging. *In* Airborne and In-Water Underwater Imaging, pp. 10–19. Ed. by G. D. Gilbert. Proceedings of SPIE, 3761. 198 pp.

McLean, J. W., and Freeman, J. D. 1996. Effects of ocean waves on airborne lidar imaging. Applied Optics, 35: 3261–3269.

Menin, A., and Paulus, R. 2003. Fish counting by acoustic means. Oceans, 6: 166–168.

Mishra, D. R., Narumalani, S., Rundquist, D., Lawson, M., and Perk, R. 2007. Enhancing the detection and classification of coral reef and associated benthic habitats: a hyperspectral remote sensing approach. Journal of Geophysical Research, 112: C08014: 18 pp. doi:10.1029/2006JC003892.

Mitra, K., and Churnside, J. H. 1999. Transient radiative transfer equation applied to oceanographic lidar. Applied Optics, 38: 889–895.

Mitson, R. B. 1963. Marine Fish Culture in Britain: V. An electronic device for counting the nauplii of *Artemia salina* L. Journal du Conseil Permanent International pour l'Exploration de la Mer, 28: 262–269.

Mobley, C. D. 1994. Light and Water. Academic Press, San Diego, CA, USA. 592 pp.

Morais, E. F., Campos, M. F. M., Padua, F. L. C., and Carceroni, R. L. 2005. Particle filter-based predictive tracking for robust fish counting. *In* Proceedings of the 18th Brazilian Symposium on Computer Graphics and Image Processing (SIBGRAPI 2005), 9–12 October 2005, Natal, RN, Brazil, pp. 367–374. Published by IEEE Computer Society, Los Alamos, CA, USA.

Müller, C. 2007. Behavioural reactions of cod (*Gadus morhua*) and plaice (*Pleuronectes platessa*) to sound resembling offshore wind turbine noise. PhD thesis, Humboldt University, Berlin.

Mumby, P. J., and Edwards, A. J. 2002. Mapping marine environments with IKONOS imagery: enhanced spatial resolution can deliver greater thematic accuracy. Remote Sensing of the Environment, 82: 248–257.

Mumby, P. J., Green, E. P., Clark, C. D., and Edwards, A. J. 1998. Digital analysis of multispectral airborne imagery of coral reefs. Coral Reefs, 17: 59–69.

Nakken, O., and Olsen, K. 1977. Target strength measurements of fish. Rapports et Procès-Verbaux des Réunions du Conseil Permanent International pour l'Exploration de la Mer, 170: 52–69.

Nielsen, J. R., and Lundgren, B. 1999. Hydroacoustic *ex situ* target strength measurements on juvenile cod (*Gadus morhua* L.). ICES Journal of Marine Science, 56: 627–639.

Nielsen, L. T., Jakobsen, H. H., and Hansen, P. J. 2010. High resilience of two coastal plankton communities to twenty-first century seawater acidification: evidence from microcosm studies. Marine Biology Research, 6: 542–555.

Norcross, B. L., and Mueter, F. J. 1999. The use of an ROV in the study of juvenile flatfish. Fisheries Research, 39: 241–251.

Okamoto, M., Morita, S., and Sato, T. 2000. Fundamental study to estimate fish biomass around coral reef using 3-dimensional underwater video system. *In* Oceans 2000: Where Marine Science and Technology Meet. Proceedings of the MTS/IEEE Oceans Conference, 11–14 September 2000, Providence, RI, 2: 1389–1392.

Oliver, C. W., and Edwards, E. F. 1996. Dolphin-safe Research Program Progress Report II (1992–1996). Southwest Fisheries Science Center Administrative Report LJ-96–13. National Marine Fisheries Service, Southwest Fisheries Science Center, La Jolla, CA, USA. 91 pp.

Olla, B. L., Davis, M. W., and Schreck, C. B. 1997. Effects of simulated trawling on sablefish and walleye pollock: the role of light intensity, net velocity and towing duration. Journal of Fish Biology, 50: 1181–1194.

Olla, B. L., Davis, M. W., and Rose, C. S. 2000. Differences in orientation and swimming of walleye pollock *Theragra chalcogramma* in a trawl net under light and dark conditions. Concordance between field and laboratory observations. Fisheries Research, 44: 261–266.

Olsson, M., Hardy, K., and Sanderson, J. 2007. Underwater applications of high-power light-emitting diodes. Sea Technology, 48(8): 31–34.

O'Neill, F. G., McKay, S. J., Ward, J. N., Strickland, A., Kynoch, R. J., and Zuur, A. F. 2003. An investigation of the relationship between sea state induced vessel motion and cod-end selection. Fisheries Research, 60: 107–130.

Oppelt, N., and Mauser, W. 2007. Airborne visible/infrared imaging spectrometer AVIS: design, characterization and calibration. Sensors, 7: 1934–1953.

Osborn, J. 1997. Analytical and digital photogrammetry. *In* Animal Groups in Three Dimensions, pp. 36–60. Ed. by J. K. Parrish and W. M. Hamner. Cambridge University Press, Cambridge, UK. 378 pp.

Osofsky, S. T. 2001. Characterization of a vertical blurring effect unique to streak tube imaging lidar. *In* Ocean Optics: Remote Sensing and Underwater Imaging, pp. 1–7. Ed. by R. J. Frouin and G. D. Gilbert. Proceedings of SPIE, 4488. 280 pp.

Özbilgin, H., and Glass, C. W. 2004. Role of learning in mesh penetration behaviour of haddock (*Melanogrammus aeglefinus*). ICES Journal of Marine Science, 61: 1190–1194.

Özbilgin, H., and Wardle, C. S. 2002. Effect of seasonal temperature changes on the escape behaviour of haddock, *Melanogrammus aeglefinus*, from the codend. Fisheries Research, 58: 323–331.

Palandro, D., Andre-Foue, S., Dustan, T. P., and Muller-Karger, E. 2003. Change detection in coral reef communities using Ikonos satellite sensor imagery and historic aerial photographs. International Journal of Remote Sensing, 24: 873–878.

Parrish, B. B., Blaxter, J. H. S., and Dixon, W. 1962. Photography of fish behaviour in relation to trawls. ICES Document CM 1962/Comparative Fishing Committee: 77.

Parrish, B. B., Hemmings, C. C., Chapman, C. J., Main, J., and Lythgoe, J. 1964. Further observations by frogmen on the reactions of fish to the seine net. ICES Document CM 1964/ Comparative Fishing Committee: 134.

Partridge, B. L., Pitcher, T. J., Cullen, J. M., and Wilson, J. 1980. The three-dimensional structure of fish schools. Behavioral Ecology and Sociobiology, 6: 277–288.

Pearlman, J. S., Barry, P. S., Segal, C. C., Shepanski, J., Beiso, D., and Carman, S. L. 2003. Hyperion, a space-based imaging spectrometer. IEEE Transactions on Geoscience and Remote Sensing, 41: 1160–1173.

Petrell, R. J., Shi, X., Ward, R. K., Naberg, A., and Savage, C. R. 1997. Determining fish size and swimming speed in cages and tanks using simple video techniques. Aquacultural Engineering, 16: 63–84.

Philpot, W., Davis, C. O., Bissett, W. P., Mobley, C. D., Kohler, D. D. R, Lee, Z., Bowles, J., *et al.* 2004. Bottom characterization from hyperspectral image data. Oceanography, 17: 76–85.

Piasente, M., Knuckey, I. A., Eayrs, S., and McShane, P. E. 2004. *In situ* examination of the behaviour of fish in response to demersal trawl nets in an Australian trawl fishery. Marine and Freshwater Research, 55: 825–835.

Pienaar, L. V., and Thomson, A. C. 1969. Allometric weight-length regression models. Journal of the Fisheries Research Board of Canada, 26(1): 123–131.

Pitcher, T. J., Magurran, A. E., and Edwards, J. I. 1985. Schooling mackerel and herring choose neighbours of similar size. Marine Biology, 86: 319–322.

Pizarro, O., and Singh, H. 2003. Toward large-area mosaicing for underwater scientific applications. IEEE Journal of Oceanic Engineering, 20: 651–672.

Porcella, L., and Nishijima, J. 2006. Alamitos Fish Ladder Year 2 – Monitoring Report 2004–2005, Project No. 62742011. Santa Clara Valley Water District, Guadalupe. 9 pp.

Reid, D. G., Allen, V. J., Bova, D. J., Jones, E. G., Kynoch, R. J., Peach, K. J., Fernandes, P. G., *et al.* 2007. Anglerfish catchability for swept-area abundance estimates in a new survey trawl. ICES Journal of Marine Science, 64: 1503–1511.

Reilly-Matthews, B. 2007. Particle imaging and analysis instrumentation minimizes taste and odor complaints. American Water Works Association Journal, 99: 50–54.

Remondino, F., and Fraser, C. 2006. Digital camera calibration methods: considerations and comparisons. *In* ISPRS Commission V Symposium: Image Engineering and Vision Metrology, 25–27 September 2006, Dresden, Germany. International Archives of the Photogrammetry, Remote Sensing and Spatial Information Sciences, 36(5): 262–272.

Rhoads, D. C., Carey, D., Saade, E. J., and Hecker, B. 1997. Capabilities of laser line scan technology for aquatic habitat mapping and fishery resource characterization. US Army Engineer Waterways Experimental Station, Vicksburg, MS, USA, Technical Report EL-97–7. 61 pp.

Riegl, B., Korrubel, J. L., and Martin, C. 2001. Mapping and monitoring of coral communities and their spatial patterns using a surface-based video method from a vessel. Bulletin of Marine Science, 69: 869–880.

Roff, J. C., and Hopcroft, R. R. 1986. High precision microcomputer based measuring system for ecological research. Canadian Journal of Fisheries and Aquatic Sciences, 43: 2044–2048.

Rogers, C. S., and Miller, J. 2001. Coral bleaching, hurricane damage and benthic cover on coral reefs in St John, US Virgin Islands: a comparison of surveys with the chain transect method and videography. Bulletin of Marine Science, 69: 459–470.

Roithmayr, C. M. 1970. Airborne low-light sensor detects luminescing fish schools at night. Commercial Fisheries Review, 32: 42–51.

Rooper, C. N., and Zimmermann, M. 2007. A bottom–up methodology for integrating underwater video and acoustic mapping for seafloor substrate classification. Continental Shelf Research, 27: 947–957.

Rose, C. S. 1995. Behaviour of North Pacific groundfish encountering trawls: applications to reduce bycatch. *In* Solving Bycatch – Considerations for Today and Tomorrow, pp. 235–241. University of Alaska, Fairbanks. Alaska Sea Grant College Program Report No. 96-03.

Rosenkranz, G. E., and Byersdorfer, S. C. 2004. Video scallop survey in the eastern Gulf of Alaska, USA. Fisheries Research, 69: 131–140.

Rosenkranz, G. E., Gallager, S. M., Shepard, R. W., and Blakeslee, M. 2008. Development of a high-speed, megapixel benthic imaging system for coastal fisheries research in Alaska. Fisheries Research, 92: 340–344.

Ruff, B. P., Marchant, J. A., and Frost, A. R. 1995. Fish sizing and monitoring using a stereo image analysis system applied to fish farming. Aquacultural Engineering. 14: 155–173.

Ryan, T. E., Kloser, R. J., and Macaulay, G. J. 2009. Measurement and visual verification of fish target strength using an acoustic-optical system attached to a trawlnet. ICES Journal of Marine Science, 66: 1238–1244.

Ryer, C. H., and Olla, B. L. 2000. Avoidance of an approaching net by juvenile walleye pollock *Theragra chalcogramma* in the laboratory: the influence of light intensity. Fisheries Research, 45: 195–199.

Rzhanov, Y. 2005. Video mosaics. *In* Report of the National Marine Fisheries Service Workshop on Underwater Video Analysis. 4–6 August 2004, p. 49. Ed. by D. A. Somerton and C. T. Gledhill. US Department of Commerce, NOAA Technical Memorandum NMFS-F/SPO-68. 69 pp.

Samoilys, M. A., and Carlos, G. 2000. Determining methods of underwater visual census for estimating the abundance of coral reef fishes. Environmental Biology of Fishes, 57: 289–304.

Sawada, K., Takao, Y., Miyanohana, Y., and Kinacigl, H. T. 2002. Introduction of the precise TS measurement for fisheries acoustics. Turkish Journal of Veterinary and Animal Sciences, 26: 209–214.

Sawada, K., Takahashi, H., Takao, Y., Watanabe, K., Horne, J. K., McClatchie, S., and Abe, K. 2004. Development of an acoustic-optic system to estimate target-strengths and tilt angles from fish aggregations. *In* Oceans '04: Bridges Across the Oceans. Proceedings of the MTS/IEEE Techno-Ocean Conference, 9–12 November 2004, Kobe, Japan, 1: 395–400.

Sawada, K., Takahashi, H., Abe, K., Ichii, T., Watanabe, K., and Takao, Y. 2009. Target-strength, length, and tilt-angle measurements of Pacific saury (*Cololabis saira*) and Japanese anchovy (*Engraulis japonicus*) using an acoustic-optical system. ICES Journal of Marine Science, 66: 1212–1218.

Scaramuzza, D., Martinelli, A., and Siegwart, R. 2006. A flexible technique for accurate omnidirectional camera calibration and structure from motion. *In* Proceedings of the Fourth IEEE International Conference on Computer Vision Systems, January 2006, New York (ICVS 2006). 8 pp.

Shardlow, T. F., and Hyatt, K. D. 2004. Assessment of the counting accuracy of the Vaki infrared counter on chum salmon. North American Journal of Fisheries Management, 24: 249–252.

Sheng, J., Malkiel, E., Katz, J., Adolf, J., Belas, R., and Place, A. R. 2007. Digital holographic microscopy reveals prey-induced changes in swimming behaviour of predatory dinoflagellates. Proceedings of the National Academy of Sciences, 104: 17512–17517.

Shieh, A. C. R., and Petrell, R. J. 1998. Measurement of fish size in salmon (*Salmo salar* L.) cages using stereographic video techniques. Aquacultural Engineering, 17: 29–43.

Shifrin, K. S. 1988. Physical Optics of Ocean Water. American Institute of Physics, New York. 285 pp.

Shortis, M. R., Clarke, T. A., and Robson, S. 1995. Practical testing of the precision and accuracy of target image centring algorithms. *In* Videometrics IV, pp. 65–76. Ed. by S. F. El-Hakim. Proceedings of SPIE, 2598. 400 pp.

Shortis, M. R., Miller, S., Harvey, E. S., and Robson, S. 2000. An analysis of the calibration stability and measurement accuracy of an underwater stereo-video system used for shellfish surveys. Geomatics Research Australasia, 73: 1–24.

Shortis, M. R., Ogleby, C. L., Robson, S., Karalis, E. M., and Beyer, H. A. 2001. Calibration modelling and stability testing for the Kodak DC200 series digital still camera. *In* Videometrics and Optical Methods for 3D Shape Measurement, pp. 148–153. Ed. by S. F. El-Hakim and A. Gruen. Proceedings of SPIE, 4309. 356 pp.

Shortis, M. R., Seager, J. W., Robson, S., and Harvey, E. S. 2003. Automatic recognition of coded targets based on a Hough transform and segment matching. *In* Videometrics VII, pp. 202–208. Ed. by S. F. El-Hakim, A. Gruen, and J. S. Walton. Proceedings of SPIE, 5013. 278 pp.

Shortis, M. R., Bellman, C. J., Robson, S., Johnston, G. J., and Johnson, G. W. 2006. Stability of zoom and fixed lenses used with digital SLR cameras. International Archives of Photogrammetry and Remote Sensing, 36(5): 285–290.

Shortis, M. R., Seager, J. W., Williams, A., Barker, B. A., and Sherlock, M. 2009a. Using stereo-video for deep water benthic habitat surveys. Marine Technology Society Journal, 42: 28–37.

Shortis, M. R., Harvey, E., and Abdo, D. 2009b. A review of underwater stereo-image measurement for marine biology and ecology applications. Oceanography and Marine Biology: An Annual Review, 47: 257–292.

Sieracki, C. K., Sieracki, M. E., and Yentsch, C. S. 1998. An imaging-in-flow system for automated analysis of marine microplankton. Marine Ecology Progress Series. 168: 285–296.

Smith, I. P., Johnstone, A. D. F., and Dunkley, D. A. 1996. Evaluation of a portable electrode array for a resistivity fish counter. Fisheries Management and Ecology, 3: 129–141.

Snow, W. L., Childers, B. A., and Shortis, M. R. 1993. The calibration of video cameras for quantitative measurements. Proceedings of the 39th International Instrumentation Symposium, 2–6 May 1993, Albuquerque, NM, USA, pp. 103–130. Instrument Society of America (ISA). 1227 pp.

Somerton, D. A., and Gledhill, C. T. (Eds). 2005. Report of the National Marine Fisheries Service Workshop on Underwater Video Analysis, August 4–6, 2004. US Department of Commerce, NOAA Technical Memorandum NMFS-F/SPO-68. 69 pp.

Squire, J. L., and Krumboltz, H. 1981. Profiling pelagic fish schools using airborne optical lasers and other remote sensing techniques. Marine Technological Society Journal, 15: 27–31.

Steeves, G. D., Peterson, R. H., and Clark, L. D. 1998. A quantitative stereoscopic video system for visually measuring the linear dimensions of free-swimming fish. *In O*ceans '98: Engineering for Sustainable Use of the Oceans Proceedings of the IEEE/OES Oceans Conference 28 September–1 October 1998, Nice, France, 3: 1405–1408.

Stokesbury, K. D. E., Harris, B. P., Marino II, M. C., and Nogueira, J. I. 2004. Estimation of sea scallop abundance using a video survey in off-shore US waters. Journal of Shellfish Research, 23: 33–40.

Stokesbury, K. D. E., Harris, B. P., Marino II, M. C., and Nogueira, J. I. 2007. Sea scallop mortality in a marine protected area. Marine Ecology Progress Series, 349: 151–158.

Stoner, A. W., and Kaimmer, S. M. 2008. Reducing elasmobranch bycatch: laboratory investigation of rare earth metal and magnetic deterrents with spiny dogfish and Pacific halibut. Fisheries Research, 92: 162–168.

Strong, M. B., and Lawton, P. 2004. URCHIN — Manually deployed geo-referenced video system for Under-water Reconnaissance and Coastal Habitat Inventory. Canadian Technical Report of Fisheries and Aquatic Sciences, 2553. 28 pp.

Sun, H., Benzie, P. W., Burns, N., Hendry, D. C., Player, M. A., and Watson, J. 2008. Underwater digital holography for studies of marine plankton. Philosophical Transactions of the Royal Society, 366: 1789–1806.

Sun, H., Hendry, D. C., Player, M. A., and Watson, J. 2007. *In situ* underwater electronic holographic camera for studies of plankton. IEEE Journal of Oceanic Engineering, 32: 373–382.

Takahashi, H., Sawada, K., Watanabe, K., Horne, J. K., McClatchie, S., Takao, Y., and Abe, K. 2004. Development of a stereo TV camera system to complement fish school measurements by a quantitative echo sounder. *In* Oceans '04: Bridges Across the Oceans. Proceedings of the MTS/IEEE Techno-Ocean Conference, 9–12 November 2004, Kobe, Japan, 1: 408–414.

Tenningen, E., Churnside, J. H., Slotte, A., and Wilson, J. J. 2006. Lidar target-strength measurements on Northeast Atlantic mackerel (*Scomber scombrus*). ICES Journal of Marine Science, 63: 677–682.

Terabayashi, K., Mitsumoto, H., Morita, T., Aragaki, Y., Shimomura, N., and Umeda, K. 2009. Measurement of three-dimensional environment with a fish-eye camera based on structure from motion – error analysis. Journal of Robotics and Mechatronics, 21: 680–688.

Thomas, G. L., and Thorne, R. E. 2001. Nighttime predation by Steller sea lions. Nature, 411: 1013.

Thompson, A., and Taylor, B. N. 2008. Guide for the Use of the International System of Units (SI). NIST Special Publication No. 811, 2008 edn. National Institute of Standards and Technology, Gaithersburg, MD, USA. 85 pp.

Towler, R. H., Jech, J. M., and Horne, J. K. 2003. Visualizing fish movement, behaviour, and acoustic backscatter. Aquatic Living Resources, 16: 277–282.

Trefethen, P. S., and Collins, G. B. 1975. Techniques for appraising adult salmon and trout populations in the Columbia River basin. *In* Report of the Symposium on Methodology for the Survey, Monitoring and Appraisal of Fishery Resources in Lakes and Large Rivers, 2–4 May 1974, Aviemore, Scotland. EIFAC Technical Paper No. 23 (Suppl. 1, Vol. 2): 490–501.

Tremblay, M. J., Smith, S. J., Todd, B. J., Clement, P. M., and McKeown, D. L. 2009. Associations of lobsters (*Homarus americanus*) off southwestern Nova Scotia with bottom type from images and geophysical maps. ICES Journal of Marine Science, 66: 2060–2067.

Tsai, R. Y. 1986. An efficient and accurate camera calibration technique for 3D machine vision. *In* Proceedings of the IEEE Computer Society Conference on Computer Vision and Pattern Recognition, 22–26 June 1986, Miami, FL, USA. Pp. 364–374.

Tsai, R. Y. 1987. A versatile camera calibration technique for high-accuracy 3D machine vision metrology using off-the-shelf TV cameras and lenses. IEEE International Journal of Robotics and Automation, 3: 323–344.

Tyo, J. S., Rowe, M. P., Pugh, E. N., and Engheta, N. 1996. Target detection in optically scattering media by polarization-difference imaging. Applied Optics, 35: 1855–1870.

Ulich, B. L., Lacovara, P., Moran, S. E., and DeWeert, M. J. 1997. Recent results in imaging lidar. *In* Advances in Laser Remote Sensing for Terrestrial and Oceanographic Applications, pp. 95–108. Ed. by R. M. Narayanan and J. E. Kalshoven. Proceedings of SPIE, 3059. 208 pp.

Van Long, L., and Aoyama, T. 1985. Photographic measurement for obtaining the length, aspect and bearing of free-swimming fish from their spatial position. Bulletin of the Japanese Society of Scientific Fisheries, 52: 191–195.

Van Long, L., Aoyama, T., and Inagaki, T. 1985. A stereo photographic method for measuring the spatial position of fish. Bulletin of the Japanese Society of Science and Fisheries. 51: 183–190.

van Rooij, J. M., and Videler, J. J. 1996. Estimating oxygen uptake rate from ventilation frequency in the reef fish *Sparisoma viride*. Marine Ecology Progress Series, 132: 31–41.

Vandermeulen, H. 2007. Drop and towed camera systems for ground-truthing high frequency sidescan in shallow waters. Canadian Technical Report of Fisheries and Aquatic Sciences, 2687. 17 pp.

Wagner, P. G. 2007. Fish counting at large hydroelectric projects. *In* Reconciling Fisheries with Conservation: Proceedings of the Fourth World Fisheries Congress, 3–5 May 2004, Vancouver, Canada, pp. 173–195. Ed. by J. L. Nielsen, J. J. Dodson, K. Friedland, T. R. Hamon, J. Musick, and E. Vespoor. American Fisheries Society Symposium Series No. 49. Bethesda, Maryland. 1946 pp.

Walker, J. G., Chang, P. C. Y., and Hopcraft, K. I. 2000. Visibility depth improvement in active polarization imaging in scattering media. Applied Optics, 39: 4933–4941.

Walsh, S. J, and Hickey, W. M. 1993. Behavioural reactions of demersal fish to bottom trawls at various light conditions. ICES Marine Science Symposia, 196: 68–76.

Wang, X-F., Tang, Y., Zhang, Z-Z., and Liu, H-Y. 2008. Feasibility of using digital photography for environmental monitoring of animals in an artificial reef. International Archives of the Photogrammetry, Remote Sensing and Spatial Information Sciences, 37(B6b): 339–342.

Wardle, C. S. 1983. Fish reaction to towed fishing gears. *In* Experimental Biology at Sea, pp. 167–196. Ed. by A. G. MacDonald and G. Priedel. Academic Press, London, UK.

Wardle, C. S., and Hall, C. D. 1993. Marine video. *In* Video Techniques in Animal Ecology and Behavior, pp. 89–111. Ed. by S. D. Wratten. Chapman and Hall, London. 192 pp.

Weber, P., Wagner, M., and Schneckenburger, H. 2010. Fluorescence imaging of membrane dynamics in living cells. Journal of Biomedical Optics, 15: 046017.

Widder, E. A., Robison, B. H., Reisenbichler, K. R., and Haddock, S. H. D. 2005. Using red light for *in situ* observations of deep-sea fishes. Deep-Sea Research I, 52: 2077–2085.

Williams, I. D., Polunin, N. V. C., and Hendrick, V. J. 2001. Limits to grazing by herbivorous fishes and the impact of low coral cover on macroalgal abundance on a coral reef in Belize. Marine Ecology Progress Series, 222: 187–196.

Williams, K., Towler, R., and Wilson. C. 2010. Cam-Trawl: a combination trawl and stereo-camera system. Sea Technology, 51(12): 45–50.

Yamano, H., and Tamura, M. 2004. Detection limits of coral reef bleaching by satellite remote sensing: simulation and data analysis. Remote Sensing of the Environment, 90: 86–103.

Yanase, K., Eayrs, S., and Arimoto, T. 2007. Influence of water temperature and fish length on the maximum swimming speed of sand flathead, *Platycephalus bassensis*: implications for trawl selectivity. Fisheries Research, 84: 180–188.

Yoklavich, M. M., Grimes, G. B., and Wakefield, W. W. 2003. Using laser line scan imaging technology to assess deepwater habitats in the Monterey Bay National Marine Sanctuary. Marine Technology Society Journal, 37: 18–26.

Zege, E. P., Katsev, I. L., Prikhach, A. S., and Keeler, R. N. 1999. Comparison of airborne lidar performance when operating in the obscuration and reflection modes. *In* Airborne and In-Water Underwater Imaging, pp. 142–153. Ed. by G. D. Gilbert. Proceedings of SPIE, 3761. 198 pp.

Zege, E. P., Katsev, I. L., Prikhach, A. S., and Keeler, R. N. 2001. Simulating the performance of airborne and in-water laser imaging systems. *In* Ocean Optics: Remote Sensing and Underwater Imaging, pp. 94–105. Ed. by R. J. Frouin and G. D. Gilbert. Proceedings of SPIE, 4488. 280 pp.

Zhang, Z. 2000. A flexible new technique for camera calibration. IEEE Transactions on Pattern Analysis and Machine Intelligence (PAMI), 22: 1330–1334.

Zorn, H. M., Churnside, J. H., and Oliver, C. W. 2000. Laser safety thresholds for cetateans and pinnipeds. Marine Mammal Science, 16: 186–200.

8 Author contact information

Editors

James Churnside
NOAA Earth System Research Laboratory
325 Broadway, Boulder, CO 80305, USA
james.h.churnside@noaa.gov

Michael Jech
NOAA Northeast Fisheries Science Center
166 Water Street, Woods Hole, MA 02543, USA
michael.jech@noaa.gov

Eirik Tenningen
Institute of Marine Research
PO Box 1870, Nordnes
5817 Bergen, Norway
eirik.tenningen@imr.no

Contributing authors

Pierre M. Clement
DFO Bedford Institute of Oceanography
PO Box 1006
Dartmouth, NS B2Y 4C6, Canada
pierre.clement@dfo-mpo.gc.ca

Arne Fjälling
National Board of Fisheries
Institute of Coastal Research
178 93 Drottningholm, Sweden
arne.fjalling@fiskeriverket.se

Jules S. Jaffe
Marine Physical Laboratory
Scripps Institute of Oceanography
9500 Gilman Avenue
La Jolla, CA 92093, USA
jules@mpl.ucsd.edu

Emma G. Jones
National Institute of Water and Atmospheric Research Ltd
41 Market Place
Auckland Central, 1010, New Zealand
emma.jones@niwa.co.nz

Bo Lundgren
Technical University of Denmark
National Institute of Aquatic Resources
North Sea Science Park, Willemoesvej
PO Box 101
DK-9850 Hirtshals, Denmark
bl@aqua.dtu.dk

Gavin J. Macaulay
Institute of Marine Research
Postboks 1870 Nordnes
5817 Bergen, Norway
gavin.macaulay@imr.no

Howard McElderry
Archipelago Marine Research Ltd
525 Head Street
Victoria, BC V9A 5S1, Canada
howardm@archipelago.ca

Richard O'Driscoll
National Institute of Water and Atmospheric Research Ltd
Private Bag 14-901
Kilbirnie, Wellington, New Zealand 6241
r.odriscoll@niwa.co.nz

Tim E. Ryan
CSIRO Marine and Atmospheric Research
Castray Esplanade
Hobart, TAS 7001, Australia
tim.ryan@csiro.au

Mark R. Shortis
School of Mathematical and Geospatial Sciences
RMIT University
GPO Box 2476
Melbourne 3001, Australia
mark.shortis@rmit.edu.au

Stephen J. Smith
DFO Bedford Institute of Oceanography
1 Challenger Drive
Dartmouth, NS B2Y 4A2, Canada
stephen.smith@dfo-mpo.gc.ca

W. Waldo Wakefield
NOAA Northwest Fisheries Science Center
2032SE OSU Drive
Newport, OR 97365, USA
waldo.wakefield@noaa.gov

9 Abbreviations and acronyms

ADCP	acoustic Doppler current profiler
AUV	autonomous underwater vehicle
BRD	bycatch reduction device
CCD	charge-coupled device
CCTV	closed circuit television
CMOS	complementary metal oxide semiconductor
CV	coefficient of variation
DEM	digital-elevation map
DSLR	digital single-lens reflex
DVL	Doppler velocimeter log
EM	video-based electronic monitoring
EMCCD	electron multiplying charge-coupled device
EXIF	exchangeable image file format
FILLS	fluorescent imaging laser line scanning
FLIR	forward-looking infrared imaging systems
FLOE	Fish Lidar, Oceanic, Experimental (NOAA's airborne fish lidar)
fps	frames per second
GigE	Gigabyte Ethernet
GIS	geographic information system
GOOS	Global Ocean Observing System
GPS	global positioning system
GPSTime	GPS time-string
GUI	graphical user interface
HD	high definition
HDi	interlaced high definition
HDp	progressive high definition
HID	high-intensity-discharge
HiPaP	high-precision acoustic positioning
ICCD	intensified charge-coupled device
INS	inertial navigation system
IOOS	Integrated Ocean Observing System
IR	infrared

ISIT	intensified silicon intensifier-target
JAI	Joint Architectural Intelligence (www.jai.com)
JPEG	joint photographic experts group
LBL	long baseline (a positioning system)
LED	light-emitting diode
LLS	laser line scanning
LOPC	laser optical plankton counter
MEMS	microelectromechanical system
MODIS	moderate resolution imaging spectoradiometer
NMEA	National Marine Electronics Association
NOAA	National Oceanic and Atmospheric Administration (USA)
NTSC	National Television System Committee
OBIS	Ocean Biogeographic Information System
PAL	phase alternating line (video standard)
PAR	photosynthetically active radiation
PHILLS	portable hyper-spectral imager for low-light spectroscopy
PINRO	Knipovich Polar Research Institute of Marine Fisheries and Oceanography (Russia)
QE	quantum efficiency
RFID	radio frequency identification
RMS	root mean squared
ROV	remotely operated vehicle
SBL	short baseline
SeaWIFS	Sea-viewing Wide Field-of-view Sensor
SIT	silicon intensifier-target
SLR	single-lens reflex
SST	sea surface temperature
TS	target strength
USBL	ultra-short baseline
VICASS	video image capturing and sizing system
VMS	Vision Measurement System
WGFAST	ICES Working Group on Fishery Acoustics Science and Technology

10 Websites

Calibration toolbox

http://www.vision.caltech.edu/bouguetj/calib_doc/

Commercial camera company

www.pco.de

Geometric software

www.geomsoft.com

International Ocean Colour Coordination Group

http://www.ioccg.org/

Joint Architectural Intelligence

www.jai.com

NASA ocean color website

http://oceancolor.gsfc.nasa.gov/

Ocean Research and Conservation Association

http://oceanrecon.org/

Scientific CMOS technology

www.scimos.com